PERFORMANCE ANALYSIS OF OFDM SYSTEMS WITH RANDOM RESIDUAL FREQUENCY OFFSET

by

Pradeep Chathuranga Weeraddana

A thesis submitted in partial fulfillment of the requirements for the degree of Master of Engineering in Telecommunications

Examination Committee: Dr. R.M.A.P. Rajatheva (Chairman)
Dr. Teerapat Sanguankotchakorn
Dr. Poompat Saengudomlert

Nationality: Sri Lankan
Previous Degree: Bachelor of Science in Electronic & Telecommunication Engineering
University of Moratuwa
Moratuwa, Sri Lanka

Scholarship Donor: Government of Thailand

Asian Institute of Technology
School of Engineering and Technology
Thailand
May 2007

ACKNOWLEDGEMENT

I would like to express my sincere gratitude to my thesis advisor, Dr. R.M.A.P. Rajatheva, for his guidance and unreserved help during the study period. My special thanks should go to the examination committee members Dr. Poompat Saengudomlert, Dr. Teerapat Sanguankotchakorn for their constructive opinions and invaluable suggestions.

My grateful thanks also go to the rest of the faculty members, all of the staff members in the telecommunications program for their constant support during my study period at AIT. Also I'm grateful to the assistant Professor Hlaing Minn, University of Texas Dallas for extending his generous cooperation with my research study. His cooperation was much helpful in realizing the modern research trend in wireless communications.

For financial support, I thank the Royal Thai Government. Without this scholarship, this thesis as well as the study at AIT would not have been possible.

Moreover, I would like to convey my heartfelt appreciation to the PhD student, Mr. Prathapasinghe Dharmawansa for his precious instructions and guidance throughout my study time at AIT, where I benefited much due to his generosity, and Mr. Surachai Chieochan from my senior batch, the person who developed this valuable document format.

I am also greatly indebted to my sisters and friends for their love and support throughout my study period at AIT.

Last but not least I would like to thank my parents. They have been an inspiration throughout my life, and always supported my dreams and aspirations, and if I do say so myself, I think they did a fine job raising me. I'd like to pay my gratitude for all of them, and all they have done for me. This thesis is dedicated to my parents.

ABSTRACT

Orthogonal frequency division multiplexing (OFDM) is a multicarrier modulation scheme that achieves high spectral efficiency by using minimally densely spaced orthogonal subcarriers without increasing the transmitter and receiver complexities. Despite its promises OFDM systems are vulnerable to the carrier frequency offset (CFO) arising from transceiver oscillator mismatches and/or Doppler shifts.

The principle motive behind this thesis study is to investigate the performance degradation in OFDM systems due to CFO induced by transmitter/receiver oscillator frequency mismatches. Our derivations are distinct from the other existing results and derivations available in the open literature as most of them considered CFO to be a constant, in contrast we treat it as a random parameter which is the case in reality.

We begin with a derivation of new approximated intercarrier interference (ICI) expression which enables us to carry out the subsequent derivations associated with new bit error rate (BER) and symbol error rate (SER) expressions for binary phase shift keying (BPSK) and 4-quadrature amplitude modulation (QAM) OFDM systems with random CFO or random residual CFO.

Those derived results can be classified into two parts based on the correlation between the residual CFO or CFO and the channel, i.e., performance analysis with channel independent residual CFO or CFO and performance analysis with channel dependent residual CFO. The BER/SER expressions in BPSK/4-QAM OFDM systems with uniformly distributed CFO and Gaussian distributed residual CFO are obtained under the channel independent case and additive white Gaussian (AWGN), frequency-flat and selective Rayleigh fading channels are considered separately. Moreover, in the case of channel dependent scenario, we derive BER/SER expressions in BPSK/4-QAM OFDM systems with frequency-flat Rayleigh fading where the residual CFO is Gaussian distributed conditioned on the channel parameters. The simulation results are provided to verify the accuracy of the new BER/SER expressions.

Table of Contents

List of Abbreviations

ADSL	Asymmetric Digital Subscriber Loop
AOA	Angle of Arrival
AOD	Angle of Departure
AWGN	Additive White Gaussian Noise
BER	Bit Error Rate
BPSK	Binary Phase Shift Keying
CFO	Carrier Frequency Offset
CIR	Channel Impulse Response
CRB	Cramer-Rao Bound
CSI	Channel State Information
DD	Decision-Directed
DAB	Digital Audio Broadcasting
DFT	Discrete Fourier Transform
DVB	Digital Video Broadcasting
FDM	Frequency Division Multiplex
FFT	Fast Fourier Transform
IBI	Inter Block Interference
ICI	Inter Carrier Interference
IDFT	Inverse Discrete Fourier Transform
IFFT	Inverse Fast Fourier Transform
ISI	Inter Symbol Interference
OFDM	Orthogonal Frequency Division Multiplexing
MCM	Multi Carrier Modulation
MIMO	Multiple Input Multiple Output
ML	Maximum Likelihood
MSE	Mean Square Error
PDF	Probability Density Function
P/S	Parallel to Serial

QPSK	Quadrature Phase Shift Keying
RV	Random Variable
SER	Symbol Error Rate
SISO	Single Input Single Output
SNR	Signal to Noise Ratio
S/P	Serial to Parallel

List of Symbols

N	Number of carriers in the OFDM system
G	Number of guard samples in the OFDM symbol
T_s	Data symbol period
T	OFDM block period
T_c	Coherence time of the channel
u_T	Unit step function
f_c	Carrier frequency
$\Im(.)$	Imaginary part of a complex number
$\Re(.)$	Real part of a complex number
h_m	Time domain channel coefficients
H_m	Frequency domain channel coefficients
$E\{.\}$	Statistical expectation
$Var\{.\}$	Statistical Variance
L	Number of tap coefficients in the tap-delay line
$\boldsymbol{I}_m$	Identity Matrix with size $m \times m$
$\mathbf{0}_{m\times n}$	All zero Matrix with size $m \times n$
v	Normalized CFO
v_Δ	Normalized residual CFO
$\hat{v}$	Estimated normalized CFO
δ_{lk}	Kronecker delta
$P_b(\xi)$	Bit Error rate
$P_s(\xi)$	Symbol Error rate
ω	Angular frequency
$Q(.)$	Q-function
$\mathcal{N}(m, \sigma^2)$	Normal distribution with mean and variance m and σ^2 respectively

List of Figures

CHAPTER 1

INTRODUCTION

1.1 Overview

In this chapter we concisely describe the OFDM systems, It's applications, advantages disadvantages of using OFDM in wireless communication and employed techniques to mitigate the impairments of OFDM systems. In addition the statement of the problem, objectives of the research, scopes and limitations are presented followed by the outline of the thesis.

1.1.1 Multi Carrier Modulation (MCM) Schemes

MCM scheme as the name suggests is a modulation technique in which multiple number of carriers are used for modulating the information signals. A functional block diagram of MCM scheme is shown in Figure 1.1. The serial data bits carrying information are first converted to parallel bit streams and every block of N data bits entering will be multiplexed on to N channels where each of these bits are modulated by a different carrier signal. As illustrated in figure 1.1 those carrier signals are ϕ_1 to ϕ_{N-1}.

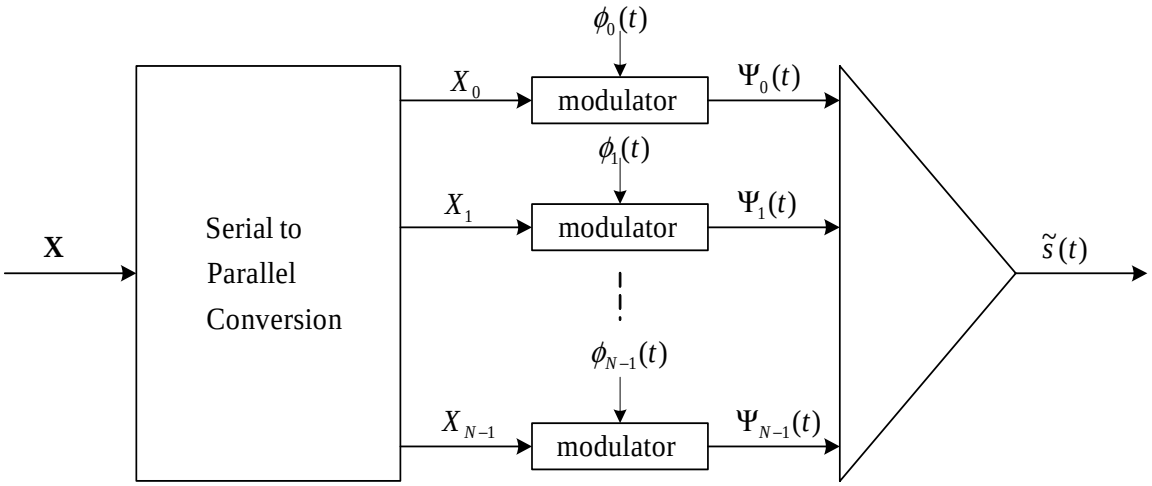

Figure 1.1: Multi carrier modulation scheme

1.1.2 OFDM Systems and Applications of OFDM

OFDM can be considered as one of the most popular MCM scheme with densly spaced subcarrierrs and overlapping spectra which was patented in the United States in 1970. The innovation of the OFDM technique was arround late 1960s, gradually spreading over various wireless communication applications and standards with it's rapid maturity to survive under upredictable wireless channel conditions.

In the OFDM these carrier signals are taken to be orthoganal in time. Thus OFDM time-domain waveforms are chosen such that the mutual orthoganality is ensured even though sub carrier spectra may overlap. Manipulation of the discrete Fourier transform (DFT) in the modulation and demodulation of parallel data transmission techniques (**Weinstein and Ebert**, 1971) shows the possibility of removing the whole bunch of oscillators tuned to each subcarrier frequencies and demodulators with coherent detection as required by FDM. Thus the use of fast Fourier transform (FFT) and inverse fast Fourier transform (IFFT) in implementations ensures a fully digitalized realization of OFDM transceivers which can be easily embedded in to special-purpose hardware components. So that, with the FFT algorithm to compute DFT, a new direction on the practicality of an efficient OFDM system evolved resulting FFT based OFDM systems. The main functional block diagram of an FFT based OFDM system is shown below in Figure 1.2.

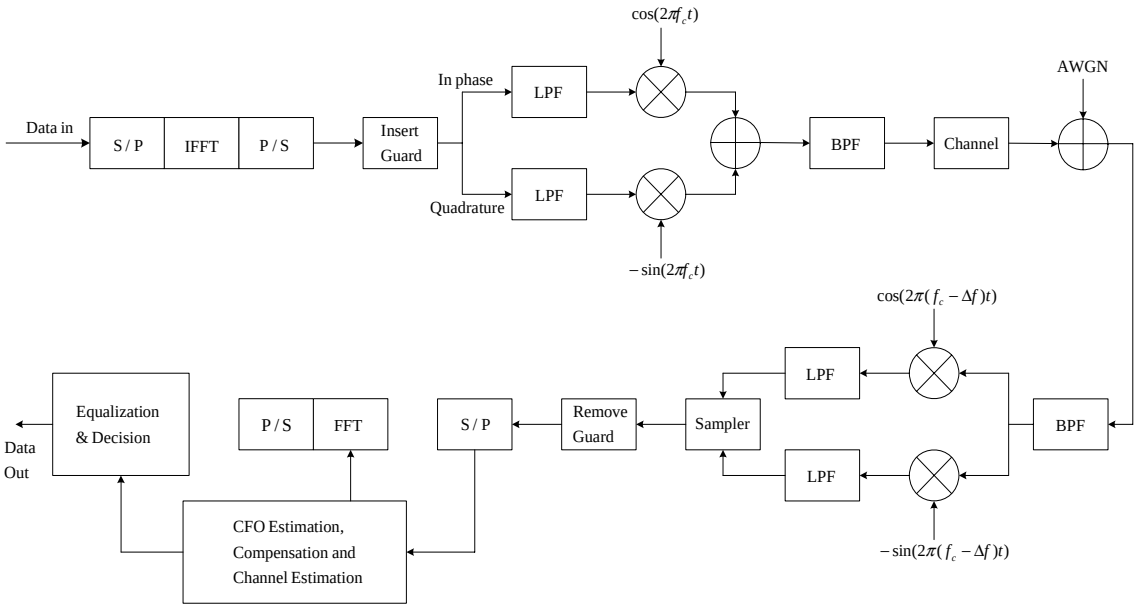

Figure 1.2: Block diagram of an FFT based OFDM system.

The physical layers of many wireless network standards, such as IEEE 802.11a, IEEE 802.16a, HIPERLAN/2 (**IEEE Std 802.11a-1999(R2003)**, 2003; **IEEE Std 802.16^{TM}-2004**, 2004) and wire-line digital communication systems such as ADSL are some of the main application areas of OFDM (**Chow et al.**, 1991; **Cioffi**). Furthermore it has been approved as the new European digital audio broadcasting (DAB) standards as well as for the terrestrial digital audio broadcasting (DVB) systems.

1.1.3 Advantages of Using OFDM

OFDM is in particular capable of dealing with the multipath reception, one of the main problem which is encountered in wireless communication systems. Many narrow-band digital signals which are transmitted simultaneously are overlapped to create the wideband OFDM spectrum. Higher the number of simultaneous or parallel transmitted channels, lesser the data rate that each separate carrier should carry, consequently

increases the symbol duration thus compelling the multipath signals or waves to be suppressed inside one symbol duration.

Splitting of data among a huge number of carriers which are overlapped and closely packed, corresponds to the segment frequency division multiplex inside the term OFDM. The data generated from one single source is capable of populating the whole bandwidth possessed by the OFDM system. The data sequence coming serially is converted to a parallel mode and transmitted. By doing so, the amount of data per carrier is comparatively reduced to a small number consequently reducing the bitrate per carrier as well. This ultimately directs to a significant reduction in the influence of intersymbol interference (ISI).

One important fact to be noted in OFDM systems is that, the overall bandwidth acquired by the OFDM system is far beyond the fading channel's correlation bandwidth. So that, even with some of the carrier signals are distorted due to the fact multipath fading, the transmitted OFDM signal can be hopefully regenerated at the receiver by adequately employing techniques such as error control coding. The phenomenon behind this is that the rest of the undistorted or less distorted carriers can still be received and demodulated without any errors. Rayleigh fading environments can cause burst errors. Randomization of these kind of errors can be effectively addressed by OFDM systems with the use of interleaving of transmitted symbols after the serial to parallel conversion of these symbols. Irrespective of the width of the OFDM bandwidth and channel response, each subcarrier experiences only a frequency-flat fading environment. In other words a frequency-selective fading environment can be strategically partitioned in to a number of frequency-flat fading environments because of the entire spectrum of the OFDM system is composed of so many independent and orthogonal narrowband subcarrier spectrums. So that the equalization process would be more easier than in a typical serial data transmission system.

In addition, the introduction of a guard interval (cyclic prefix or suffix) in to the raw OFDM block at the transmitter decreases the OFDM system's susceptibility to inter symbol interference (ISI) or inter block interference (IBI) which arises due to the phenomenon called delay spread (**Cimini**, 1985). Nevertheless, in-band fading or in other words inter carrier interference (ICI) may still remain.

1.1.4 Impairments of OFDM and Mitigation Techniques

Carrier frequency offset due to time dispersion, frequency mismatches between transmitter and receiver oscillators and phase noise imparted to the signal in up-conversion and down-conversion processes at the transmitter/receiver can be considered as the main impairments inherent in OFDM systems. Orthogonal frequency division multiplexing is a bandwidth efficient signaling scheme where the orthogonality among the subcarriers should be maintained to a high degree of precision. Since the spectra of the sub-carriers are overlapping, an accurate frequency synchronization technique is needed. However, due to the unavoidable factors which were mentioned earlier, the orthogonality of subcarriers will be compromised resulting in intercarrier interference (ICI). That is the useful energy of a particular sub carrier spills over the other sub carriers which degrades the performance of OFDM systems significantly (**Stantchev and Fettweis**, 2000).

There are two different approaches to address the ICI problem induced by the car-

rier frequency offset. The first approach performs CFO estimation and compensation. There exist several CFO estimation techniques which can be categorized as training based methods (**Moose**, 1994; (**schmidl and Cox**, 1997; **Morelli and Mengali**, 1999, 2000; **Lei and Tung-Sang**, 2004; **Hlaing Minn et al.** [a] [b] [c], 2006; **Hlaing Minn and Xing S.**, 2005) and semi-blind or blind methods (**Van De Beek et al.**, 1997; **Tureli, Liu and Zoltowski**, 2000). The training based methods offer faster synchronization, lower complexity, and more reliable performance at the cost of training overhead while the semi-blind or blind methods save training overhead at the expense of longer latency, higher complexity, and less reliable performance. The second approach applies a self ICI cancellation (**Zhao and Häggaman**, 1996; **Armstrong**, 1999) at the sacrifice of data rate. In all current OFDM systems, the first approach is adopted. After the CFO estimation and compensation, there still exists a residual CFO which affects the system error performance.

In the literature the error performance analysis has been treated by a number of authors. Most of the time the followed procedures have utilised the fact that, CFO is constant. However, in practice the CFO error is a random variable with an appropriate probability density function. The BER analysis of OFDM systems with a random CFO represents a more practical performance but it has not been addressed in the literature.

In this thesis we mainly focus on the random nature of the normalised residual carrier frequency offset rather than treating it as a constant parameter in the bit error rate expressions.

1.2 Statement of the Problem

The principal weakness of OFDM technique is its sensitivity to frequency offset errors caused by Doppler shifts and/or transmitter receiver oscillator instabilities. As the subcarriers are closely spaced in frequency compared to the channel bandwidth,the frequency offset must be kept within a small fraction of the subcarrier spacing to avoid severe bit error rate degradation. So the performance impact due to those impairments are of high importance.

1.3 Objectives of the Research

This thesis investigates a novel approach of analyzing the performance of OFDM systems treating the normalised residual CFO as a random variable. Our main consideration is focused on the Error performance analyzing for single input single output (SISO) OFDM systems with CFO, for different type of channel models assuming perfect channel state information (CSI) is known at the receiver. This includes the additive white Gaussian channel, flat fading channel and frequency selective channel. A brief classification of the main objectives of the thesis is as follows.

1. Develop a new approximated ICI expression which enable us to analyse performance of OFDM systems with random residual CFO.

2. Performance analysis of BPSK OFDM systems with channel-independent residual CFO or CFO

   (a) AWGN channel with uniformly distributed CFO

(b) Frequency-flat Rayleigh fading channel with uniformly distributed CFO

(c) Frequency-selective Rayleigh fading channel with uniformly distributed CFO

(d) AWGN channel with Gaussian distributed residual CFO (under perfect power control [1])

(e) Frequency-flat Rayleigh fading channel with Gaussian distributed residual CFO (under perfect power control)

3. Performance analysis of BPSK OFDM systems with channel-dependent residual CFO

   (a) Frequency-flat Rayleigh fading channel with Gaussian distributed residual CFO (under no power control)

4. An alternative approach to BER analysis in frequency-flat/frequency-selective channels in BPSK OFDM systems

   (a) Frequency-flat Rayleigh fading channel

   (b) Frequency-selective Rayleigh fading channel

5. Performance analysis of 4-QAM OFDM systems with channel-independent residual CFO or CFO

   (a) AWGN channel with uniformly distributed CFO

   (b) Frequency-flat Rayleigh fading channel with uniformly distributed CFO

   (c) AWGN channel with Gaussian distributed residual CFO (under perfect power control

   (d) Frequency-flat Rayleigh fading channel with Gaussian distributed residual CFO (under perfect power control)

6. Performance analysis of 4-QAM OFDM systems with channel-dependent residual CFO

   (a) Frequency-flat Rayleigh fading channel with Gaussian distributed residual CFO (under no power control)

1.4 Scope and Limitations

This thesis study is subject to the following limitations.

1. Channel tap coefficients are assumed to be independent of each other and treat as circularly symmetric complex Gaussian random variables.

2. The ideal channel state information is assumed in some derivations.

3. A quasi-static channel model is assumed.

[1] Perfect power control makes certain combinations of channel parameters to be constant with the use of proper pilot symbol design. See section 3.2.4

4. For each sub channel over a given frame, a symbol spaced length L tap-delay-line model is assumed in the case of frequency selective fading.

5. Message symbols are assumed to be equi-probable for simulation purposes and in all analytical derivations.

6. In all analytical derivations, The CFO-induced, symbol-index-dependent phase shift is not considered. Every symbol is assumed to be phase synchronized so that the above phase shift is neglected by assuming perfect phase synchronization of all the symbols.

1.5 Outline of the Thesis

The rest of this thesis is structured and organized as follows. Chapter two, which is the literature review, discusses the basic mathematical description and the behaviours of OFDM systems, estimation techniques used in OFDM, and the literature related to the performance analysis in OFDM systems. In chapter three we present a detailed analysis of performance degradation due to CFO of BPSK OFDM systems and the corresponding simulation results and discussions. Chapter four consists of a detailed analysis of the performance degradation due to CFO of 4-QAM OFDM systems followed with the corresponding simulation results and discussions. Chapter five outlines the conclusion and recommendations for further studies.

CHAPTER 2

LITERATURE REVIEW

2.1 Mathematical Description of OFDM Systems

OFDM is a block modulation scheme where data symbols are transmitted in parallel by employing a large number of subcarriers. A block of N serial data symbols, each of duration T_s, is converted in to a block of N parallel data symbols, each of duration $T = NT_s$. Figure 2.1 shows how the OFDM modulated signal is generated. The serial input data symbols are given by $X_n = \{X_{n,0}, X_{n,1}, \cdots, X_{n,N-1}\}$. In the case of OFDM

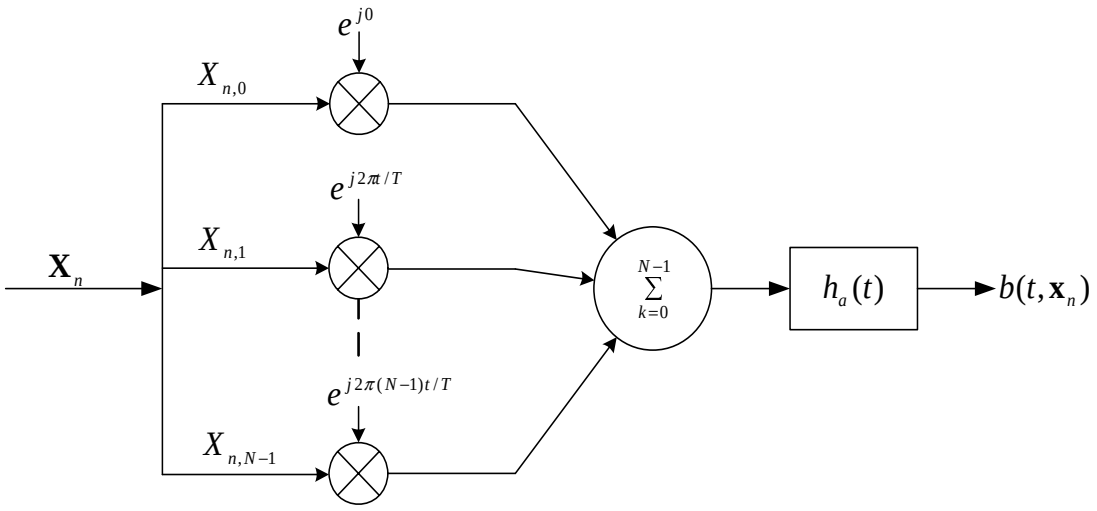

Figure 2.1: OFDM Modulation.

the set of orthogonal functions are chosen from the set $\phi_k(t) = \{\exp(j2\pi f_k t), \quad 0 \leq k \leq N-1\}$, where f_k is choose in such a way that the orthogonality of the subcarriers are preserved. So that, in order to preserve the orthogonality of the subcarriers everywhere $(t \in (-\infty, \infty))$, the subcarrier functions required to be windowed by the rectangular pulse u_T [1] and then the minimum separation of the subcarrier spacing is found to be $\frac{1}{T}$. Thus without loss of generality f_k can be replaced with $\frac{k}{T}$. The complex envelope of an OFDM system is given by (**Stüber**, 2001),

$$\tilde{s}(t) = A \sum_{n} b(t - nT, \boldsymbol{X}_n) \tag{2.1}$$

where

$$b(t, \boldsymbol{X}_n) = h_a(t) \sum_{k=0}^{N-1} X_{n,k} \exp\left\{ j \frac{2\pi(k - \frac{N-1}{2})t}{T} \right\} \tag{2.2}$$

where n represents the block index, and the amplitude shaping pulse $h_a(t) = u_T(t)$ as mentioned previously. The data symbols $X_{n,k}$ can be taken from any two dimensional

[1] This is unit step function, valued one from o to T and zero elsewhere

signal constellation. As we discussed in the previous chapter OFDM modulation and demodulation can be achieved in the discrete-domain by using DFT. Without loss of generality we can rewrite the complex envelope given by (2.1), after removing the block index n and the frequency offset term $\exp\{-j\frac{\pi(N-1)t}{T}\}$, as

$$\tilde{s}(t) = A\sum_{k=0}^{N-1} X_k \exp\left\{j\frac{2\pi kt}{NT_s}\right\}u_T(t) \tag{2.3}$$

Sampling the complex envelope at epochs $t = nT_s$ gives the sequence

$$x_n = \tilde{s}(nT_s) = A\sum_{k=0}^{N-1} X_k \exp\left\{j\frac{2\pi kn}{N}\right\} \tag{2.4}$$

so that the sequence $\boldsymbol{x} = \{x_0, x_1, \cdots, x_{N-1}\}$ represents the inverse discrete Fourier transform (IDFT) coefficients of the sequence $\boldsymbol{X} = \{X_0, X_1, \cdots, X_{N-1}\}$ with $A = \frac{1}{N}$. This IDFT coefficient vector $\boldsymbol{x}$ is used in the fast Fourier transform (FFT) based OFDM transmitter to generate the required analog signal to be transmitted.

2.2 Generic FFT Based OFDM Transmitter and Receiver

The IDFT operation given by (2.4) is a complex domain operation. That is, the regeneration of $\boldsymbol{X}$ at the receiver requires both the real and imaginary parts of the elements of $\boldsymbol{x}$. This necessitates the transmission of both the real and imaginary parts of each x_n's for successful symbol reception. However an additional bandwidth is not required as both can be up converted separately using orthogonal functions $\cos(2\pi f_c t)$, and $\sin(2\pi f_c t)$, as shown in Figure 2.2. Here Im and Re blocks correspond to extracting imaginary and real parts of the coming serial symbol stream $\boldsymbol{x}$ respectively and $s(t)$ is the transmitted signal. At the receiver, as shown in the Figure 2.2, descrete

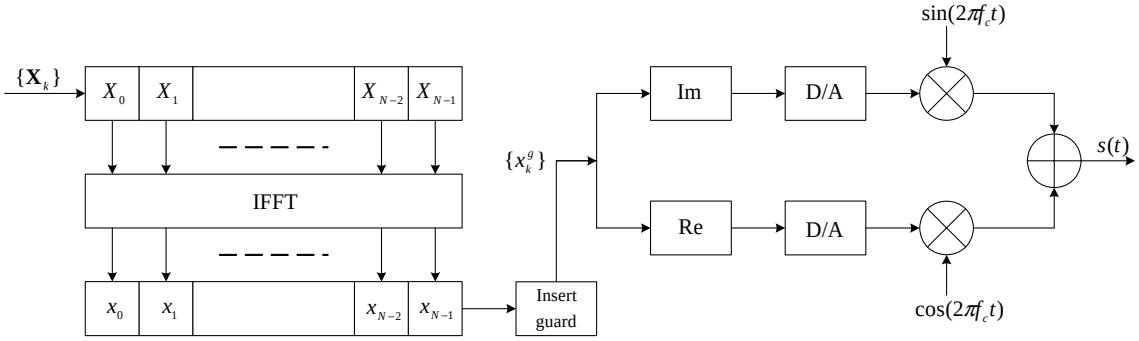

Figure 2.2: OFDM Transmitter.

complex sequence $\boldsymbol{z} = \{z_0, z_1, .., z_{N-1}\}$ is regenerated from the received signal $r(t)$ and successive operations yield $\boldsymbol{Z} = \{Z_0, Z_1, \cdots, Z_{N-1}\}$, which is the complex demodulated symbol sequence. In practice $r(t)$ is the distorted signal of $s(t)$ due to various factors such as addition of noise, influences of the channel responses. The following section briefly discusses some of OFDM's potentials in alleviating the effects arise due to undesired channel response and ISI.

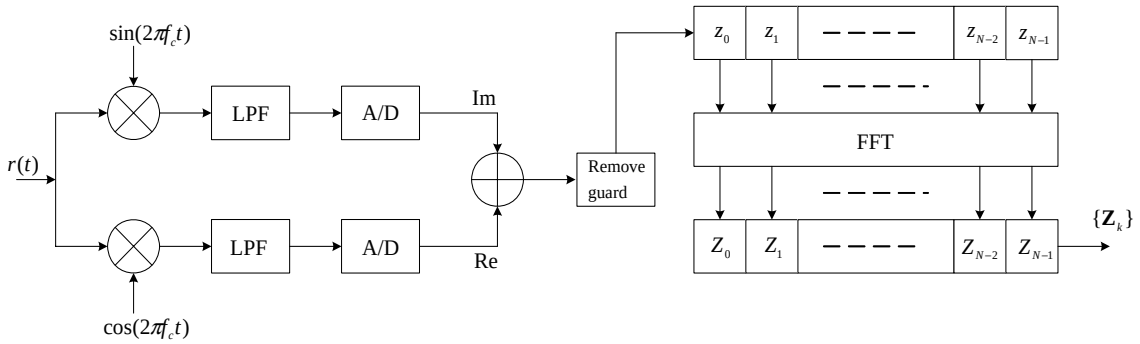

Figure 2.3: OFDM Receiver.

2.3 ISI mitigation and Influence of the Channel and Noise on OFDM Systems

As we mentioned in the previous chapter, because of the whole bandwidth occupied by an OFDM system is a composite of a number of overlapping, orthogonal and narrow subcarrier spectrums or sub-bands, the fading environment over each of these can be considered as relatively flat. If we consider the sub-band span over the whole OFDM spectrum, it would be a very small fraction. So that the equalization process would be more easier than in a typical serial data transmission system. That is, OFDM can transform a frequency-selective ISI channel into a frequency-flat channel, which is one of the main advantage of using OFDM. Considering a non-ideal band limited channel we can say that, data transmission with symbol duration T_s may introduce ISI as discussed in the previous chapter which demands receivers with complex equalization methods such as Viterbi. In what follows we discuss ISI vulnerability of OFDM, how the OFDM systems can mitigate the use of complex equalizers at the receiver and how the frequency-selective channel is partitioned in to several frequency-flat fading channels.

Assume that the channel is time-invariant over the period $t \in (0, T)$, hence $T_c >> T$ in the wideband channel, where T_c is the coherence time of the channel. So that we call the channel is quasi-static. Now let the channel be modelled by an L-tap delay line as shown in the Figure 2.4.

Here h_i's are the complex tap gains, x_k^g is the transmitted sequence of IDFT samples x_k with padded cyclic suffix, y_k^g is the corresponding channel out put, n_k^g is the additive white Gaussian noise samples, and z_k^g is the received signal samples at the receiver. To eliminate the ISI altogether at the expence of a small decrease in capacity, a guard interval of length $GT_s \geq LT_s$ can be inserted between suucessively modulated OFDM blocks. A guard interval consisting of a cyclic prefix or suffix of length G which is appended to the sequence $\boldsymbol{x}$ at the transmitter. Figure 1.2 and 2.2 show the location of where this is operation is performed and Figure 2.5 dipicts this process in detail. If a cyclic suffix is assumed, the transmitted sequence with guard interval can be denoted by (**Stüber**, 2001)

$$x_n^g = x_{(n)_N} = A \sum_{k=0}^{N-1} X_k \exp\left\{ j \frac{2\pi k n}{N} \right\} \quad n = 0, 1, \cdots, N + G - 1 \tag{2.5}$$

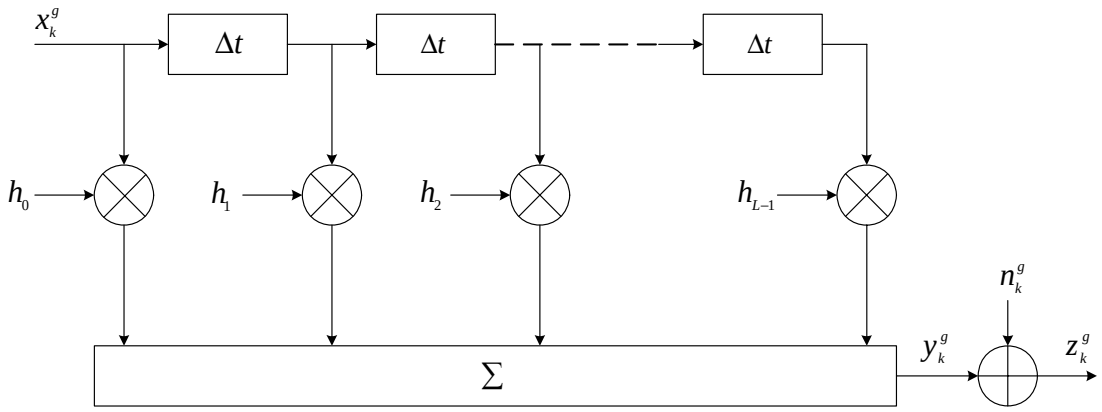

Figure 2.4: $\mathcal{L}$ - Tap Delay Line.

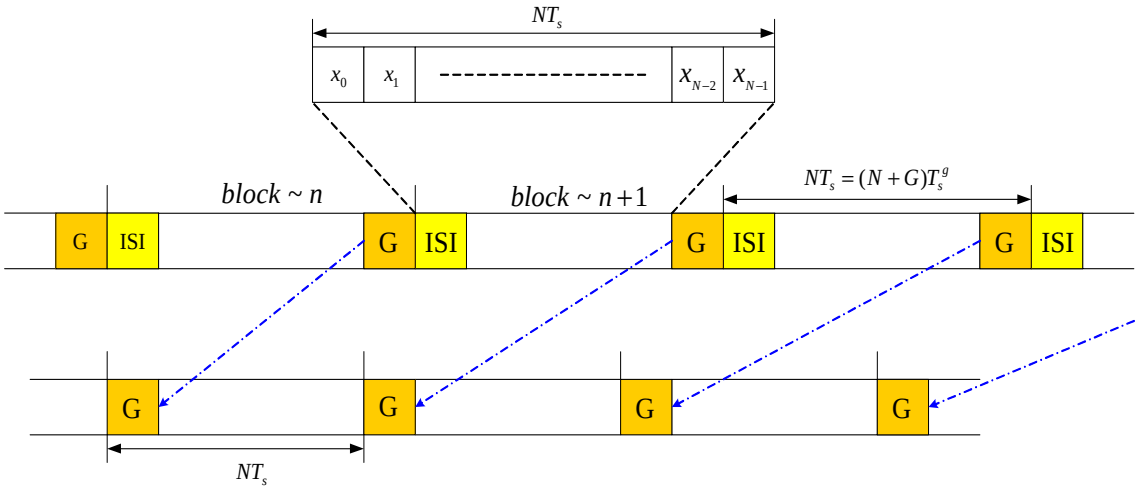

Figure 2.5: Insertion & removal of cyclic prefix.

where $(n)_N$ is the residue of n modulo N. When an OFDM block is received, the first $G \geq L$ samples are assumed to be corrupted by ISI from the previous block. The ISI is removed by replicating these samples with the cyclic suffix according to (**Stüber**, 2001),

$$z_n = z^g_{G+(n-G)_N} \quad n = 0, 1, \cdots, N-1. \tag{2.6}$$

Writing the complex envelope of sequence y_k^g, we have

$$y_k^g = \sum_{m=0}^{L-1} h_m x^g_{k-m} = \sum_{m=0}^{N-1} h_m x^g_{k-m} \tag{2.7}$$

and hence z_k^g can be written as

$$z_k^g = y_k^g + n_k^g = \sum_{m=0}^{N-1} h_m x^g_{k-m} + n_k^g. \tag{2.8}$$

The second equality in (2.7) is due to the fact that, practically $N >> L$ and hence

h_m's where $m > L-1$ are considered to be equal to zero. Using the equations (2.6) and (2.8) we can write z_k as,

$$z_k = \sum_{m=0}^{N-1} h_m x_{(k-m)_N} + n'_k; \quad k = 0, 1, \cdots, N-1. \tag{2.9}$$

Now, the first term of (2.9) can be considered as the circular convolution of the two sequences h_k's and x_k's. Here n'_k is again represents the AWGN noise samples. Thus, we have the received complex sequence of samples z_k as

$$z_k = h_k \odot x_k + n_k = IDFT(H_m X_m) + n'_k \tag{2.10}$$

where $\odot$ stands for the descrete convolution operation, H_m is the N-point DFT coefficients of the zero padded sequence $\{h_0, h_1, \cdots, h_{L-1}, 0, 0, \cdots, 0\}$, and X_m denotes the transmitted complex symbols. Now considering the DFT operation at the receiver we can obtain,

$$DFT\{z_k\} = Z_m = DFT\{IDFT(H_m X_m)\} + DFT\{n_k\} = H_m X_m + N_m \tag{2.11}$$

where Z_m and N_m are the N-point DFT coefficients of the sequences z_k and n_k respectively. This reveals the fact that, the OFDM's ability to correct a frequency-selective fading channel in to a frequency-flat fading channel with a multipath diversity gain given by H_m.

2.4 Impairments of OFDM

2.4.1 Carrier Frequency Offset(CFO) Due to Time Dispersion

As a consequence of low Doppler frequency the Rayleigh fading channel impulse response (CIR) taps fluctuate only slowly compared to the duration of the OFDM symbol, then a time-invariant CIR can be associated with each transmitted OFDM symbol. Naturally all of the Rayleigh-fading tap values are changing gradually over the duration of a number of consecutive OFDM symbols implying that the channel transfer function of a specific OFDM symbol is time-invariant for the duration of one OFDM symbol. But if the Raleigh-fading CIR taps are changing rapidly owing to high relative movement of the transmitter and the receiver leads high Doppler frequency to be introduced. This causes the OFDM system experiences ICI which can be interpreted in frequency domain as a frequency domain channel transfer function fluctuation during the reception of the OFDM symbol. However due to this scenario, the orthogonality of the sinc-shaped subchannel spectra may be destroyed by the channel inducing ICI.

2.4.2 Constant Carrier Frequency Offset

Carrier frequency errors result in a shift of the received signal's spectrum in the frequency domain which are created by factors such as differences in sampling clock frequencies of the transmitter and the receiver and clock jitter. If the frequency error is an integer multiple of the subcarrier spacing, then the subcarriers are still mutually

orthogonal, but the received data symbols,which map to the OFDM spectrum, are in the wrong position in the demodulated spectrum, resulting in a bit error rate (BER) of 0.5. if the CFO is not an integer multiple of the subcarrier spacing, then energy spilling over between the subcarriers, resulting in loss of their orthogonality causing ICI.

2.4.3 Phase Noise

Practical Oscillators suffer from phase noise which is a random perturbation of the phase of the steady sinusoidal waveform. Practical modulators or demodulators usually work either at base band or a convenient intermediate frequency(IF). As we must transmit our signal at some allocated radio frequency(RF) it follows that in practice the modulated signal must be shifted up to RF in the transmitter, and down from RF to IF or base band in the receiver. In practice to perform these up conversions and down conversions of the frequencies, we require the use of oscillators and those will introduce the phase noise, which will be imparted to the signal. Thus the phase noise contribution of both the transmitter and the receiver can be considered as an additional multiplicative effect of the radio channel. For OFDM schemes, multiplication of the received time domain signal with a time-varying channel transfer function is equivalent to convolving the frequency domain spectrum of the OFDM signal with the frequency domain channel transfer function.Usually the phase noise spectrum's bandwidth is wider than the subcarrier spacing resulting in energy spillage into other sub-channels and therefore in intersubcarrier interference. The effects of phase noise on OFDM systems have been intensively investigated in the literature (**Armada**, 1998; **Pollet et al.**, 1995; **Shentu et al.**,2003).

2.5 Impairments Mitigation Techniques in OFDM

In recent years numerous research contributions have appeared on the topic of the channel estimation techniques designed for employment in single user, single transmit antenna assisted OFDM systems, since the availability of an accurate channel transfer function estimate is essential for coherent symbol detection at an OFDM receiver. The techniques proposed in the literature can be classified as $pilot-assisted, decision-directed$(DD) and *blind* channel estimation methods.

2.5.1 Pilot Assisted Estimations

In this case s subset of the available subcarriers is dedicated to the transmission of specific pilot symbols known to the receiver. This is used at the cost of a reduction of the number of useful subcarriers available for data transmission. For instance a family of $pilot-assisted$ channel estimation techniques was investigated by Moose (**Moose**, 1994), T Schmidl and D Cox (**Schmidl and Cox**, 1997), Morelli and Mengali (**Morelli and Mengali**, 1999, 2000), Jing Lei and Tung-Sang (**Jing Lei and Tung-Sang**, 2004) and Minn (**Hlaing Minn et al.** [a] [b] [c], 2006; **Hlaing Minn and Xing S.**, 2005).

2.5.2 Decision-Directed Estimations

By contrast, in the context of decision-direct channel estimations the subcarrier data symbols are considered as pilots. In the absence of symbol errors and also depending on the rate of channel fluctuation (**Hanzo et al.**, 2003)., it was found that accurate channel estimates can be obtained, which are often better quality in terms of the estimator's mean square error (MSE). A comprehensive analysis of this technique was performed by authors such as Zhao and Häggman (**Zhao and Häggman**, 1996), Armstrong (**Zhao and Häggman**, 1996) and Edfors (**Edfors et al.**, 1998)

2.5.3 Blind Estimations

In the estimation techniques described above, the use of pilot symbols are unavoidable, On the contrary, there are no pilot symbols used in the blind channel estimation techniques and thus high spectral efficiency at the expense of high complexity, long delay, and/or less robust/accurate estimation is inevitable. The existing blind channel estimation techniques which are utilized in OFDM systems can be categorized in to two parts. The first one is known as statistical methods. The transmitted signal properties such as cyclostationarity which is due to the insertion of cyclic prefix are investigated in this method and those cyclic properties and the statistics of the received signal is manipulated in order to obtain the acceptable channel statistics (**Heath and Giannakis**, 1999). On the other hand the second part utilises a method which is known as subspace decomposition of the correlation matrix of the pre-DFT received blocks (**Cai and Akansu**, 2000; **Muquet et al.**, 2002). Furthermore, Van de Beek (**Van de Beek et al.**, 1997), Tureli (**Tureli et al.**, 1997), are also among the authors who studied the blind channel estimation techniques.

2.6 Performance Analysis of OFDM with CFO

A careful literature survey reveals two main performance analysis methods in OFDM systems. One approach is to treat ICI as a Gaussian process based on the central limit theorem (**Russell and Stüber**, 1995; **Rugini and Banelli**, 2005) which does not yield satisfactory results at high signal to noise ratios (SNR)(**Keller and Hanzo**, 2000). In contrast the approach due to Sathananthan and Tellambura (**Sathananthan and Tellambura**, 2001), uses the characteristic function and the Beaulieu series to derive exact bit error rate (BER) expressions for AWGN channel in the presence of ICI where the probability of error is always expressed conditioned on normalized frequency offset. Some authors (**Dharmawansa et al.** [a] [b], 2006) have derived exact BER/SER expressions for AWGN , frequency flat and frequency selective channels in the presence of fixed CFO error.

A number of methods have been proposed for estimation and compensation of frequency offset in OFDM systems. The technique proposed by Moose (**Moose**, 1994) contains an algorithm to estimate offset so that it may be removed prior to demodulation. T Schmidl and D Cox (**schmidl and Cox**, 1997) have presented a method for the rapid and robust synchronisation of OFDM signals, and acquisition is obtained upon the receipt of just one training sequence. Many authors have proposed the use of pilot symbols or tones (**Morelli and Mengali**, 1999, 2000; **Jing Lei and Tung-Sang**,

2004; **Hlaing Minnet al.** [a] [b] [c], 2006; **Hlaing Minn and Xing S.**, 2005) where these can be used either in continuous or packet based burst transmissions.

From the above various methods, the estimator proposed by Morelli and Mengali (**Morelli and Mengali**, 2000), which is a joint maximum likelihood (ML) estimate where the channel coefficients and the normalize frequency offset error is measured jointly, is used in some of our derivations.

CHAPTER 3

BER ANALYSIS OF BPSK OFDM SYSTEMS WITH RANDOM RESIDUAL FREQUENCY OFFSET

3.1 Introduction

In this chapter, we derive closed form bit error rate (BER) expressions for orthogonal frequency division multiplexing (OFDM) systems with residual carrier frequency offset (CFO). Most of the published work treat CFO as a nonrandom parameter. But in our study we consider it as a random parameter. The BER performance of binary phase shift keying (BPSK) OFDM system is analyzed in the cases of additive white Gaussian noise (AWGN), frequency-flat and frequency-selective Rayleigh fading channels. We further discuss how these expressions can be related to systems with practical estimators. The simulation results are provided to verify the accuracy of these error rate expressions.

3.2 System Model and Analysis

We consider a quasi-static channel and first present the signal model for a frequency-selective fading channel from which the models for AWGN and frequency-flat fading channels can easily be obtained. We consider an OFDM system with N subcarriers. The following notations were used in the subsequent derivations.

Notations: $(.)^H$, $(.)^T$, and $\overline{(.)}$ denote the Hermitian transpose, the transpose, and the conjugate operations, respectively. Furthermore $|z|$, $\angle z$, $\Re(z)$ and $\Im(z)$ denote the absolute value, angle, real and imaginary components of the complex quantity z, respectively. $\mathbf{1}_k$ and $\mathbf{0}_k$ represent the all-one column vector and the all-zero column vector of length k while $\boldsymbol{I}_k$ and $\mathbf{0}_{k\times n}$ denote the $k \times k$ identity matrix and the $k \times n$ all-zero matrix, respectively. The N-point unitary discrete Fourier transform (DFT) matrix is denoted by $\boldsymbol{F} = [\boldsymbol{f}_0 \boldsymbol{f}_1 \dots \boldsymbol{f}_{N-1}]$ where $\boldsymbol{f}_k = [1\ e^{-j2\pi k/N} \cdots e^{-j2\pi(N-1)/N}]^T/\sqrt{N}$. We define $\boldsymbol{F}_L = [\boldsymbol{f}_0 \boldsymbol{f}_1 \cdots \boldsymbol{f}_{L-1}]$. $[\boldsymbol{X}]_{k,n}$ represents the (k,n)th element of the matrix $\boldsymbol{X}$, and $diag\{\boldsymbol{x}\}$ denotes a diagonal matrix with diagonal elements defined by $\boldsymbol{x}$. $E\{.\}$ represents the statistical expectation and $Var\{.\}$ represents the statistical variance. The discrete-time received sequence after passing through a L-tap delay line can be written as (**Wang and Giannakis**, 2000),

$$\bar{x}(n) = \sum_{l=0}^{L-1} e^{j\frac{2\pi vn}{N}} h(l)\bar{u}(n-l) + \bar{n}(l). \tag{3.1}$$

The exponential term in this equation is introduced to reflect the influence of CFO v, $h(l)$ are tap coefficients (see Figure 2.4), $\bar{\boldsymbol{u}}(i)$ is time domain symbol sequence of i^{th} transmitted OFDM block after the cyclic prefix addition, and $\boldsymbol{n}_k^g$ is the sequence of AWGN noise samples. Note that the sequences $\boldsymbol{x}_k^g$, $\boldsymbol{n}_k^g$ and $\boldsymbol{z}_k^g$ in Figure 2.4 is equivalent to the sequences $\bar{\boldsymbol{u}}(i)$, $\bar{\boldsymbol{n}}(i)$ and $\bar{\boldsymbol{x}}(i)$ in (3.1) respectively. This received sequence equation (3.1) can be implemented as given in Figure 3.1 and it shows the OFDM signal transmission model with cyclic prefix (CP) which we use throughout our

derivations. As shown in Figure 3.1 $\boldsymbol{s}(i)$ represents the time domain symbol sequence of i^{th} transmitted OFDM block.

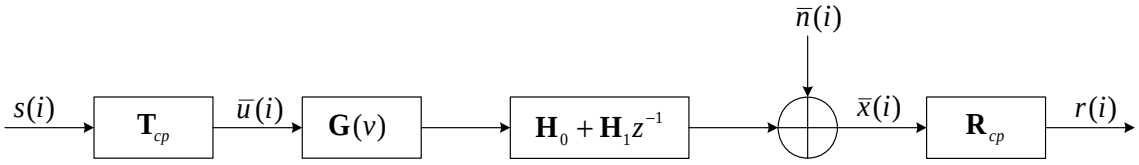

Figure 3.1: Mathematical Channel Model, (**Wang and Giannakis**, 2000)

In what follows, we briefly outline the main arguments and the procedures to derive the received signal vector in terms of system specific parameters (**Wang and Giannakis**, 2000). The transmitted OFDM block or signal vector in the time-domain is given by $\boldsymbol{s}(i)$. $\bar{\boldsymbol{u}}(i)$ is the signal vector after the addition of CP. This signal vector passes through the channel and AWGN noise samples $\bar{\boldsymbol{n}}(i)$ are added to give $\bar{\boldsymbol{x}}(i)$ and finally we have the received signal vector $\tilde{\boldsymbol{r}}(i)$ after the removal of cyclic prefix where,

$$\begin{aligned}
\boldsymbol{s}(i) &= [s_{iN}\ s_{iN+1}\ \cdots\ s_{iN+N-1}]^T \\
\bar{\boldsymbol{u}}(i) &= [\bar{u}_{iP}\ \bar{u}_{iP+1}\ \cdots\ \bar{u}_{iP+P-1}]^T \\
\bar{\boldsymbol{n}}(i) &= [\bar{n}_{iP}\ \bar{n}_{iP+1}\ \cdots\ \bar{n}_{iP+P-1}]^T \\
\bar{\boldsymbol{x}}(i) &= [\bar{x}_{iP}\ \bar{x}_{iP+1}\ \cdots\ \bar{x}_{iP+P-1}]^T \\
\tilde{\boldsymbol{r}}(i) &= [\tilde{r}_{iN}\ \tilde{r}_{iN+1}\ \cdots\ \tilde{r}_{iN+N-1}]^T
\end{aligned}$$

where P is the block length after the cyclic prefix was added and it is chosen such that $P >> L-1$ and N is the DFT length. Note that the i in afore mentioned signal vectors denote the block index of the transmitted/received signals. Let $L' = L-1$ for notational simplicity and $P = N + L'$ in order to get rid of the ISI. Now we can simply show that

$$\bar{\boldsymbol{x}}(i) = \boldsymbol{G}(v)\boldsymbol{H}_0\bar{\boldsymbol{u}}(i) + \boldsymbol{G}(v)\boldsymbol{H}_1\bar{\boldsymbol{u}}(i-1) + \bar{\boldsymbol{n}}(i) \tag{3.2}$$

where $\boldsymbol{G}(v) = diag[1\ e^{j2\pi v/N}\ \cdots\ e^{j2\pi(P-1)v/N}]$ and

$$\boldsymbol{H}_0 = \begin{bmatrix} h(0) & 0 & 0 & \dots & 0 \\ \vdots & h(0) & 0 & \dots & 0 \\ h(L') & \dots & \ddots & \dots & \vdots \\ \vdots & \ddots & \dots & \ddots & 0 \\ 0 & \dots & h(L') & \dots & h(0) \end{bmatrix}, \boldsymbol{H}_1 = \begin{bmatrix} 0 & \dots & h(L') & \dots & h(1) \\ \vdots & \ddots & 0 & \ddots & \vdots \\ 0 & \dots & \ddots & \dots & h(L') \\ \vdots & \vdots & \vdots & \ddots & \vdots \\ 0 & \dots & 0 & \dots & 0 \end{bmatrix}.$$

To obtain ISI-free blocks, the cyclic prefix or guard chips are added in the transmitted

block $\boldsymbol{s}(i)$ according to the relation $\bar{\boldsymbol{u}}(i) = \boldsymbol{T}_{cp}\boldsymbol{s}(i)$ where

$$\boldsymbol{T}_{cp} = \begin{bmatrix} \boldsymbol{0}_{L' \times (N-L')} & \boldsymbol{I}_{L'} \\ \boldsymbol{I}_{N-L'} & \boldsymbol{0}_{(N-L') \times L'} \\ \boldsymbol{0}_{L' \times (N-L')} & \boldsymbol{I}_{L'} \end{bmatrix}.$$

It is obvious from equation (3.2) that, i^{th} block $\bar{\boldsymbol{x}}(i)$ is made out of not only from the block $\bar{\boldsymbol{u}}(i)$ but also from the previous block $\bar{\boldsymbol{u}}(i-1)$. That is, careful observations reveal that, the first L' entries in the block $\bar{\boldsymbol{x}}(i)$ are deteriorated by the previous block. So, to remove the first L' entries in $\bar{\boldsymbol{x}}(i)$, the receive matrix $\boldsymbol{R}_{cp}$ is defined as $\boldsymbol{R}_{cp} = [\boldsymbol{0}_{N \times L'} \quad \boldsymbol{I}_N]$ and hence we have $\tilde{\boldsymbol{r}}(i) = \boldsymbol{R}_{cp}\bar{\boldsymbol{x}}(i)$. It can easily be shown that the matrix multiplication $\boldsymbol{R}_{cp}\boldsymbol{G}(v)\boldsymbol{H}_1\bar{\boldsymbol{u}}(i-1) = \boldsymbol{0}_{N \times 1}$ and thus using (3.2) we get the relation

$$\tilde{\boldsymbol{r}}(i) = \boldsymbol{R}_{cp}\boldsymbol{G}(v)\boldsymbol{H}_0\bar{\boldsymbol{u}}(i) + \boldsymbol{R}_{cp}\bar{\boldsymbol{n}}(i) = \boldsymbol{R}_{cp}\boldsymbol{G}(v)\boldsymbol{H}_0\boldsymbol{T}_{cp}\boldsymbol{s}(i) + \boldsymbol{R}_{cp}\bar{\boldsymbol{n}}(i). \tag{3.3}$$

After some matrix manipulations, (3.3) can easily be written as

$$\tilde{\boldsymbol{r}}(i) = \boldsymbol{G}_{\boldsymbol{T}}(v)\boldsymbol{R}_{cp}\boldsymbol{H}_0\boldsymbol{T}_{cp}\boldsymbol{s}(i) + \tilde{\boldsymbol{w}}(i) \tag{3.4}$$

where $\tilde{\boldsymbol{w}}(i) = \boldsymbol{R}_{cp}\bar{\boldsymbol{n}}(i)$ and $\boldsymbol{G}_{\boldsymbol{T}}(v)$ is a truncated version of $\boldsymbol{G}(v)$ such that

$$\boldsymbol{G}_{\boldsymbol{T}}(v) = diag[e^{j2\pi L'v/N} \; e^{j2\pi(L'+1)v/N} \; \cdots \; e^{j2\pi(P-1)v/N}].$$

Let the matrix multiplication $\boldsymbol{R}_{cp}\boldsymbol{H}_0\boldsymbol{T}_{cp} = \tilde{\boldsymbol{H}}$ where $\tilde{\boldsymbol{H}}$ constitute a circulant matrix (**Wang and Giannakis**, 2000) such that $\tilde{\boldsymbol{H}} = \sqrt{N}\boldsymbol{F}^H\boldsymbol{H}\boldsymbol{F}$, where $\boldsymbol{H} = diag\{\boldsymbol{F}_{\boldsymbol{L}}\boldsymbol{h}\} = diag[H_0 \; H_1 \; \cdots \; H_{N-1}]^T$ and $\boldsymbol{h} = [h_0 \; h_1 \; \cdots \; h_{L-1}]^T$. Note that we use h_m and $h(m)$; $m = 0, 1, \cdots, L-1$ interchangeably. So (3.4) gives us

$$\tilde{\boldsymbol{r}}(i) = \sqrt{N}\boldsymbol{G}_{\boldsymbol{T}}(v)\boldsymbol{F}^H\boldsymbol{H}\boldsymbol{F}\boldsymbol{s}(i) + \tilde{\boldsymbol{w}}(i). \tag{3.5}$$

Pre-multiplying (3.5) by the matrix $\boldsymbol{G}_c$ where $\boldsymbol{G}_{\boldsymbol{c}}(v) = e^{-j2\pi L'v/N}\boldsymbol{I}_N$ we can easily obtain the received symbol vector as

$$\boldsymbol{r}(i) = \sqrt{N}\boldsymbol{\Gamma}(v)\boldsymbol{F}^H\boldsymbol{H}\boldsymbol{c}(i) + \boldsymbol{w}(i) \tag{3.6}$$

where $\boldsymbol{\Gamma}(v) = \boldsymbol{G}_{\boldsymbol{c}}(v)\boldsymbol{G}_{\boldsymbol{T}}(v) = diag[1 \; e^{j2\pi v/N} \; \cdots \; e^{j2\pi(N-1)v/N}]$, $\boldsymbol{w}(i) = \boldsymbol{G}_{\boldsymbol{c}}\tilde{\boldsymbol{w}}(i)$, $\boldsymbol{r}(i) = \boldsymbol{G}_{\boldsymbol{c}}\tilde{\boldsymbol{r}}(i)$ and $\boldsymbol{c}(i) = [c_{iN} \; c_{iN+1} \; \cdots \; c_{iN+N-1}]^T$ denote the frequency domain symbol sequence in the i^{th} OFDM block transmitted, which is simply obtained by the unitary DFT operation $\boldsymbol{c}(i) = \boldsymbol{F}\boldsymbol{s}(i)$. Without loss of generality, the block index i can be dropped and hence in the presence of a normalized (by the subcarrier spacing) CFO v, the time-domain received signal vector after the cyclic prefix removal can be given by (**Hlaing Minn et al.** [a], 2006)

$$\boldsymbol{r} = \boldsymbol{\Gamma}(v)\boldsymbol{S}\boldsymbol{h} + \boldsymbol{w} = \sqrt{N}\boldsymbol{\Gamma}(v)\boldsymbol{F}^H\boldsymbol{H}\boldsymbol{c} + \boldsymbol{w} \tag{3.7}$$

where $\boldsymbol{r} = [r_0 \; r_1 \; \cdots \; r_{N-1}]^T$, $\boldsymbol{c} = [c_0 \; c_1 \; \cdots \; c_{N-1}]^T$, $\boldsymbol{w} = [w_0 \; w_1 \; \cdots \; w_{N-1}]^T$, and $\boldsymbol{h} = [h_0 \; h_1 \; \cdots \; h_{L-1}]^T$ as defined before. Here $\{h_n\}$ denote the channel impulse

response (CIR) coefficients and L is the number of CIR taps. Assume that $\{w_n\}$ are independent and identically distributed zero-mean circularly-symmetric complex Gaussian noise samples each having a variance of σ^2 per dimension. $\{c_n\}$ are independent equi-probable frequency domain transmit symbols and the corresponding time-domain signal vector is given by $\boldsymbol{s}=[s_0\ s_1\ \cdots\ s_{N-1}]^T=\boldsymbol{F}^H\boldsymbol{c}$. The time-domain signal matrix in (3.7) is defined by $[\boldsymbol{S}]_{k,n}=s_{k-n}$, $0\le k\le N-1$, $0\le n\le L-1$ with $s_k=\frac{1}{\sqrt{N}}\sum_{n=0}^{N-1}c_n e^{j2\pi nk/N}$ for $k=L-1,\cdots,N-1$.

Let $\hat{v}$ be the estimated frequency offset, $\hat{v}=v+v_\Delta$ where we denote the residual CFO as v_Δ. After the frequency offset compensation and DFT, the received signal vector is given by

$$\boldsymbol{R}=\sqrt{N}\boldsymbol{F}\boldsymbol{\Gamma}^H(v_\Delta)\boldsymbol{F}^H\boldsymbol{H}\boldsymbol{c}+\boldsymbol{w'} \tag{3.8}$$

where $\boldsymbol{R}=[R_0\ R_1\ \cdots\ R_{N-1}]^T$, $\boldsymbol{w'}=[n'_0\ n'_1\ \cdots\ n'_{N-1}]^T$ and $\boldsymbol{w'}$ has the same statistical properties as $\boldsymbol{w}$. Note that if we use CFO instead of residual CFO (see section 3.3.1) we can still use the equation given by (3.8) by replacing v_Δ by v in further processing. Evaluating the (k,l)th element of $\boldsymbol{F}\boldsymbol{\Gamma}^H(v_\Delta)\boldsymbol{F}^H$ and denoting it as I'_{l-k} (ICI coefficient), we can obtain

$$I'_{l-k}=\frac{1}{N}\sum_{n=0}^{N-1}\exp\left\{j2\pi(l-k-v_\Delta)\frac{n}{N}\right\};\quad k,l=0,1,\cdots,N-1. \tag{3.9}$$

Then, using (3.8) we can express the received symbol on the kth subcarrier as

$$R_k=\sqrt{N}c_kH_kI'_0+\sqrt{N}\sum_{l=0,l\neq k}^{N-1}c_lH_lI'_{l-k}+n'_k;\ k=0,1,\cdots,N-1. \tag{3.10}$$

The expressions for AWGN and frequency-flat fading channels can be derived using (3.10).

Next, we analyze the ICI coefficients. With the assumption that the CFO or residual CFO is very small and using the approximation $\exp(jx)\simeq(1+jx)$ for small real-valued x, we get

$$I'_{l-k}\approx\frac{1}{N}\sum_{n=0}^{N-1}\exp\left\{j2\pi(l-k)\frac{n}{N}\right\}-jv_\Delta\frac{2\pi}{N^2}\sum_{n=0}^{N-1}n.\exp\left\{j2\pi(l-k)\frac{n}{N}\right\}. \tag{3.11}$$

With some trigonometric manipulations (**Gradshteyn and Ryzhik**, 1980), we can further reduce the above relation. It is obvious that (3.11) can be written as

$$I'_{l-k}\approx\delta_{lk}-jv_\Delta\frac{2\pi}{N^2}\sum_{n=0}^{N-1}\Big[n\cos(\beta n)+jn\sin(\beta n)\Big]$$

where δ_{lk} is Kronecker delta and $\beta=\frac{2\pi(l-k)}{N}$. When $l\neq k$ we can write $\sum_{n=0}^{N-1}n\cos(\beta n)=\left[\frac{N\sin\left(\frac{2N-1}{2}\beta\right)}{2\sin\left(\frac{\beta}{2}\right)}-\frac{1-\cos(N\beta)}{4\sin^2\left(\frac{\beta}{2}\right)}\right]$ (**Gradshteyn and Ryzhik**, 1980). With some trigonometric manipulation, we can derive

$$\sum_{n=0}^{N-1}n\cos(\beta n)=-\frac{N}{2}.$$

Similarly, when $l \neq k$, we can write $\sum_{n=0}^{N-1} n \sin(\beta n) = \left[\frac{\sin(N\beta)}{4\sin^2\left(\frac{\beta}{2}\right)} - \frac{N\cos\left(\frac{2N-1}{2}\beta\right)}{2\sin\left(\frac{\beta}{2}\right)}\right]$ (**Gradshteyn and Ryzhik**, 1980), which yields

$$\sum_{n=0}^{N-1} n \sin(\beta n) = -\frac{N}{2}\cot\left[\frac{\pi(l-k)}{N}\right].$$

When $l = k$ and $\beta = 0$, we have $\sum_{n=0}^{N-1} n\cos(\beta n) = \frac{N(N-1)}{2}$ and $\sum_{n=0}^{N-1} n\sin(\beta n) = 0$. Using the above results we can deduce (3.12).

$$I'_{l-k} \approx \begin{cases} \frac{\pi v_\Delta}{N}[-\cot(\frac{\pi(l-k)}{N}) + j] & , \text{ if } l \neq k \\ 1 - j\pi\frac{N-1}{N}v_\Delta & , \text{ if } l = k \end{cases} \tag{3.12}$$

We will use (3.12) in our BER analysis since the residual CFO is typically small in practical OFDM systems.

3.3 Performance Analysis with Channel-Independent CFO or Residual CFO for BPSK OFDM Systems

We can treat the CFO or residual CFO and the CIR as independent parameters under some conditions. An example is a scenario where the transceivers use highly-stable crystal oscillators and skip CFO estimation to save energy. Under this condition, we may consider the CFO to be uniformly distributed and independent of the channel. Another example is a scenario where the receiver performs CFO estimation and compensation in a system with perfect power control. Under this scenario the residual CFO can be treated as a Gaussian random variable independent of the channel.

For the channel-independent CFO or residual CFO case, BER is obtained by solving the following integral

$$P_b(\xi) = \int\int P_b(\xi|v_\Delta, \boldsymbol{h})\, f_v(v_\Delta) f(\boldsymbol{h}) dv_\Delta d\boldsymbol{h} \tag{3.13}$$

where $f_v(v_\Delta)$ and $f(\boldsymbol{h})$ are pdfs of CFO or residual CFO and channel respectively, and $P_b(\xi|v_\Delta, \boldsymbol{h})$ represents the BER conditioned on v_Δ and $\boldsymbol{h}$. In the following sections 3.3.1-3, we consider the uniformly distributed CFO, while in the section 3.3.4 we address a Gaussian-distributed residual CFO. These can be considered as a generalization of what is discussed in (**Dharmawansa et al.** [a] [b], 2006).

3.3.1 AWGN Channel with Uniformly Distributed CFO

For the AWGN channel, we have $\boldsymbol{H} = \frac{1}{\sqrt{N}}\boldsymbol{I}_N$. We can simply deduce from (3.10) that

$$R_k = c_k I'_0 + \sum_{l=0, l\neq k}^{N-1} c_l I'_{l-k} + n'_k; \quad k = 0, 1, \cdots, N-1. \tag{3.14}$$

Now consider the following trigonometric identity used by (**Dharmawansa et al.** [b], 2006), which is useful in our main derivations.

$$\prod_{k=0}^{M-1} \cos(\phi_k) \equiv \frac{1}{2^{M-1}} \sum_{k=1}^{2^{M-1}} \cos\left(\mathbf{\Phi}^T \mathbf{e}_k\right) \tag{3.15}$$

where $\mathbf{\Phi} = (\phi_0\ \phi_1\ \ldots\ \phi_{M-1})^T$, $\mathbf{e}_k$ is the kth column of a more general $M \times 2^{M-1}$ matrix $\mathbf{E}_M$. The kth row of $\mathbf{E}_M^T$ is essentially the binary representation of the number $2^M - k$, where zeros are replaced with -1s. For example the matrix $\mathbf{E}_M$ for the values of $M = 3$ can be written as

$$\mathbf{E}_3 = \begin{pmatrix} 1 & 1 & 1 & 1 \\ 1 & 1 & -1 & -1 \\ 1 & -1 & 1 & -1 \end{pmatrix}$$

$c_k \in \{-1, 1\}$ for BPSK modulation and considering the first subcarrier with the transmitted symbol 1, we can derive the characteristic function (CHF) of the real part of R_o, $\Re(R_0)$ as (**Sathananthan and Tellambura**, 2001)

$$\phi_{\Re(R_0)}(\omega) = \exp\left\{ j\omega\Re(I_0') - \frac{\omega^2\sigma^2}{2} \right\} \prod_{l=1}^{N-1} \cos\{\omega\Re(I_l')\} \tag{3.16}$$

and using (3.15) we can obtain

$$\phi_{\Re(R_0)}(\omega) = \frac{1}{2^{N-1}} \exp\left\{ j\omega - \frac{\omega^2\sigma^2}{2} \right\} \sum_{l=1}^{2^{N-2}} \cos\{\omega v_\Delta \boldsymbol{P}^T \boldsymbol{e}_k\} \tag{3.17}$$

where $\boldsymbol{P}=\frac{\pi}{N}[\cot(\frac{\pi}{N})\ \cot(\frac{2\pi}{N})\ \ldots\ \cot(\frac{(N-1)\pi}{N})]^T$ and $j = \sqrt{-1}$. Using the Euler's relationship $\cos(x) = \frac{\exp(jx)+\exp(-jx)}{2}$ and after rearranging the terms of (3.17) we get (**Dharmawansa et al.** [b], 2006)

$$\phi_{\Re(R_0)}(\omega) = \frac{1}{2^{N-1}} \sum_{k=1}^{2^{N-2}} \left(\exp\left\{ j\omega\theta_k - \frac{\omega^2\sigma^2}{2} \right\} + \exp\left\{ j\omega\beta_k - \frac{\omega^2\sigma^2}{2} \right\} \right) \tag{3.18}$$

where $\theta_k=(1 + a_k v_\Delta)$, $\beta_k=(1 - a_k v_\Delta)$ and $a_k=\boldsymbol{P}^T \boldsymbol{e}_k$. A careful observation of (3.18) reveals that it is the CHF of a mixture of Gaussian density functions. For BPSK signal constellation, an error occurs if $\Re(R_0) < 0$ and thus the conditional bit error probability can be written as

$$P_b(\xi|v_\Delta) = \frac{1}{2^{N-1}} \sum_{k=1}^{2^{N-2}} \left\{ Q\left(\sqrt{2\gamma}(1 + a_k v_\Delta)\right) + Q\left(\sqrt{2\gamma}(1 - a_k v_\Delta)\right) \right\}. \tag{3.19}$$

Then with the assumption that the CFO v_Δ is uniformly distributed over the region $[-b, b]$, the BER can be written as

$$P_b(\xi) = \frac{1}{2b}\int_{-b}^{b} P_b(\xi|v_\Delta)\, dv_\Delta \tag{3.20}$$

After some algebraic manipulations, (3.19) gives the bit error probability as (see Appendix)

$$P_b(\xi) = \frac{1}{b2^{N-1}}\Bigg[\sum_{k=1,a_k\neq 0}^{2^{N-2}}\left\{\frac{\lambda_k}{a_k}Q\left(\sqrt{2\gamma}\lambda_k\right) - \frac{\mu_k}{a_k}Q\left(\sqrt{2\gamma}\mu_k\right)\right\} + \sum_{k=1,a_k\neq 0}^{2^{N-2}}\left\{\frac{-1}{2\sqrt{\pi\gamma}a_k}e^{-\gamma\lambda_k^2} + \frac{1}{2\sqrt{\pi\gamma}a_k}e^{-\gamma\mu_k^2}\right\} + \sum_{k=1,a_k=0}^{2^{N-2}}\left\{2b\; Q\left(\sqrt{2\gamma}\right)\right\}\Bigg] \tag{3.21}$$

where λ_k=$(1 + a_k b)$, μ_k=$(1 - a_k b)$, γ=$\frac{E_b}{N_0}$=$\frac{1}{2\sigma^2}$ and $Q(x)$ is the Gaussian Q-function.

3.3.2 Frequency-flat Rayleigh Fading Channel with Uniformly Distributed CFO

In the frequency-flat Rayleigh fading case, we have $\boldsymbol{H} = (\alpha/\sqrt{N})\boldsymbol{I}_N$ where α is a zero-mean circularly-symmetric complex Gaussian random variable with a variance of σ_R^2 per dimension which is taken to be 0.5. Then, (3.10) becomes

$$R_k = \alpha c_k I'_0 + \alpha\sum_{l=0,l\neq k}^{N-1} c_l I'_{l-k} + n'_k; \quad k = 0, 1, .., N-1. \tag{3.22}$$

Simply compensating for the phase information of complex Gaussian random variable α, we can obtain the following relation from (3.22).

$$e^{-j\angle\alpha}R_0 = |\alpha|c_0 I'_0 + |\alpha|\sum_{l=1}^{N-1} c_l I'_l + e^{-j\angle\alpha}n'_0 \tag{3.23}$$

Now we can write the CHF of the term $\Re(e^{-j\angle\alpha}R_0)$ and following the same set of arguments as in the section 3.2.1, we can obtain the conditional bit error probability as

$$P_b(\xi|v_\Delta,\alpha) = \frac{1}{2^{N-1}}\sum_{k=1}^{2^{N-2}}\left\{Q\left(\sqrt{2\gamma}|\alpha|(1 + a_k v_\Delta)\right) + Q\left(\sqrt{2\gamma}|\alpha|(1 - a_k v_\Delta)\right)\right\}. \tag{3.24}$$

Note that $|\alpha|$ is Rayleigh distributed with its pdf given by

$$f(|\alpha|) = \frac{|\alpha|}{\sigma_R^2}\exp\left(-\frac{|\alpha|^2}{2\sigma_R^2}\right). \tag{3.25}$$

Performing the integration $\frac{1}{2b}\int_{-b}^{b} P_b\left(\xi|v_\Delta,\alpha\right) dv_\Delta$ we can get the conditional BER $P_b\left(\xi|\alpha\right)$ as (see **Appendix**)

$$P_b\left(\xi|\alpha\right) = \frac{1}{b2^{N-1}}\Bigg[\sum_{k=1,a_k\neq 0}^{2^{N-2}}\left\{\frac{\lambda_k}{a_k}Q\left(\sqrt{2\gamma}\lambda_k|\alpha|\right) - \frac{\mu_k}{a_k}Q\left(\sqrt{2\gamma}\mu_k|\alpha|\right)\right\} + \sum_{k=1,a_k\neq 0}^{2^{N-2}}\left\{\frac{-1}{2\sqrt{\pi\gamma}a_k|\alpha|}e^{-\gamma\lambda_k^2|\alpha|^2} + \frac{1}{2\sqrt{\pi\gamma}a_k|\alpha|}e^{-\gamma\mu_k^2|\alpha|^2}\right\} + \sum_{k=1,a_k=0}^{2^{N-2}}\left\{2b\ Q\left(\sqrt{2\gamma}|\alpha|\right)\right\}\Bigg] \quad (3.26)$$

Now the dependence of α on the conditional BER $P_b\left(\xi|\alpha\right)$ is removed by averaging $P_b\left(\xi|\alpha\right)$ with the pdf of $|\alpha|$, Thus, after some algebraic manipulations, we obtain the bit error probability as (**Marvin and Alouini**, 2005)

$$P_b\left(\xi\right) = \frac{1}{2^{N-1}b}\sum_{k=1,a_k\neq 0}^{2^{N-2}}\Bigg\{\frac{\lambda_k}{2a_k}\left(1-\lambda_k\sqrt{\frac{2\gamma\sigma_R^2}{1+2\gamma\sigma_R^2\lambda_k^2}}\right) - \frac{\mu_k}{2a_k}\left(1-\mu_k\sqrt{\frac{2\gamma\sigma_R^2}{1+2\gamma\sigma_R^2\mu_k^2}}\right) + \frac{-1}{2\sqrt{2\gamma\sigma_R^2}a_k\sqrt{1+2\gamma\lambda_k^2\sigma_R^2}} + \frac{1}{2\sqrt{2\gamma\sigma_R^2}a_k\sqrt{1+2\gamma\mu_k^2\sigma_R^2}}\Bigg\} + \frac{1}{2^{N-1}}\sum_{k=1,a_k=0}^{2^{N-2}}\left(1-\sqrt{\frac{2\sigma_R^2\gamma}{1+2\sigma_R^2\gamma}}\right). \quad (3.27)$$

3.3.3 Frequency-selective Rayleigh Fading Channel with Uniformly Distributed CFO

In the case of a frequency-selective channel, the received symbol on the kth subcarrier is given by (3.10). We assume an L sample-spaced tap-delay-line model for the channel with the time domain tap coefficients $\{h_l,\ l=0,1,\cdots,L-1\}$ modeled as zero mean circularly symmetric complex Gaussian random variables having variances $\{\sigma_{h_l}^2\}$ with uniform power delay profile and $\sigma_{h_0}^2+\sigma_{h_1}^2+\cdots+\sigma_{h_{L-1}}^2=1$. Furthermore, the channel is assumed to be quasi-static. Define $\alpha_l=\sqrt{N}H_l$ for $l=0,1,\cdots,N-1$, $\boldsymbol{\alpha}=[\alpha_1\ \alpha_2\ \cdots\ \alpha_{N-1}]^T$. One very important factor that we should pay our attention is the correlation between different α_i's. and $\sigma_n^2=|\alpha_0|^2\sigma^2$. In the frequency-selective Rayleigh fading case, we have $\boldsymbol{H}=\frac{1}{\sqrt{N}}diag[(\alpha_0,\alpha_1,\cdots,\alpha_{N-1})]$. Then, using (3.10) and considering the first subcarrier with the transmitted symbol 1, we can write

$$R_0 = \alpha_0 I_0' + \sum_{l=1}^{N-1} c_l I_l' \alpha_l + n_0' \quad (3.28)$$

Now taking the real part of (3.28) after the phase of the complex random variable α_0 is compensated, yields

$$\Re(\bar{\alpha_0}R_0) = |\alpha_0|^2 + \sum_{l=1}^{N-1} \Re(c_l I'_l \alpha_l \bar{\alpha_0}) + \Re(\bar{\alpha_0} n'_0) \tag{3.29}$$

where $\bar{\alpha_0} = |\alpha_0| e^{-j\angle\alpha_0}$. Hence, we can obtain the conditional CHF of the random variable $\Re(\bar{\alpha_0}R_0)|\alpha_0, \boldsymbol{\alpha}, v_\Delta$ as (**Dharmawansa et al.** [b], 2006)

$$\phi_{\Re(\bar{\alpha_0}R_0)|\alpha_0,\boldsymbol{\alpha},v_\Delta}(\omega) = \frac{1}{2^{N-1}} \sum_{k=1}^{2^{N-2}} \left(\exp\left\{ j\omega\theta_k - \frac{\omega^2\sigma_n^2}{2} \right\} + \exp\left\{ j\omega\beta_k - \frac{\omega^2\sigma_n^2}{2} \right\} \right) \tag{3.30}$$

where $\theta_k = (|\alpha_0|^2 + \Re\left(\overline{\alpha}_0 \boldsymbol{P}_k^T \boldsymbol{\alpha}\right))$, $\beta_k = (|\alpha_0|^2 - \Re\left(\overline{\alpha}_0 \boldsymbol{P}_k^T \boldsymbol{\alpha}\right))$, and $\boldsymbol{P}_k = diag(I'_1, ..., I'_{N-1})\boldsymbol{e}_k$. Hence the conditional BER can be obtained as

$$P_b\left(\xi|\alpha_0, \boldsymbol{\alpha}, v_\Delta\right) = \frac{1}{2^{N-1}} \sum_{k=1}^{2^{N-2}} \left\{ Q\left(\frac{|\alpha_0|^2 + \Re\left(\overline{\alpha}_0 \boldsymbol{P}_k^T \boldsymbol{\alpha}\right)}{\sigma_n} \right) + Q\left(\frac{|\alpha_0|^2 - \Re\left(\overline{\alpha}_0 \boldsymbol{P}_k^T \boldsymbol{\alpha}\right)}{\sigma_n} \right) \right\} \tag{3.31}$$

Let us define $z_k = \Re\left(\overline{\alpha}_0 \boldsymbol{P}_k^T \boldsymbol{\alpha}\right)$. It is obvious that the conditional random variable $z_k|\alpha_0, v_\Delta$ is Gaussian with mean and variance to be determined.

Now we have the following (**Kay** , 1993) :

$$\begin{aligned} \boldsymbol{C} = E\left\{ \left(\alpha_0\ \boldsymbol{\alpha}^T\right)^T \left(\overline{\alpha}_0\ \boldsymbol{\alpha}^H\right) \right\} &= \begin{pmatrix} c_{\alpha_0\alpha_0} & \boldsymbol{C}^H_{\boldsymbol{\alpha}\alpha_0} \\ \boldsymbol{C}_{\boldsymbol{\alpha}\alpha_0} & \boldsymbol{C}_{\boldsymbol{\alpha}\boldsymbol{\alpha}} \end{pmatrix} = N\boldsymbol{F}_L \boldsymbol{C}_h \boldsymbol{F}_L^H \\ E\{\boldsymbol{\alpha}|\alpha_0\} &= \alpha_0 c^{-1}_{\alpha_0\alpha_0} \boldsymbol{C}_{\boldsymbol{\alpha}\alpha_0} \\ \boldsymbol{C}_{\boldsymbol{\alpha}|\alpha_0} &= \boldsymbol{C}_{\boldsymbol{\alpha}\boldsymbol{\alpha}} - c^{-1}_{\alpha_0\alpha_0} \boldsymbol{C}_{\boldsymbol{\alpha}\alpha_0} \boldsymbol{C}^H_{\boldsymbol{\alpha}\alpha_0} \end{aligned} \tag{3.32}$$

where $\boldsymbol{C_h}$ is the $L \times L$ time-domain channel covariance matrix, $c_{\alpha_0\alpha_m} = E\{\alpha_0\overline{\alpha}_m\}$, $0 \leq l, m \leq N-1$, and $\boldsymbol{C}_{\boldsymbol{\alpha}\alpha_0} = [c_{\alpha_1\alpha_0} c_{\alpha_2\alpha_0} \dots c_{\alpha_{N-1}\alpha_0}]^T$. Then we can derive the conditional mean and variance of the random variable z_k (**Dharmawansa et al.** [b], 2006; **Miller K. S.**, 1969) as,

$$E\left\{z_k|\alpha_0, v_\Delta\right\} = \frac{\pi v_\Delta}{N} |\alpha_0|^2 c^{-1}_{\alpha_0\alpha_0} \Re\left(\boldsymbol{V}_k^T \boldsymbol{C}_{\boldsymbol{\alpha}\alpha_0}\right) = \frac{\pi v_\Delta}{N} |\alpha_0|^2 a'_k \tag{3.33}$$

and

$$\mathrm{Var}\left(z_k|\alpha_0, v_\Delta\right) = \frac{\pi^2 {v_\Delta}^2}{2N^2} |\alpha_0|^2 \boldsymbol{V}_k^T \boldsymbol{C}_{\boldsymbol{\alpha}|\alpha_0} \overline{\boldsymbol{V}}_k = \frac{\pi^2 {v_\Delta}^2}{2N^2} |\alpha_0|^2 b_k \tag{3.34}$$

where $a'_k = c^{-1}_{\alpha_0\alpha_0} \Re\left(\boldsymbol{V}_k^T \boldsymbol{C}_{\boldsymbol{\alpha}\alpha_0}\right)$ and $b_k = \boldsymbol{V}_k^T \boldsymbol{C}_{\boldsymbol{\alpha}|\alpha_0} \overline{\boldsymbol{V}}_k$. Here $\boldsymbol{P}_k$ and $\boldsymbol{V}_k$ are related by $\boldsymbol{P}_k = \frac{\pi v_\Delta}{N} \boldsymbol{V}_k$. Rearranging the random variables inside the Q function in (3.31) yields (**Dharmawansa et al.** [b], 2006)

$$P_b\left(\xi|\alpha_0, \boldsymbol{\alpha}, v_\Delta\right) = \frac{1}{2^{N-1}} \sum_{k=1}^{2^{N-2}} \left\{ Q\left(\mu_{+k} + \lambda_k Y_k\right) + Q\left(\mu_{-k} - \lambda_k Y_k\right) \right\} \tag{3.35}$$

where $Y_k \sim \mathcal{N}(0,1)$, $\mu_{+k} = \frac{|\alpha_0|}{\sigma}\left(1 + \frac{\pi}{N} v_\Delta a'_k\right)$, $\mu_{-k} = \frac{|\alpha_0|}{\sigma}\left(1 - \frac{\pi}{N} v_\Delta a'_k\right)$ and $\lambda_k = \sqrt{\frac{b_k}{2\sigma^2}} \frac{\pi v_\Delta}{N}$.

Then the BER conditioned on α and v_Δ can be obtained as (**Verdu**, 1998)

$$P_b\left(\xi|\alpha_0, v_\Delta\right)=\frac{1}{2^{N-1}}\sum_{k=1}^{2^{N-2}}\left\{Q\left(\frac{\mu_{+k}}{\sqrt{1+\lambda_k^2}}\right)+Q\left(\frac{\mu_{-k}}{\sqrt{1+\lambda_k^2}}\right)\right\}. \tag{3.36}$$

Further manipulating and averaging (3.36) with respect to α_0 give

$$P_b\left(\xi|v_\Delta\right)=\frac{1}{2}-\frac{1}{2^N}\sum_{k=1}^{2^{N-2}}\left\{\frac{M\left(1+m_k v_\Delta\right)}{2\sqrt{p+q_k v_\Delta+r_k {v_\Delta}^2}}-\frac{M\left(1-m_k v_\Delta\right)}{2\sqrt{p-q_k v_\Delta+r_k {v_\Delta}^2}}\right\} \tag{3.37}$$

where $M=\sqrt{2\sigma_R^2\gamma}$, γ is the same as defined before, $m_k=\frac{\pi}{N}{a'}_k$, $p=(1+2\sigma_R^2\gamma)$, $q_k=\frac{4\sigma_R^2\gamma\pi{a'}_k}{N}$, and $r_k=\frac{\pi^2}{N^2}\gamma(b_k+{a'}_k^2)$. Now removing the dependence of random CFO in (3.37), we obtain the BER as

$$P_b\left(\xi\right)=\frac{1}{b2^N}\sum_{k=1,m_k\neq 0}^{2^{N-2}}\left[2b-[A]_{-b}^{b}-[B]_{-b}^{b}\right]+\frac{1}{b2^N}\sum_{k=1,m_k=0}^{2^{N-2}}\left[2b-\left[\frac{M}{\sqrt{r_k}}\sinh^{-1}\left(\frac{v_\Delta}{L'}\right)\right]_{-b}^{b}\right] \tag{3.38}$$

where

$$A=\frac{Mm_k}{2r_k}\left[\sqrt{p+q_k v_\Delta+r_k {v_\Delta}^2}\right]+\left[\frac{M(1-\frac{q_k m_k}{2r_k})}{2\sqrt{r_k}}\sinh^{-1}\left(\frac{v_\Delta}{L'}+\frac{q_k}{2r_k L'}\right)\right] \tag{3.39}$$

$$B=\frac{-Mm_k}{2r_k}\left[\sqrt{p-q_k v_\Delta+r_k {v_\Delta}^2}\right]+\left[\frac{M(1-\frac{q_k m_k}{2r_k})}{2\sqrt{r_k}}\sinh^{-1}\left(\frac{v_\Delta}{L'}-\frac{q_k}{2r_k L'}\right)\right] \tag{3.40}$$

$$L'=\sqrt{\frac{p}{q_k}-\frac{q_k^2}{4r_k^2}} \tag{3.41}$$

and L' is always positive.

3.3.4 AWGN and Frequency-flat Rayleigh Fading Channels with Perfect Power Control

To evaluate (3.13), we should know the pdf of v_Δ. As far as maximum likelihood (ML) estimators are concerned, we can observe the nature of the pdf of v_Δ conditioned on the channel. Asymptotic properties of the maximum likelihood estimate (MLE) indicate that if the regularity conditions are satisfied, then the MLE of the unknown parameter $\boldsymbol{\theta}$ is asymptotically Gaussian-distributed as

$$\hat{\boldsymbol{\theta}}\sim\mathcal{N}(\boldsymbol{\theta},\boldsymbol{I}^{-1}(\boldsymbol{\theta})) \tag{3.42}$$

where $\boldsymbol{I}(\boldsymbol{\theta})$ is the Fisher information matrix evaluated at the true value of the unknown parameter (**Kay**, 1993). Hence, it is reasonable to use the conditional pdf of v_Δ as

$$f_v(v_\Delta|\boldsymbol{h})=\mathcal{N}(0,\boldsymbol{I}^{-1}(\boldsymbol{\theta}))=\mathcal{N}(0,CRB|_{\boldsymbol{h}}) \tag{3.43}$$

where $CRB|_{\boldsymbol{h}}$ is the Cramer-Rao lower bound conditioned on the CIR. For a training signal consisting of $(P+1)$ identical parts, each having L samples, and if the CFO estimation is based on PL samples (excluding the cyclic prefix with L samples), the CRB conditioned on the channel $\boldsymbol{h}$ is given by (**Hlaing Minn et al.** [b], 2006)

$$CRB|_{\boldsymbol{h}} = \frac{3N^3\sigma^2}{\pi^2 PL^3(P^2-1)\boldsymbol{h}^H\boldsymbol{S}^H\boldsymbol{S}\boldsymbol{h}}. \tag{3.44}$$

For most of the training designs (**Hlaing Minn et al.** [b] [c], 2006), we have $\boldsymbol{S}^H\boldsymbol{S}=E_{av}\boldsymbol{I}$, and hence

$$CRB|_{\boldsymbol{h}} = \frac{3N^3\sigma^2}{\pi^2 PL^3(P^2-1)E_{av}\boldsymbol{h}^H\boldsymbol{h}}. \tag{3.45}$$

If we assume perfect power control, we can say $\boldsymbol{h}^H\boldsymbol{S}^H\boldsymbol{S}\boldsymbol{h}$ is constant and hence for a receiver with a CFO estimator, the pdf of the residual CFO can be considered as a Gaussian pdf independent of the channel resulting simply $f(v_\Delta|\boldsymbol{h}) = f(v_\Delta)$. If we consider arbitrary training signal samples $\{s_k\}$, the CRB for v derived for the ML joint estimation of v and $\boldsymbol{h}$ is given by (**Morelli and Mengali**, 2000)

$$CRB|_{\boldsymbol{h}} = \frac{N^2\sigma^2}{4\pi^2\boldsymbol{h}^H\boldsymbol{S}^H\boldsymbol{\Lambda}(\boldsymbol{I}_N-\boldsymbol{B})\boldsymbol{\Lambda}\boldsymbol{S}\boldsymbol{h}} \tag{3.46}$$

where

$$\boldsymbol{B}=\boldsymbol{S}(\boldsymbol{S}^H\boldsymbol{S})^{-1}\boldsymbol{S}^H \tag{3.47}$$

and $\boldsymbol{\Lambda} = diag\{0,1,\ldots,N-1\}$. In our derivation, we use (3.46).

3.3.4.1 AWGN channel

For the AWGN channel, (3.13) simply reduces to a single integral evaluation as we do not have to average with respect to the channel. The signal model for AWGN channel can be obtained from (3.7) as

$$\boldsymbol{r} = \boldsymbol{\Gamma}(\boldsymbol{v})\boldsymbol{s} + \boldsymbol{w} \tag{3.48}$$

where $\boldsymbol{s} = [s_0 s_1 \ldots s_{N-1}]^T$ is the training signal vector. The CRB of the CFO estimation for the signal model in (3.48) is given by (**Hlaing Minn and Xing**, 2005)

$$CRB = \frac{N^2\sigma^2}{4\pi^2\boldsymbol{s}^H\boldsymbol{\Lambda}^2\boldsymbol{s}} = \Omega \tag{3.49}$$

Then we evaluate the BER as

$$P_b(\xi) = \frac{1}{2^{N-1}}\sum_{k=1}^{2^{N-2}} 2E\left\{Q\left(\sqrt{2\gamma}+\sqrt{2\gamma}a_k v_\Delta\right)\right\} \tag{3.50}$$

where the expectation is with respect to v_Δ. Re-arranging the random variables inside the Q function in (3.50) gives

$$P_b(\xi) = \frac{1}{2^{N-1}} \sum_{k=1}^{2^{N-2}} 2E\left\{ Q\left(\sqrt{2\gamma} + \sqrt{2\gamma\Omega} a_k \frac{v_\Delta}{\sqrt{\Omega}} \right) \right\}$$
$$= \sum_{k=1}^{2^{N-2}} 2E\left\{ Q\left(\sqrt{2\gamma} + \sqrt{2\gamma\Omega} a_k X \right) \right\} \quad (3.51)$$

where $X \sim \mathcal{N}(0,1)$. Then, using (**Verdu**, 1998) we obtain the BER as

$$P_b(\xi) = \frac{1}{2^{N-1}} \sum_{k=1}^{2^{N-2}} 2Q\left(\sqrt{\frac{2\gamma}{1+2\gamma\Omega a_k^2}} \right). \quad (3.52)$$

3.3.4.2 Frequency-flat Rayleigh fading channel

When the frequency-flat fading channel is considered, (3.46) can be reduced to

$$CRB|_\alpha = \frac{2N^2}{\left(8\pi^2 \boldsymbol{s}^H \boldsymbol{\Lambda}(\boldsymbol{I}_N - \boldsymbol{B})\boldsymbol{\Lambda}\boldsymbol{s}\right)} \frac{\sigma^2}{|\alpha_0|^2} = \frac{\Lambda}{|\alpha_0|^2} \quad (3.53)$$

where α_0 is complex Gaussian with variance σ_R^2 per dimension. Under the perfect power control, we can equivalently consider that $|\alpha_0|^2$ is constant while fixing $\boldsymbol{s}$. Thus we assume the pdf of residual CFO to be

$$f_v(v_\Delta|\alpha_0) = f_v(v_\Delta) = \mathcal{N}(0,\Lambda). \quad (3.54)$$

Using (3.13), (3.24), (3.54) and the same mathematical arguments used in deriving (3.52), we obtain the BER for the frequency-flat Rayleigh fading channel under perfect power control as

$$P_b(\xi) = \frac{1}{2^{N-1}} \sum_{k=1}^{2^{N-2}} 2Q\left(\sqrt{\frac{2\gamma}{1+2\gamma\Lambda a_k^2}} \right). \quad (3.55)$$

3.4 Performance Analysis with Channel-Dependent Residual CFO for BPSK OFDM Systems

For the channel-dependent residual CFO scenario, the bit error probability can be expressed as

$$P_b(\xi) = \int\int P_b(\xi|v_\Delta, \boldsymbol{h})\, f_v(v_\Delta|\boldsymbol{h}) f(\boldsymbol{h}) dv_\Delta d\boldsymbol{h}. \quad (3.56)$$

The closed form solution to (3.56) for the frequency-flat Rayleigh fading channel is presented in the following. However, solving the above problem for the frequency-selective case appears to be intractable and hence we adopt an alternative approach for the frequency-selective case which will be presented in Section 3.4.

3.4.1 Frequency-flat Rayleigh Fading Channel

The variance of the conditional Gaussian random variable $v_\Delta|\alpha$ for the frequency-flat Rayleigh fading channel is given by (3.53) for the MLE estimator (**Morelli and Mengali**, 2000) we use in this paper. Manipulating the equations (3.24), (3.25), (3.43), (3.53) and (3.56) yields the BER conditioned on α as

$$P_b\left(\xi|\alpha\right) = \frac{1}{2^{N-1}} \sum_{k=1}^{2^{N-2}} 2Q\left(\frac{\mu}{\sqrt{1+\eta_k^2}}\right) \tag{3.57}$$

where $\mu{=}\sqrt{2\gamma}|\alpha|$ and $\eta_k{=}\sqrt{2\gamma\lambda}a_k$. Further averaging with respect to the Rayleigh variable $|\alpha|$, we obtain the BER as

$$P_b\left(\xi\right) = \frac{1}{2^{N-1}} \sum_{k=1}^{2^{N-2}} \left\{1 - \sqrt{\frac{\frac{2\gamma}{1+2\gamma\lambda a_k^2}\sigma_R^2}{1+\frac{2\gamma}{1+2\gamma\lambda a_k^2}\sigma_R^2}}\right\}. \tag{3.58}$$

3.5 An Alternative Approach to BER Analysis in Frequency-Selective Channel for BPSK OFDM Systems

Since the BER calculation in the frequency-selective fading channel seems to be intractable using the procedure used earlier, we propose the following method with relaxed assumptions and we denote this as an *analysis with relaxed assumptions*. In this analytical development we assume that v_Δ and $\boldsymbol{h}$ are independent and v_Δ is uniformly distributed. Even though these assumptions are not entirely justifiable for the MLE1 estimator in (**Morelli and Mengali**, 2000), analytical results so obtained closely match with the simulation results. We applied this approach for both frequency-flat and frequency-selective scenarios as follows.

3.5.1 Frequency-Flat Rayleigh Fading Channel

The estimates of v and h_0 can be written as (**Morelli and Mengali**, 2000)

$$\hat{v} = \arg_{\tilde{v}} \max\left\{\boldsymbol{r}^H\Gamma(\tilde{v})\boldsymbol{B}\Gamma^H(\tilde{v})\boldsymbol{r}\right\} \tag{3.59}$$

$$\hat{h_0} = (\boldsymbol{S}^H\boldsymbol{S})^{-1}\boldsymbol{S}^H\Gamma^H(\hat{v})\boldsymbol{r} \tag{3.60}$$

where $\boldsymbol{B}$ is given in (3.47) and $\boldsymbol{S} = \boldsymbol{s}$ since $L = 1$. Substituting (3.7) into (3.60) and using the approximation $e^{\frac{-j2\pi l v_\Delta}{N}} \simeq (1 - \frac{j2\pi l v_\Delta}{N})$ for very small v_Δ, we can find an approximation for $\hat{h}_0$ as

$$\hat{h_0} \approx \left[1 - \frac{j2\pi v_\Delta}{N^2}\sum_{k=1}^{N-1} k|s_k|^2\right]h_0 + w_{new} \tag{3.61}$$

where w_{new} is a zero-mean circularly-symmetric complex Gaussian variable with variance $\frac{\sigma^2}{N}$ per dimension. For simplicity we define $q{=}\left[1 - \frac{j2\pi v_\Delta}{N^2}\sum_{k=1}^{N-1} k|s_k|^2\right]$. From

(3.22) we have

$$R_0 = \Big[1 + \frac{\pi v_\Delta}{N} \sum_{l=1}^{N-1} c_l a_l\Big] h_0 + n_0'; l = 0, 1, \cdots, N-1 \tag{3.62}$$

where we have used $I_l'=\frac{\pi v_\Delta}{N} a_l$ for $l \neq 0$ and $I_0'=1$ under very small v_Δ assumption, and $c_0=1$. Let $p=\Big[1+\frac{\pi v_\Delta}{N}\sum_{l=1}^{N-1} c_l a_l\Big]$. Now we want to find $Pr\Big[\Re(\frac{R_0}{\hat{h}_0})<0|c_0=1\Big]$. Applying the results from Appendix B of (**Proakis**, 1995), we obtain

$$P_b(\xi|v_\Delta, c_1, c_2, ...c_{N-1}) = 1 - \frac{v_2}{v_1 + v_2} \tag{3.63}$$

where

$$v_1=\sqrt{w^2 + \frac{1}{4(\mu_{\hat{h_0}\hat{h_0}}\mu_{R_0R_0} - |\mu_{\hat{h_0}R_0}|^2)}} - w \tag{3.64}$$

$$v_2=\sqrt{w^2 + \frac{1}{4(\mu_{\hat{h_0}\hat{h_0}}\mu_{R_0R_0} - |\mu_{\hat{h_0}R_0}|^2)}} + w \tag{3.65}$$

$$w = \frac{\mu_{\hat{h_0}R_0} + \mu^*_{\hat{h_0}R_0}}{4(\mu_{\hat{h_0}\hat{h_0}}\mu_{R_0R_0} - |\mu_{\hat{h_0}R_0}|^2)} \tag{3.66}$$

and $\mu_{XY}=\frac{1}{2}E\Big[(X - E\{X\})(Y - E\{Y\})^*\Big]$. Furthermore, we can derive the following statistical relationships conditioned on v_Δ and all data symbols ($c_1\ c_2\ \cdots\ c_{N-1}$): $\mu_{R_0R_0} = \frac{|p|^2\sigma^2_{h_0}}{2} + \sigma^2$, $\mu_{\hat{h_0}\hat{h_0}} = \frac{|q|^2\sigma^2_{h_0}}{2} + \frac{\sigma^2}{N}$, $\mu_{\hat{h_0}R_0} = \frac{p^*q\sigma^2_{h_0}}{2}$, $\mu_{R_0\hat{h_0}} = \frac{q^*p\sigma^2_{h_0}}{2}$, $w = \frac{\Re(pq^*)}{2\sigma^2(\frac{|p|^2}{N}+|q|^2+\frac{2\sigma^2}{N\sigma^2_{h_0}})}$ where $\sigma^2_{h_0}$ is the variance of h_0. After some algebraic manipulations, we can show that

$$P_b(\xi|v_\Delta, c_1, c_2, ...c_{N-1}) = \frac{1}{2} - \frac{a_1' + b_1' v_\Delta + c_1' {v_\Delta}^2}{\sqrt{a_3' + b_3' v_\Delta + c_3' {v_\Delta}^2 + d_3' {v_\Delta}^3 + e_3' {v_\Delta}^4}} \tag{3.67}$$

where $a_1'=0.5$, $b_1'=-\frac{\pi a}{2N}$, $c_1'=-\frac{\pi^2 g\lambda}{N^3}$, $a_2'=\frac{2\sigma^2}{\sigma^2_{h_0}}(1+\frac{1}{N}+\frac{2\sigma^2}{N\sigma^2_{h_0}})$, $b_2'=-\frac{2\sigma^2}{\sigma^2_{h_0}}(\frac{2\pi a}{N^2})$, $c_2'=\frac{2\sigma^2}{\sigma^2_{h_0}}\Big[\frac{\pi^2}{N^3}(a^2+g^2)+\frac{4\pi^2\lambda^2}{N^4}\Big]$, $a_3'=(4{a_1'}^2+a_2')$, $b_3'=(8a_1'b_1'+b_2')$, $c_3'=\Big[4({b_1'}^2+2a_1'c_1')+c_2'\Big]$, $d_3'=8b_1'c_1'$, $e_3'=4{c_1'}^2$, $a=\sum_{l=1}^{N-1} c_l \cot(\frac{\pi l}{N})$, $\lambda=\sum_{k=1}^{N-1} k|s_k|^2$ and $g=\sum_{l=1}^{N-1} c_l$. Averaging (3.67) over all possible data symbol combinations and v_Δ yields

$$P_b(\xi) = \frac{1}{2^{N-1}} \sum_{c_1\in\{-1,1\}} \sum_{c_2\in\{-1,1\}} ..... \sum_{c_{N-1}\in\{-1,1\}} \frac{1}{2b} \times \left[\int_{-b}^{b} \frac{1}{2} - \frac{a_1' + b_1' v_\Delta + c_1' {v_\Delta}^2}{\sqrt{a_3' + b_3' v_\Delta + c_3' {v_\Delta}^2 + d_3' {v_\Delta}^3 + e_3' {v_\Delta}^4}} dv_\Delta\right]. \tag{3.68}$$

In general, closed form solution does not exist for (3.68). But a closed form solution can be derived ignoring the terms with coefficients d_3' and e_3'. This is really the case when $v_\Delta \to 0$. However, at high SNR this is not acceptable and we have to use numerical integration techniques given in software packages such as MatLab and Mathematica.

3.5.2 Frequency-selective Rayleigh fading channel

The estimate of the channel co-efficient vector is obtained as (**Morelli and Mengali**, 2000)

$$\hat{\boldsymbol{h}} = \left[\hat{h}_0\ \hat{h}_1\ \cdots\ \hat{h}_{L-1}\right]^T = (\boldsymbol{S}^H\boldsymbol{S})^{-1}\boldsymbol{S}^H\boldsymbol{\Gamma}^H(\hat{v})\boldsymbol{r} \tag{3.69}$$

where $\boldsymbol{S}$, $\boldsymbol{\Gamma}$, $\boldsymbol{r}$ are as defined in (3.7) and $\hat{v}$ is the estimate of the normalized CFO. Denoting $\hat{\boldsymbol{\alpha}}_e$ as the N-point DFT of $\hat{\boldsymbol{h}}$, i.e., $\hat{\boldsymbol{\alpha}}_e = [\hat{\alpha}_0\ \hat{\alpha}_1\ \ldots\ \hat{\alpha}_{N-1}]^T = \sqrt{N}\boldsymbol{F}_L\hat{\boldsymbol{h}}$, and after some matrix manipulations, we obtain

$$\hat{\alpha}_0 = \frac{1}{\sqrt{N}}\mathbf{1}_N^T\boldsymbol{A}_e\boldsymbol{F}^H\left[\alpha_0\ \boldsymbol{\alpha}^T\right]^T + \mathbf{1}_N^T\boldsymbol{B}_e\boldsymbol{w} \tag{3.70}$$

where

$$\begin{aligned}
\boldsymbol{A}_e &= \begin{pmatrix} \boldsymbol{A} & \mathbf{0}_{L\times(N-L)} \\ \mathbf{0}_{(N-L)\times L} & \mathbf{0}_{(N-L)\times(N-L)} \end{pmatrix} \\
\boldsymbol{B_e} &= [((\boldsymbol{S}^H\boldsymbol{S})^{-1}\boldsymbol{S}^H)^T, \mathbf{0}_{N\times(N-L)}]^T \\
\boldsymbol{A} &= (\boldsymbol{S}^H\boldsymbol{S})^{-1}\boldsymbol{S}^H\boldsymbol{\Gamma}^H(v_\Delta)\boldsymbol{S}.
\end{aligned}$$

From (14) when $c_0 = 1$, we can deduce that

$$R_0 = \alpha_0 + a\boldsymbol{P}^T\boldsymbol{\alpha} + n_0{}' \tag{3.71}$$

where $a{=}\frac{\pi v_\Delta}{N}$, $\boldsymbol{P}{=}[c_1a_1\ c_2a_2\ \cdots\ c_{N-1}a_{N-1}]^T$, and we have used (3.12) with $I_l'{=}aa_l$ for $l \neq 0$ and $I_0'{=}1$ under very small v_Δ assumption. Here we apply the same procedure which was used to derive (3.68). The random variables $\hat{\alpha}_0$ and R_0 conditioned on v_Δ and the data sequence $[c_1\ c_2\ \cdots\ c_{N-1}]^T$ are complex Gaussian. Hence we can derive the following statistics:

$$\mu_{R_0R_0} = A_1 + B_1v_\Delta + C_1v_\Delta^2 \tag{3.72}$$

where $A_1{=}\frac{1}{2}\left[2\sigma^2 + c_{\alpha_0\alpha_0}\right]$, $B_1{=}\frac{\pi}{N}\Re\big(\boldsymbol{C}^H_{\boldsymbol{\alpha}\alpha_0}\overline{\boldsymbol{P}}\big)$, $C_1{=}\frac{\pi^2}{2N^2}\left[\boldsymbol{P}^T\boldsymbol{C}_{\boldsymbol{\alpha}\boldsymbol{\alpha}}\overline{\boldsymbol{P}}\right]$, and

$$\mu_{\hat{\alpha_0}\hat{\alpha_0}} = \frac{1}{2}\left[\mathbf{1}_N^T\boldsymbol{A}_e\boldsymbol{C}_h\boldsymbol{A}_e^H\mathbf{1}_{\boldsymbol{N}} + 2\sigma^2\mathbf{1}_N^T\boldsymbol{B}_e\boldsymbol{B}_e^H\mathbf{1}_{\boldsymbol{N}}\right]. \tag{3.73}$$

With the assumption of independent and identically distributed (iid) time-domain channel coefficients and using the relation $e^{\frac{-j2\pi lv_\Delta}{N}}{\approx}(1{-}\frac{j2\pi lv_\Delta}{N})$ for very small v_Δ values, we can deduce from (3.73) that

$$\mu_{\hat{\alpha_0}\hat{\alpha_0}} = \frac{1}{2} + \frac{r}{2} + \frac{1}{2L}\mu v_\Delta^2 \tag{3.74}$$

where $r{=}2\sigma^2\mathbf{1}_N^T\boldsymbol{B}_e\boldsymbol{B}_e^H\mathbf{1}_{\boldsymbol{N}}$, $\mu{=}\sum_{i=0}^{L-1}|\sum_{m=0}^{L-1}q_{mi}|^2$, $q_{mi}{=}\frac{2\pi j}{N}\sum_{k=0}^{N-1}k\big[(\boldsymbol{S}^H\boldsymbol{S})^{-1}\boldsymbol{S}^H\big]_{m,k}\times\big[\boldsymbol{S}\big]_{k,i}$. Let us denote $A_2{=}\frac{1}{2}$, $B_2{=}\frac{r}{2}$, $C_2{=}\frac{1}{2L}\mu$, $\boldsymbol{D}{=}\left[c_{\alpha_0\alpha_0}\ \boldsymbol{C}^H_{\boldsymbol{\alpha}\alpha_0}\right]$, and $\boldsymbol{E}{=}\boldsymbol{P}^T\left[\boldsymbol{C}_{\boldsymbol{\alpha}\alpha_0}\ \boldsymbol{C}_{\boldsymbol{\alpha}\boldsymbol{\alpha}}\right]$ for the notational simplicity. Then

$$\mu_{R_0\hat{\alpha_0}} = A_3 + B_3v_\Delta + C_3v_\Delta^2 \tag{3.75}$$

where $A_3{=}\frac{\lambda_2}{2\sqrt{N}}$, $B_3{=}\big[\frac{\mu_2}{2\sqrt{N}}+\frac{\pi\lambda_3}{2\sqrt{N}N}\big]$, $C_3{=}\frac{\pi\mu_3}{2\sqrt{N}N}$, $\lambda_2{=}\sum_{m=0}^{L-1}[\boldsymbol{DF}]_{1,m}$, $\mu_2{=}\sum_{m=0}^{L-1}\big(b_m^*\times[\boldsymbol{DF}]_{1,m}\big)$, $\lambda_3{=}\sum_{m=0}^{L-1}[\boldsymbol{EF}]_{1,m}$, $\mu_3{=}\sum_{m=0}^{L-1}\big([\boldsymbol{EF}]_{1,m}\,b_m^*\big)$ and $b_m{=}\sum_{k=0}^{L-1}q_{km}$. Furthermore, we can derive the corresponding w in (3.66) as

$$w=\frac{\mu_{\hat{\alpha_0}R_0}+\mu^*_{\hat{\alpha_0}R_0}}{4(\mu_{\hat{\alpha_0}\hat{\alpha_0}}\mu_{R_0R_0}-|\mu_{\hat{\alpha_0}R_0}|^2)}=\frac{K}{M} \tag{3.76}$$

where $K{=}(g_1{+}g_2v_\Delta{+}g_3v_\Delta^2)$, $M{=}4\big[(A_1A_2{+}A_1B_2{-}|A_3|^2){+}(B_1A_2{+}B_1B_2{-}2\Re(A_3B_3^*))v_\Delta + (A_1C_2+C_1B_2+C_1A_2-|B_3|^2-2\Re(A_3C_3^*))v_\Delta^2+(B_1C_2-2\Re(B_3C_3))v_\Delta^3+(C_1C_2-|C_3|^2)v_\Delta^4\big]$, $g_1{=}2\Re(A_3)$, $g_2{=}2\Re(B_3)$ and $g_3{=}2\Re(C_3)$. After some algebraic manipulations and using (3.73)-(3.76), we can come up with the following conditional error probability (**Proakis**, 1995)

$$P_b(\xi|v_\Delta,c_1,c_2,...c_{N-1})=\frac{1}{2}-\frac{g_1+g_2v_\Delta+g_3{v_\Delta}^2}{2\sqrt{g_4+g_5v_\Delta+g_6{v_\Delta}^2+g_7{v_\Delta}^3+g_8{v_\Delta}^4}} \tag{3.77}$$

where $g_4{=}g_1^2+4(A_1A_2+A_1B_2-|A_3|^2)$, $g_5{=}2g_1g_2+4(B_1A_2+B_1B_2-2\Re(A_3B_3^*))$, $g_6{=}(g_2^2+2g_1g_3)+4(A_1C_2+C_1B_2+C_1A_2-|B_3|^2-2\Re(A_3C_3^*))$, $g_7{=}2g_2g_3+4(B_1C_2-2\Re(B_3C_3))$, and $g_8{=}g_3^2{+}4(C_1C_2{-}|C_3|^2)$. Averaging (3.77) over all possible data symbol combinations and v_Δ yields

$$P_b(\xi)=\frac{1}{2^{N-1}}\sum_{c_1\in\{-1,1\}}\sum_{c_2\in\{-1,1\}}.....\sum_{c_{N-1}\in\{-1,1\}}\frac{1}{2b}\times \left[\int_{-b}^{b}\frac{1}{2}-\frac{g_1+g_2v_\Delta+g_3{v_\Delta}^2}{2\sqrt{g_4+g_5v_\Delta+g_6{v_\Delta}^2+g_7{v_\Delta}^3+g_8{v_\Delta}^4}}dv_\Delta\right]. \tag{3.78}$$

We have to use numerical integration techniques as no closed form solutions are available to evaluate (3.78).

3.6 Results and Discussion

3.6.1 Channel-Independent CFO or Residual CFO for BPSK OFDM Systems

Considering the case where CFO is uniformly distributed and independent of the channel we simulate an OFDM system with $N = 8$ and the normalized CFO is uniformly distributed over $[-b, b]$ with $b = 0.05$ and $b = 0.1$.

Fig. 3.2 shows the BER performance in the AWGN channel. The simulation results for $b = 0.05$ case match well with those calculated in (3.21) but there is a slight discrepancy for $b = 0.1$ case especially at low BER values (say below 10^{-3}). This discrepancy is simply due to the fact that the small CFO assumption in the analytical development is not closely matched by the uniform CFO with $b = 0.1$, and at these low BER values the CFO has a more dominant effect on BER than the noise does. As long as the CFO is considerably small, our analytical expressions yield highly accurate results. The results for frequency-flat and frequency-selective Rayleigh fading channels

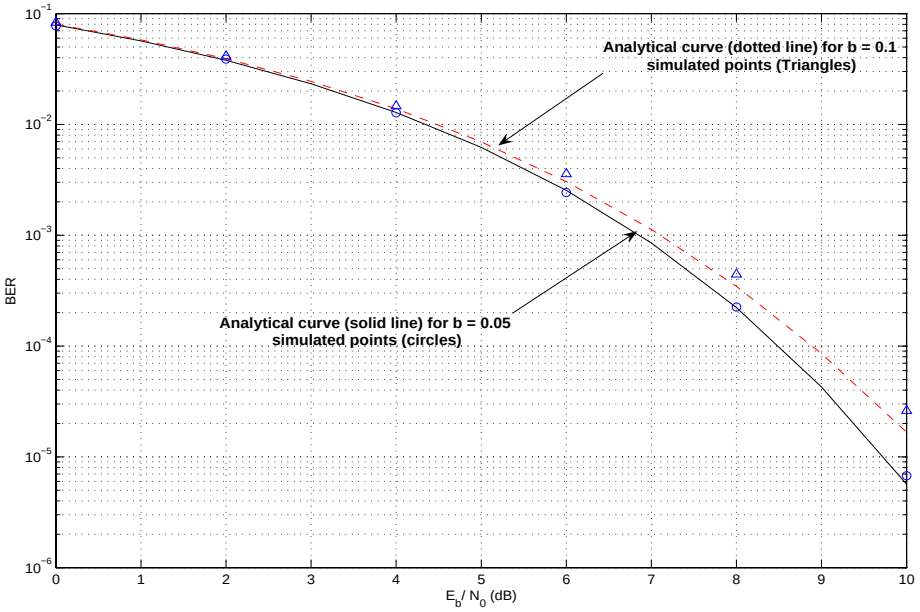

Figure 3.2: BER curves for AWGN channel with N=8 subcarriers and b=0.1, b=0.05 for BPSK OFDM Systems.

are presented in Fig. 3.3 and 3.4, respectively. The simulation results agree well with our analytical results for both $b = 0.05$ and $b = 0.1$ cases in both channels, confirming the accuracy of our analytical expressions. Here we can see that even for the case where $b = 0.1$ descrepencies are not significant. The main reason for this is the dominance of randomness of channel parameters compared to the rndomness of CFO. That is even though the appoximated CFO induces an error it is overwhelmed by the channel thus minimising the difference of effect caused by exact ICI term (corresponds to simulated points) and approximated ICI term (corresponds to analytical curve).

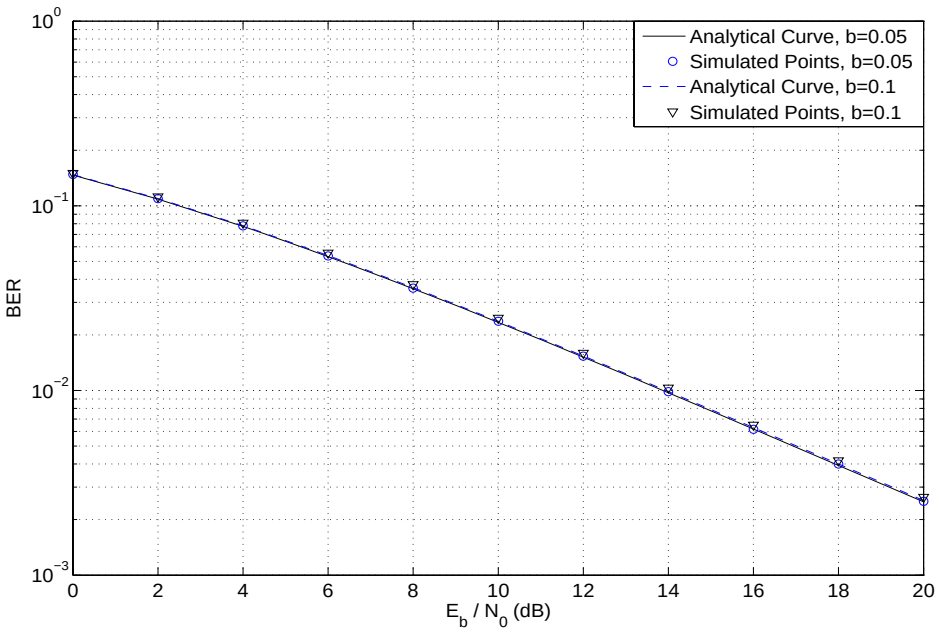

Figure 3.3: BER curves for the frequency-flat Rayleigh fading channel with N=8 subcarriers and b=0.1, b=0.05 for BPSK OFDM Systems.

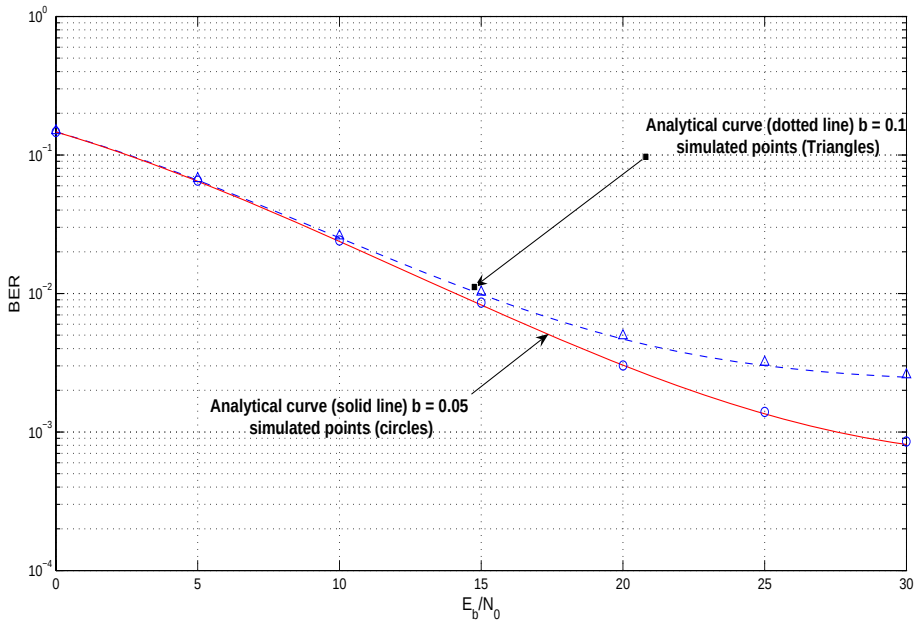

Figure 3.4: BER curves for the frequency-selective Rayleigh fading channel with N=8 subcarriers, L=5 CIR tap coefficients and b=0.1, b=0.05 for BPSK OFDM Systems.

When the channel-independent residual CFO is considered under perfect power control, the residual CFO is modeled as a Gaussian random variable. Simulation in this section is performed under two settings:

1. **Setting I** : The residual CFO is directly generated from a Gaussian density with the variance determined by the CRB conditioned on the channel. A CFO estimator is not used. The purpose of this setting is to verify the theoretical derivation.

2. **Setting II** : We apply CFO estimation and compensation at the receiver to show the accuracy of our analytical results for practical systems. For the frequency-flat fading channel, we use the CFO estimator (MLE1) from (**Morelli and Mengali**, 2000). For the AWGN channel, we can derive the ML CFO estimator based on the signal model in (3.48) as

$$\hat{v} = \arg_{\tilde{v}} \max \Re\left\{ \sum_{n=0}^{N-1} r[n]s^*[n] \exp\left(\frac{-j2\pi\tilde{v}n}{N}\right)\right\}. \tag{3.79}$$

We use an OFDM system with $N = 20$ in a quasi-static channel. In our simulation we have one OFDM preamble/training symbol followed by only one OFDM data symbol. In our analytical derivation we did not consider the CFO-induced, symbol-index-dependent phase shift of $\exp(j2\pi v_\Delta m(N+N_g)/N)$ where m is the OFDM symbol index and N_g is the number of guard samples. We simply assume that every symbol is phase synchronized so that we can neglect the above phase shift.

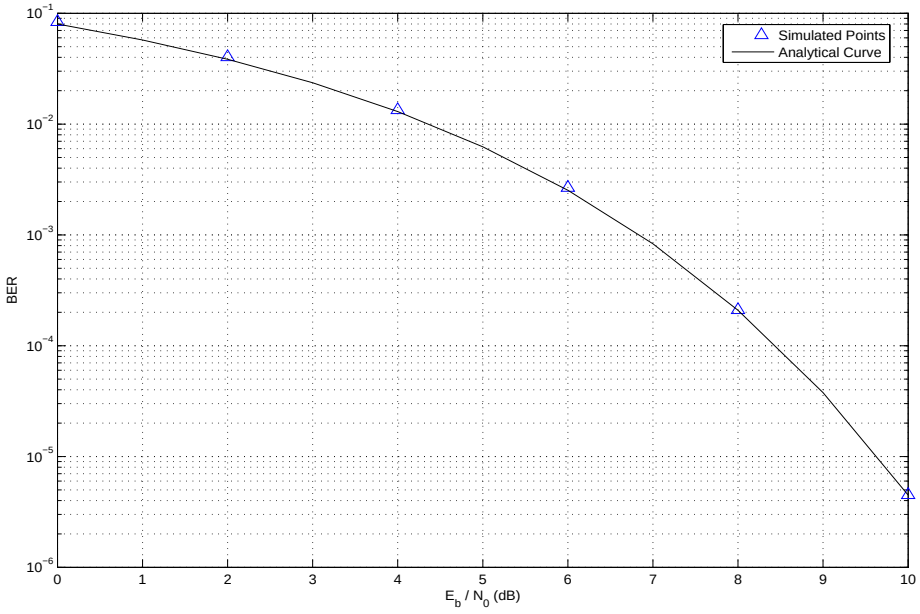

Figure 3.5: BER curves for the AWGN channel (setting I) with N=20 subcarriers for BPSK OFDM Systems.

For the AWGN channel, the simulation and analytical results for the Setting I and II are presented in Fig. 3.5 and 3.6, respectively. We observe an excellent match between the analytical and simulation results in both figures which confirms the accuracy of our derivation and the applicability of our results to practical systems with a CFO estimator.

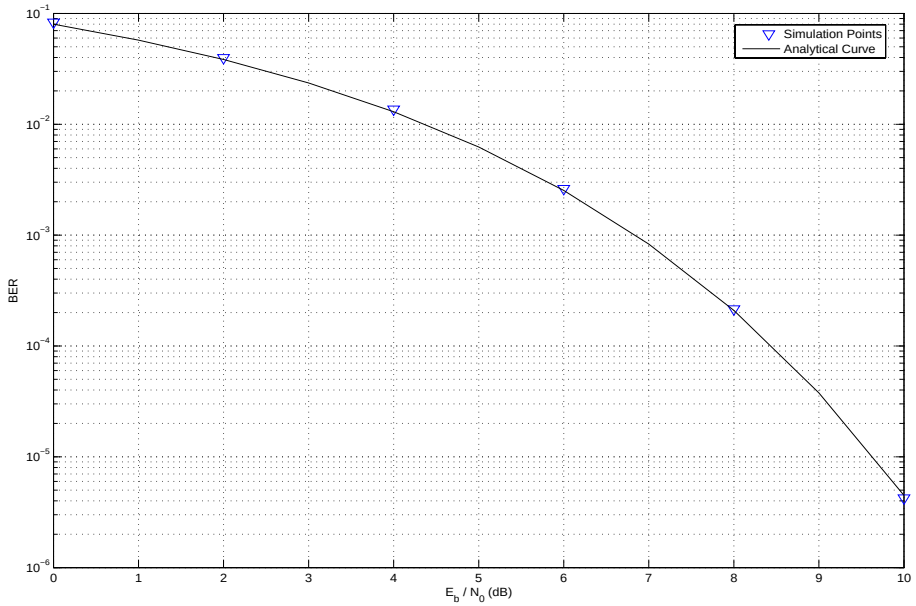

Figure 3.6: BER curves for the AWGN channel (setting II) with N=20 subcarriers for BPSK OFDM Systems.

The results for the frequency-flat Rayleigh fading channel are shown in Fig. 3.7 and 3.8 for the Setting I and II, respectively. A marginal mismatch between the simulation and the analytical results is observed for both settings at low SNR values. This slight mismatch can be ascribed to the fact that the small v_Δ approximation used in the analytical derivation is not justified by occasional large CFO estimation errors (outliers) which occur more often at lower SNR values in the simulation. Note that in practice if the channel is in deep fade the receiver will not be able to detect the signal. Hence, the above marginal mismatch is not a concern for practical systems. Also note that we can easily apply our analytical derivation to periodic training signals by using the CRB in (3.44).

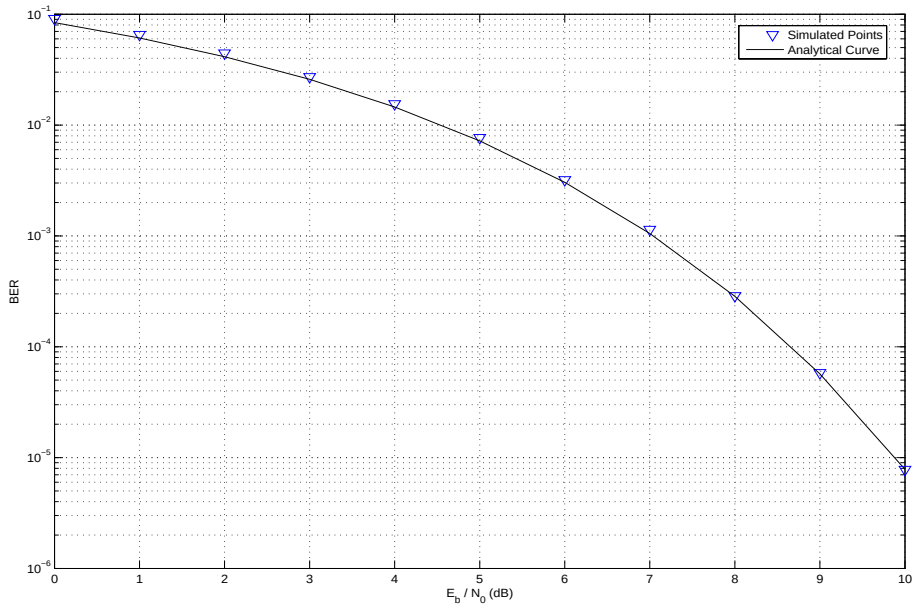

Figure 3.7: BER curves for the frequency-flat Rayleigh fading channel (setting I) with perfect power control and N=20 subcarriers for BPSK OFDM Systems.

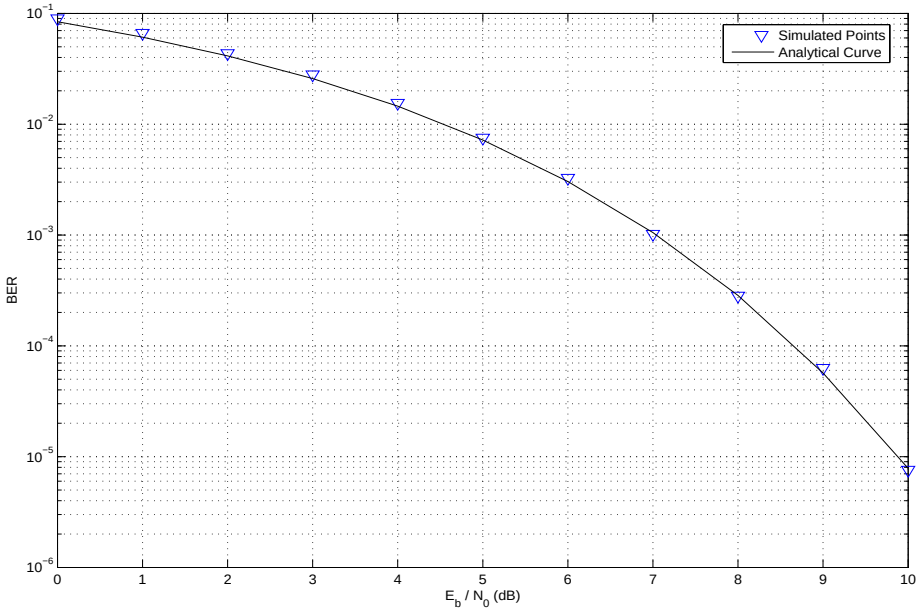

Figure 3.8: BER curves for the frequency-flat Rayleigh fading channel (setting II) with perfect power control and N=20 subcarriers for BPSK OFDM Systems.

3.6.2 Channel-Dependent Residual CFO for BPSK OFDM Systems

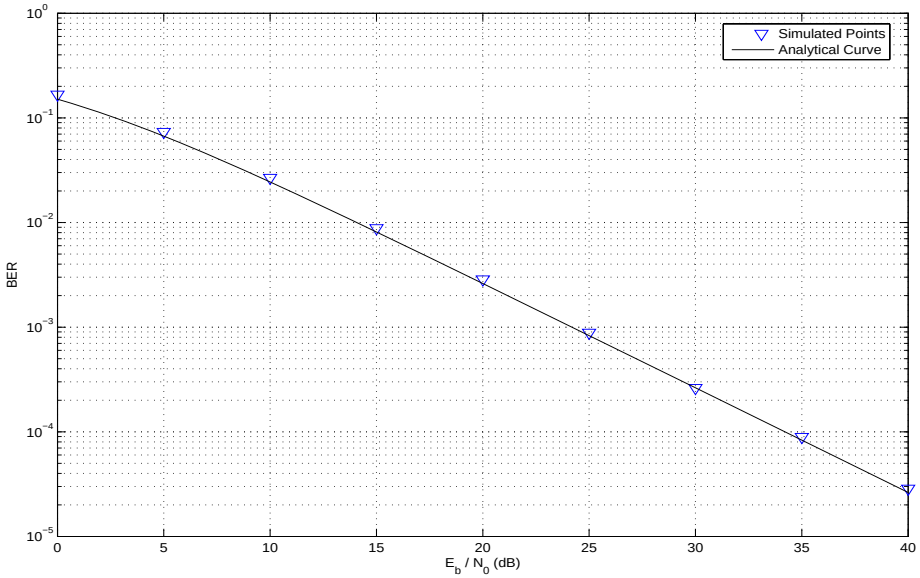

Figure 3.9: BER curves for the frequency-flat Rayleigh fading channel (setting I) with no power control and N=20 subcarriers for BPSK OFDM Systems.

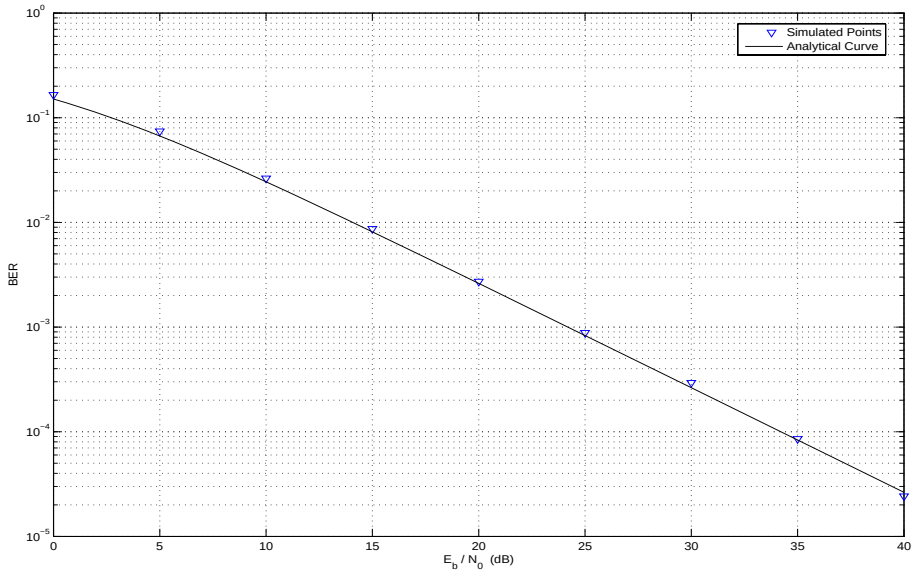

Figure 3.10: BER curves for the frequency-flat Rayleigh fading channel (setting II) with no power control and N=20 subcarriers for BPSK OFDM Systems.

In our analytical derivation corresponding to this section, the residual CFO is modeled as a Gaussian random variable conditioned on the channel realization. Here we use the same simulation settings as described in the previous section. The results for the frequency-flat Rayleigh fading channel are shown in Fig. 3.9 and 3.10 for the Setting I and II, respectively. Simulation results closely match the analytical curves verifying the accuracy and practical applicability of our BER analysis.

3.6.3 Channel-Dependent Residual CFO (With Relaxed Assumptions) for BPSK OFDM Systems

This section corresponds to the section 3.4. In the simulation, we apply the MLE1 estimator from (**Morelli and Mengali**, 2000) and hence the residual CFO is channel-dependent. However, in the analytical derivation related to this section, we assume that the residual CFO is uniformly distributed over the range $[-b, b]$ and is independent of the channel. We set the variance of the uniform residual CFO of the analytical derivation to be the same as the mean-square error (MSE) of the practical estimator in the simulation which gives the relation $b{=}\sqrt{3\text{MSE}}$. Note that the MSE of the CFO estimator depends on the SNR (E_b/N_0) and hence we set b according to the MSE at the SNR we are evaluating. Fig. 3.11 shows the analytical BER results and the

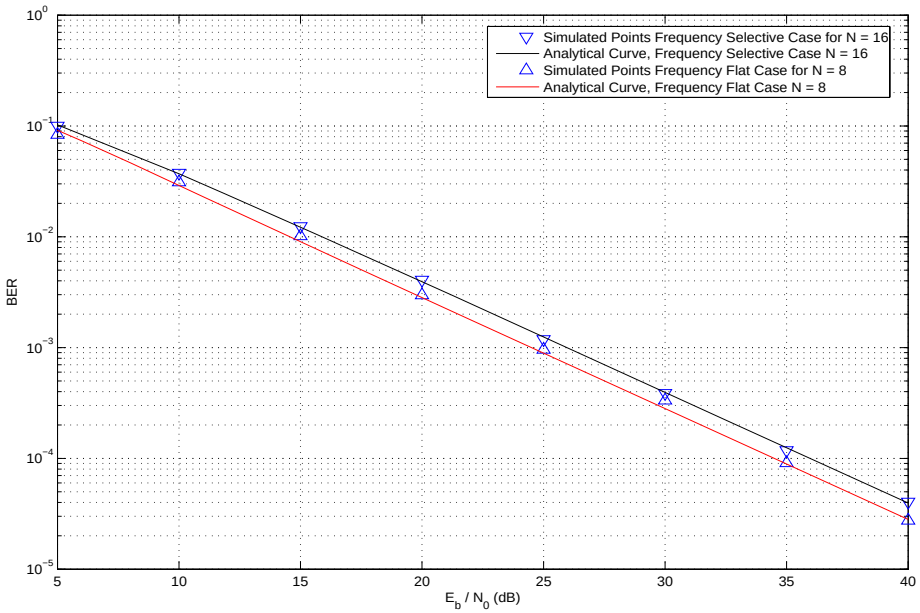

Figure 3.11: BER curves for the frequency-flat Rayleigh fading channel ($N{=}8$) and the frequency-selective Rayleigh fading channel ($N{=}16$); (with relaxed assumptions for the analytical curves) for BPSK OFDM Systems.

simulation results obtained with the CFO and channel estimation in frequency-flat and frequency-selective Rayleigh fading channels for OFDM systems with $N{=}8$ and $N{=}16$. The results show a close match between the simulated and analytical results even with the relaxed assumptions we made in the derivations of (3.68) and (3.78). In particular, the analytical results based on the relaxed assumption for the frequency-selective fading channel is quite appealing since the exact BER analysis appears to be intractable.

CHAPTER 4

SER ANALYSIS OF QUADRATURE AMPLITUDE MODULATED OFDM SYSTEMS WITH RANDOM RESIDUAL FREQUENCY OFFSET

4.1 Introduction

In this chapter, we derive symbol error rate expressions for OFDM systems with residual carrier frequency offset. The CFO or residual CFO is treated as a random parameter in this study. In particular, two scenarios, channel-independent as well as channel-dependent random CFO or residual CFO are considered. We derive SER expressions for 4-QAM OFDM systems in the cases of additive white Gaussian noise and frequency-flat Rayleigh fading channels. The simulation results are provided to verify the accuracy of the new SER expressions.

4.2 Performance Analysis with Channel-Independent CFO or Residual CFO for 4-QAM OFDM Systems

As we discussed previously in (3.13) for the channel-independent CFO or residual CFO case in 4-QAM, SER on a particular (say 0th) subcarrier of the ith OFDM symbol conditioned on the other $N-1$ sub-carrier symbols is obtained by solving

$$P_s\left(\xi|\boldsymbol{a}_i\right) = \int\int P_s\left(\xi|v_\Delta, \boldsymbol{h}, \boldsymbol{a}_i\right) f_v(v_\Delta) f(\boldsymbol{h}) dv_\Delta d\boldsymbol{h} \tag{4.1}$$

where $f_v(v_\Delta)$ and $f(\boldsymbol{h})$ are pdfs of CFO or residual CFO and channel respectively, and $P_s\left(\xi|v_\Delta, \boldsymbol{h}, \boldsymbol{a}_i\right)$ represents the SER conditioned on v_Δ, $\boldsymbol{h}$ and $\boldsymbol{a}_i$. Here $\boldsymbol{a}_i = [c_{1,i}\ c_{2,i}\ \cdots\ c_{N-1,i}]^T$. In the following sections 4.2.1 and 4.2.2, we consider the uniformly distributed CFO, while in the section 4.2.3 we address a Gaussian-distributed residual CFO. A square M-QAM modulation can be considered as a combination of two quadrature (say I and Q) $\sqrt{M}$-PAM (pulse amplitude modulation) schemes, each with half the total power. Since a correct QAM decision is made only when a correct decision is independently made on each of these PAM modulations, then the symbol error probability for a square QAM can be expressed as (**Marvin and Alouini**, 2005).

$$P_s\left(\text{error}\right)|_{M-QAM,E_s} = P_{I\sqrt{M},\frac{E_s}{2}} + P_{Q\sqrt{M},\frac{E_s}{2}} - P_{I\sqrt{M},\frac{E_s}{2}} \times P_{Q\sqrt{M},\frac{E_s}{2}} \tag{4.2}$$

where $P_{IM,E_s} = \left[P_s\left(\text{error}\right)|_{M-PAM,E_s}\right]_I$ and $P_Q = \left[P_s\left(error\right)|_{M-PAM,E_s}\right]_Q$. This holds true even for the case when the symbol error probability is conditioned on some random parameters. Writing the equation (3.10) with some slight modifications to the symbols c_k's, we can express the received symbol on the kth sub-carrier for M-PAM

OFDM as

$$R_k = \sqrt{\epsilon_s N} A_k H_k I'_0 + \sqrt{\epsilon_s N} \sum_{l=0, l\neq k}^{N-1} A_l H_l I'_{l-k} + n'_k; \quad k = 0, 1, .., N-1 \tag{4.3}$$

where $\epsilon_s = \frac{3E_s}{M^2-1}$, $A_m \in \{-(M-1)..-1, 1..(M-1)\}$ and E_s is the symbol energy. Now consider the M-QAM OFDM signal with the signal points $c_k = c_{Ik} + jc_{Q_k}$ with $c_{Ik}, c_{Q_k} \in \{-(M-1)..-1, 1..(M-1)\}$. Thus we can write the equivalent two quadrature components of M-QAM signal on the I and Q-axis of the complex plane for the zeroth sub-carrier as

$$\begin{aligned} Y_I &= \sqrt{\epsilon_s}|\alpha_0|\Re(c_0 I'_0) + \sqrt{\epsilon_s N}\sum_{l=1}^{N-1} \Re(\zeta c_l H_l I'_l) + n_I \\ Y_Q &= \sqrt{\epsilon_s}|\alpha_0|\Im(c_0 I'_0) + \sqrt{\epsilon_s N}\sum_{l=1}^{N-1} \Im(\zeta c_l H_l I'_l) + n_Q \end{aligned} \tag{4.4}$$

where $Y_I = \Re(R_0)$, $Y_Q = \Im(R_0)$, $\alpha_0 = \sqrt{N}H_0$, $\zeta = e^{-j\angle\alpha_0}$ and n_I, n_Q are i.i.d. real Gaussian random variables with zero mean and variance σ^2.

4.2.1 AWGN Channel with Uniformly Distributed CFO

For the AWGN channel, (4.4) reduces to

$$\begin{aligned} Y_I &= \sqrt{\epsilon_s}\Re(c_0 I'_0) + \sqrt{\epsilon_s}\sum_{l=1}^{N-1} \Re(c_l I'_l) + n_I \\ Y_Q &= \sqrt{\epsilon_s}\Im(c_0 I'_0) + \sqrt{\epsilon_s}\sum_{l=1}^{N-1} \Im(c_l I'_l) + n_Q. \end{aligned} \tag{4.5}$$

For an M-QAM OFDM system with $M = 4$ and a particular symbol c_0^* on the zero-th sub-carrier, we have $P_{IM,E_s}|\boldsymbol{a}_i, v_\Delta, c_0^* = P_{IM,E_s}|\boldsymbol{a}_i, v_\Delta$ and $P_{Q_{M,E_s}}|\boldsymbol{a}_i, v_\Delta, c_0^* = P_{Q_{M,E_s}}|\boldsymbol{a}_i, v_\Delta$. Then we can derive $P_{IM,E_s}|\boldsymbol{a}_i, v_\Delta$ and $P_{Q_{M,E_s}}|\boldsymbol{a}_i, v_\Delta$ using (4.5) as follows (**Marvin and Alouini**, 2005. eq.(8.3)):

$$\begin{aligned} P_{IM,E_s}|\boldsymbol{a}_i, v_\Delta = \frac{M-1}{M} Q\left(\sqrt{\epsilon_s}\frac{[\Re(c_0^* I'_0) - \frac{\pi v_\Delta}{N}\Re(X_i)]}{\sigma}\right) \\ + \frac{M-1}{M} Q\left(\sqrt{\epsilon_s}\frac{[\Re(c_0^* I'_0) + \frac{\pi v_\Delta}{N}\Re(X_i)]}{\sigma}\right) \end{aligned} \tag{4.6}$$

$$\begin{aligned} P_{Q_{M,E_s}}|\boldsymbol{a}_i, v_\Delta = \frac{M-1}{M} Q\left(\sqrt{\epsilon_s}\frac{[\Im(c_0^* I'_0) - \frac{\pi v_\Delta}{N}\Im(X_i)]}{\sigma}\right) \\ + \frac{M-1}{M} Q\left(\sqrt{\epsilon_s}\frac{[\Im(c_0^* I'_0) + \frac{\pi v_\Delta}{N}\Im(X_i)]}{\sigma}\right) \end{aligned} \tag{4.7}$$

where $X_i = \sum_{l=1}^{N-1} c_{l,i}[-\cot(\frac{\pi l}{N}) + j]$. Without loss of generality, for the 4-QAM case c_0^* is taken to be equal to $(1+j)$. Using (4.2), (4.6) and (4.7), we can derive the conditional

SER for 4-QAM OFDM as

$$\begin{aligned}P_s\left(\xi|\boldsymbol{a}_i, v_\Delta\right) =& \frac{1}{2}Q\left(\sqrt{2\gamma}[1+\alpha_{Ii}v_\Delta]\right)+\frac{1}{2}Q\left(\sqrt{2\gamma}[1+\beta_{Ii}v_\Delta]\right)+\frac{1}{2}Q\left(\sqrt{2\gamma}[1-\alpha_{Qi}v_\Delta]\right)\\ &+\frac{1}{2}Q\left(\sqrt{2\gamma}[1-\beta_{Qi}v_\Delta]\right)-\frac{1}{4}Q\left(\sqrt{2\gamma}[1+\alpha_{Ii}v_\Delta]\right)Q\left(\sqrt{2\gamma}[1-\alpha_{Qi}v_\Delta]\right)\\ &-\frac{1}{4}Q\left(\sqrt{2\gamma}[1+\alpha_{Ii}v_\Delta]\right)Q\left(\sqrt{2\gamma}[1-\beta_{Qi}v_\Delta]\right)\\ &-\frac{1}{4}Q\left(\sqrt{2\gamma}[1+\beta_{Ii}v_\Delta]\right)Q\left(\sqrt{2\gamma}[1-\alpha_{Qi}v_\Delta]\right)\\ &-\frac{1}{4}Q\left(\sqrt{2\gamma}[1+\beta_{Ii}v_\Delta]\right)Q\left(\sqrt{2\gamma}[1-\beta_{Qi}v_\Delta]\right)\end{aligned} \tag{4.8}$$

where $\alpha_{Ii} = \pi\left[\frac{N-1}{N} - \frac{\Re(X_i)}{N}\right]$, $\beta_{Ii} = \pi\left[\frac{N-1}{N} + \frac{\Re(X_i)}{N}\right]$, $\alpha_{Qi} = \pi\left[\frac{N-1}{N} - \frac{\Im(X_i)}{N}\right]$, $\beta_{Qi} = \pi\left[\frac{N-1}{N} + \frac{\Im(X_i)}{N}\right]$ and $2\gamma = \frac{2E_b}{N_0} = \frac{E_s}{N_0}$. E_b and E_s represent bit energy and symbol energy, respectively, and the complex noise variance is denoted by $N_0 = 2\sigma^2$. Now we define

$$I_1(\mu, \lambda) = \int Q\left(\mu + \lambda v_\Delta\right) f_v(v_\Delta) dv_\Delta \tag{4.9}$$

$$I_2(\mu, \lambda_1, \lambda_2) = \int Q\left(\mu + \lambda_1 v_\Delta\right) Q\left(\mu + \lambda_2 v_\Delta\right) f_v(v_\Delta) dv_\Delta \tag{4.10}$$

$$I_3(\mu, \lambda, \omega_1, \omega_2) = \int_{\omega_1}^{\omega_2} Q\left(\mu + \lambda x\right) e^{-x^2/2} dx \tag{4.11}$$

where $f_v(v_\Delta)$ is the distribution of normalized CFO or residual CFO and in this section it is considered to be a uniform distribution over $[-b, b]$ and μ is non-zero. Then we can derive

$$I_1(\mu, \lambda) = \begin{cases} Q\left(\mu\right) & \text{if } \lambda = 0 \\ \frac{1}{2b\lambda}\Big[(\mu + \lambda x)Q\left(\mu + \lambda x\right) & \\ \quad -\frac{1}{\sqrt{2\pi}}e^{-\frac{(\mu+\lambda x)^2}{2}}\Big]_{-b}^{b} & \text{if } \lambda \neq 0 \end{cases} \tag{4.12}$$

$$I_2(\mu, \lambda_1, \lambda_1) = \begin{cases} \left[g_{I_2}(x, \mu, \lambda_1, \lambda_2)\right]_{-b}^{b} & \\ +\mathcal{I}_3 & \text{if } \lambda_1, \lambda_2 \neq 0 \\ I_1(\mu, \lambda_1).I_1(\mu, \lambda_2) & \text{else} \end{cases} \tag{4.13}$$

where

$$\mathcal{I}_3 = \frac{\mu(\lambda_1 - \lambda_2)}{\sqrt{8\pi}\lambda_1\lambda_2 b} I_3\left(\frac{\mu(\lambda_1 - \lambda_2)}{\lambda_1}, \frac{\lambda_2}{\lambda_1}, \mu - \lambda_1 b, \mu + \lambda_1 b\right)$$

and $\big[g(x)\big]_{-b}^{b} = g(b) - g(-b)$ and g is any arbitrary function defined over $[-b, b]$. $g_{I_2}(x, \mu, \lambda_1, \lambda_2)$ is given by

$$g_{I_2}(x,\mu,\lambda_1,\lambda_2) = \frac{1}{2b\lambda_2}\big(\mu+\lambda_2 x\big)Q\big(\mu+\lambda_2 x\big)Q\big(\mu+\lambda_1 x\big) - \frac{1}{\sqrt{8\pi}\lambda_2 b}Q\big(\mu+\lambda_1 x\big)\exp\left(\frac{-(\mu+\lambda_2 x)^2}{2}\right) - \frac{1}{\sqrt{8\pi}\lambda_1 b}Q\big(\mu+\lambda_2 x\big)\exp\left(\frac{-(\mu+\lambda_2 x)^2}{2}\right) + \frac{(\lambda_1+\lambda_2)}{\sqrt{8\pi(\lambda_1^2+\lambda_2^2)}\lambda_1\lambda_2 b}\exp\left(\frac{-\mu^2(\lambda_1-\lambda_2)^2}{2(\lambda_1^2+\lambda_2^2)}\right)Q\left(\frac{\mu(\lambda_1+\lambda_2)}{\sqrt{\lambda_1^2+\lambda_2^2}}+\sqrt{\lambda_1^2+\lambda_2^2}x\right). \quad (4.14)$$

Using (4.12) and (4.13), we can obtain the SER conditioned on $\boldsymbol{a}_i$ which can be given as

$$P_s\left(\xi|\boldsymbol{a}_i\right) = \frac{1}{2}I_1(\sqrt{2\gamma},\sqrt{2\gamma}\alpha_{Ii}) + \frac{1}{2}I_1(\sqrt{2\gamma},\sqrt{2\gamma}\beta_{Ii}) + \frac{1}{2}I_1(\sqrt{2\gamma},-\sqrt{2\gamma}\alpha_{Qi}) + \frac{1}{2}I_1(\sqrt{2\gamma},-\sqrt{2\gamma}\beta_{Qi}) - \frac{1}{4}I_2(\sqrt{2\gamma},\sqrt{2\gamma}\alpha_{Ii},-\sqrt{2\gamma}\alpha_{Qi}) - \frac{1}{4}I_2(\sqrt{2\gamma},\sqrt{2\gamma}\alpha_{Ii},-\sqrt{2\gamma}\beta_{Qi}) - \frac{1}{4}I_2(\sqrt{2\gamma},\sqrt{2\gamma}\beta_{Ii},-\sqrt{2\gamma}\alpha_{Qi}) - \frac{1}{4}I_2(\sqrt{2\gamma},\sqrt{2\gamma}\beta_{Ii},-\sqrt{2\gamma}\beta_{Qi}). \quad (4.15)$$

Averaging over all $\boldsymbol{a}_i$ combinations leads to the SER

$$P_s\left(\xi\right) = \frac{1}{2^{2(N-1)}}\sum_i P_s\left(\xi|\boldsymbol{a}_i\right) \quad (4.16)$$

where $\sum_i \equiv \sum_{c_1\in\mathcal{A}}\sum_{c_2\in\mathcal{A}}....\sum_{c_{N-1}\in\mathcal{A}}$ and $\mathcal{A} = \big\{1+j, 1-j, -1+j, -1-j\big\}$.

4.2.2 Frequency-Flat Rayleigh Fading Channel with Uniformly Distributed CFO

When the frequency flat Rayleigh fading is concerned, the equivalent quadrature components in (4.4) reduce to

$$Y_I = \sqrt{\epsilon_s}|\alpha_0|\Re(c_0 I_0') + \sqrt{\epsilon_s}|\alpha_0|\sum_{l=0}^{N-1}\Re(\zeta c_l I_l') + n_I$$
$$Y_Q = \sqrt{\epsilon_s}|\alpha_0|\Im(c_0 I_0') + \sqrt{\epsilon_s}|\alpha_0|\sum_{l=0}^{N-1}\Im(\zeta c_l I_l') + n_Q. \quad (4.17)$$

Here we use the distribution of $|\alpha_0|$

$$f_{\alpha_0}(|\alpha_0|) = \frac{|\alpha_0|}{\sigma_R^2}\exp\big(-\frac{|\alpha_0|^2}{2\sigma_R^2}\big)$$

where α_0 is a zero-mean complex Gaussian random variable with a variance of σ_R^2 per dimension. For the notational simplicity we define the following integrals Following the same set of arguments we can easily derive the conditional SER, $P_s\big(\xi|\boldsymbol{a}_i, v_\Delta, |\alpha_0|\big)$,

replacing $\sqrt{2\gamma}$ in (4.8) with $\sqrt{2\gamma}|\alpha_0|$ as

$$\begin{aligned}P_s\big(\xi|\boldsymbol{a}_i, v_\Delta, |\alpha_0|\big) =& \frac{1}{2}Q\left(\sqrt{2\gamma}|\alpha_0|[1+\alpha_{Ii}v_\Delta]\right)+\frac{1}{2}Q\left(\sqrt{2\gamma}|\alpha_0|[1+\beta_{Ii}v_\Delta]\right)\\ &+\frac{1}{2}Q\left(\sqrt{2\gamma}|\alpha_0|[1-\alpha_{Qi}v_\Delta]\right)+\frac{1}{2}Q\left(\sqrt{2\gamma}|\alpha_0|[1-\beta_{Qi}v_\Delta]\right)\\ &-\frac{1}{4}Q\left(\sqrt{2\gamma}|\alpha_0|[1+\alpha_{Ii}v_\Delta]\right)Q\left(\sqrt{2\gamma}|\alpha_0|[1-\alpha_{Qi}v_\Delta]\right)\\ &-\frac{1}{4}Q\left(\sqrt{2\gamma}|\alpha_0|[1+\alpha_{Ii}v_\Delta]\right)Q\left(\sqrt{2\gamma}|\alpha_0|[1-\beta_{Qi}v_\Delta]\right)\\ &-\frac{1}{4}Q\left(\sqrt{2\gamma}|\alpha_0|[1+\beta_{Ii}v_\Delta]\right)Q\left(\sqrt{2\gamma}|\alpha_0|[1-\alpha_{Qi}v_\Delta]\right)\\ &-\frac{1}{4}Q\left(\sqrt{2\gamma}|\alpha_0|[1+\beta_{Ii}v_\Delta]\right)Q\left(\sqrt{2\gamma}|\alpha_0|[1-\beta_{Qi}v_\Delta]\right)\end{aligned} \tag{4.18}$$

$$T_1(\beta) = \int_{-b}^{b}\int_{0}^{\infty} Q\big(a(\beta, v_\Delta)|\alpha_0|\big) f_{\alpha_0}(|\alpha_0|) f_v(v_\Delta) d|\alpha_0| dv_\Delta$$

$$T_2(\alpha, \beta, v_\Delta) = \int_{0}^{\infty} Q\big(a(\alpha, v_\Delta)|\alpha_0|\big) Q\big(a(\beta, v_\Delta)|\alpha_0|\big) f_{\alpha_0}(|\alpha_0|) d|\alpha_0|$$

where $a(\beta, v_\Delta) = \sqrt{2\gamma}(1 + \beta v_\Delta)$. Then we can solve the above integrations to obtain

$$T_1(\beta) = \begin{cases} \frac{1}{2} - \frac{\sqrt{2\gamma}\sigma_R}{2\sqrt{1+2\gamma\sigma_R^2}} & \text{if } \beta = 0 \\ \frac{1}{2} - \frac{\left[\sqrt{1+2\gamma\sigma_R^2 x^2}\right]_{1-\beta b}^{1+\beta b}}{4\sqrt{2\gamma}\beta\sigma_R b} & \text{if } \beta \neq 0 \end{cases} \tag{4.19}$$

and $T_2(\alpha, \beta, v_\Delta)$ is given by

$$\begin{aligned}T_2(\alpha, \beta, v_\Delta) = \frac{1}{4} &- \frac{a(\alpha, v_\Delta)m(\alpha, v_\Delta)}{2\pi}\left(\frac{\pi}{2} - \cot^{-1}\left[\frac{1}{a(\beta, v_\Delta)m(\alpha, v_\Delta)}\right]\right)\\ &- \frac{a(\beta, v_\Delta)m(\beta, v_\Delta)}{2\pi}\left(\frac{\pi}{2} - \cot^{-1}\left[\frac{1}{a(\alpha, v_\Delta)m(\beta, v_\Delta)}\right]\right)\end{aligned} \tag{4.20}$$

where the function $m(\alpha, v_\Delta)$ is defined as

$$m(\alpha, v_\Delta) = \frac{\sigma_R}{\sqrt{1 + \sigma_R^2 a^2(\alpha, v_\Delta)}}.$$

Now we want to find $T_2(\alpha, \beta)$ which is given by

$$T_2(\alpha, \beta) = \int_{-b}^{b} T_2(\alpha, \beta, v_\Delta) f_v(v_\Delta) dv_\Delta.$$

After having some rearrangements in the expression (4.20) for notational simplicity, we denote $T_2(\alpha, \beta)$ as

$$T_2(\alpha, \beta) = \frac{1}{4} - T_{2'}(\alpha) - T_{2'}(\beta) + T_{2'}(\alpha, \beta) + T_{2'}(\beta, \alpha) \tag{4.21}$$

where

$$T_{2'}(\alpha) = \int_{-b}^{b} \frac{a(\alpha, v_\Delta)m(\alpha, v_\Delta)}{8b} dv_\Delta$$

$$T_{2'}(\alpha, \beta) = \int_{-b}^{b} \frac{a(\alpha, v_\Delta)m(\alpha, v_\Delta)}{4\pi b} \cot^{-1}\left[\frac{1}{a(\beta, v_\Delta)m(\alpha, v_\Delta)}\right] dv_\Delta.$$

Note that $f_v(v_\Delta) = \frac{1}{2b} : v_\Delta \in [-b, b]$. After some mathematical manipulations it can be easily shown that

$$T_{2'}(\alpha) = \frac{1}{4} - \frac{T_1(\alpha)}{2}$$

and

$$T_{2'}(\alpha, \beta) = \begin{cases} \left[g_{1T_{2'}}(x, \alpha, \beta)\right]_{1-\alpha b}^{1+\alpha b} & \text{if } \alpha \neq 0 \\ \left[g_{2T_{2'}}(x, \alpha, \beta)\right]_{-b}^{b} & \text{if } \alpha = 0 \& \beta \neq 0 \\ \frac{1}{2\pi\rho} \cot^{-1}(\rho) & \text{if } \alpha = 0 \& \beta = 0 \end{cases} \tag{4.22}$$

where $g_{1T_{2'}}(x, \alpha, \beta)$ and $g_{1T_{2'}}(x, \alpha, \beta)$ are defined as follows.

$$\begin{aligned} g_{1T_{2'}}(x, \alpha, \beta) = {} & \frac{1}{4\pi\alpha b\bar{\gamma}} \sqrt{1 + \bar{\gamma}^2 x^2} \cot^{-1}\left[\frac{\sqrt{1 + \bar{\gamma}^2 x^2}}{\bar{\gamma}(\eta x + 1 - \eta)}\right] \\ & - \frac{\eta\sqrt{1 + \eta^2 + \bar{\gamma}^2(1-\eta)^2}}{4\pi\alpha b\bar{\gamma}(1+\eta^2)} \tan^{-1}\left[\frac{x + Q}{R}\right] \\ & + \frac{1 - \eta}{4\pi\alpha b(1+\eta^2)} \ln\left[\sqrt{\bar{\gamma}^2(1+\eta^2)x^2 + 2\eta\bar{\gamma}^2(1-\eta)x + \bar{\gamma}^2(1-\eta)^2 + 1}\right] \end{aligned} \tag{4.23}$$

$$\begin{aligned} g_{2T_{2'}}(x, \alpha, \beta) = \frac{1}{4\pi\rho b}\Bigg(& x \cot^{-1}\left[\frac{\rho}{1 + \beta x}\right] - \frac{\rho}{\beta} \ln\left[\sqrt{(1 + \beta x)^2 + \rho^2}\right] \\ & + \frac{1}{\beta} \tan^{-1}\left[\frac{1 + \beta x}{\rho}\right]\Bigg) \end{aligned} \tag{4.24}$$

here $\eta = \frac{\beta}{\alpha}$, $\bar{\gamma} = \sqrt{2\gamma}\sigma_R$, $\rho = \frac{\sqrt{1+\bar{\gamma}^2}}{\bar{\gamma}}$, $Q = \frac{\eta(1-\eta)}{1+\eta^2}$ and $R = \frac{\sqrt{1+\eta^2+\bar{\gamma}^2(1-\eta)^2}}{\bar{\gamma}(1+\eta^2)}$. Now we have derived the expressions for $T_1(\beta)$ and $T_2(\alpha, \beta)$, and using (4.19) and (4.21) we can easily write the SER conditioned on $\boldsymbol{a}_i$, $P_s(\xi|\boldsymbol{a}_i)$, as given by

$$\begin{aligned} P_s(\xi|\boldsymbol{a}_i) = {} & \frac{1}{2}T_1(\alpha_{Ii}) + \frac{1}{2}T_1(\beta_{Ii}) + \frac{1}{2}T_1(-\alpha_{Qi}) + \frac{1}{2}T_1(-\beta_{Qi}) - \frac{1}{4}T_2(\alpha_{Ii}, -\alpha_{Qi}) \\ & - \frac{1}{4}T_2(\alpha_{Ii}, -\beta_{Qi}) - \frac{1}{4}T_2(\beta_{Ii}, -\alpha_{Qi}) - \frac{1}{4}T_2(\beta_{Ii}, -\beta_{Qi}) \end{aligned} \tag{4.25}$$

Averaging over all $\boldsymbol{a}_i$ combinations leads to the SER which is given in (4.16).

4.2.3 AWGN and frequency-flat Rayleigh Fading Channels with Perfect Power Control

With the arguments and results described in the section 3.2.4 we can write that,

$$f_v(v_\Delta|\boldsymbol{h}) = f_v(v_\Delta) = \mathcal{N}(0, CRB|_{\boldsymbol{h}}) \tag{4.26}$$

The expressions for the CRBs are given in (3.49) and (3.53) which was mentioned previously.

4.2.3.1 AWGN Channel

For the AWGN channel, (4.1) simply reduces to a single integral evaluation and the signal model for AWGN channel can be obtained from (3.7) as, $\boldsymbol{r} = \boldsymbol{\Gamma(v)s} + \boldsymbol{w}$ where $\boldsymbol{s} = [s_0 s_1 \dots s_{N-1}]^T$ is the training signal vector. The CRB of the CFO estimation for the aforementioned signal model is given by (3.49). Hence using the definition of $I_1(\mu, \lambda)$ (4.9) and taking $f_v(v_\Delta) = \mathcal{N}(0, \Omega)$ (**Verdu**, 1998, *eq*.3.66) we can easily show that

$$I_1(\mu, \lambda) = Q\left(\frac{\mu}{1 + \Omega\lambda^2}\right) \tag{4.27}$$

and $I_2(\mu, \lambda_1, \lambda_2)$ defined in (4.10) can be reduced to

$$I_2(\mu, \lambda_1, \lambda_2) = \frac{1}{2\pi}\int_0^{\frac{\pi}{2}-\phi_1} \exp\left(\frac{-\mu^2}{2{b_1}^2 \sin^2\phi}\right) d\phi + \frac{1}{2\pi}\int_0^{\frac{\pi}{2}-\phi_2} \exp\left(\frac{-\mu^2}{2{b_2}^2 \sin^2\phi}\right) d\phi. \tag{4.28}$$

$I_2(\mu, \lambda_1, \lambda_2)$ cannot be evaluated in closed-form and it shows similarities to the well known Craig's formula. For simplicity, define $\lambda_{1\Omega} = \sqrt{\Omega}\lambda_1$ and $\lambda_{2\Omega} = \sqrt{\Omega}\lambda_2$. So that $b_1 = \sqrt{\lambda_{1\Omega}^2 + 1}$, $b_2 = \sqrt{\lambda_{2\Omega}^2 + 1}$,

$$a_1 = \frac{\lambda_{1\Omega}^2 - \lambda_{1\Omega}\lambda_{2\Omega} + 1}{\sqrt{(\lambda_{1\Omega}^2 + 1)(\lambda_{1\Omega}^2 + \lambda_{2\Omega}^2 + 1)}}$$

$$a_2 = \frac{\lambda_{2\Omega}^2 - \lambda_{1\Omega}\lambda_{2\Omega} + 1}{\sqrt{(\lambda_{2\Omega}^2 + 1)(\lambda_{1\Omega}^2 + \lambda_{2\Omega}^2 + 1)}}$$

with $\phi_1 = \tan^{-1}(a_1 b_1)$ and $\phi_2 = \tan^{-1}(a_2 b_2)$. Then with some mathematical manipulations we obtain the SER conditioned on $\boldsymbol{a}_i$, $P_s(\xi|\boldsymbol{a}_i)$ as given in (4.15). Averaging over all $\boldsymbol{a}_i$ combinations gives the SER which is given by (4.16).

4.2.3.2 Frequency-Flat Rayleigh Fading Channel

When the frequency-flat fading channel is considered, the $CRB|_{\boldsymbol{h}}$ which was mentioned previously is given by (3.53). Because of the perfect power control, we can consider that $|\alpha_0|^2$ is constant while fixing $\boldsymbol{s}$. Thus we have the pdf of residual CFO $f(v_\Delta|\alpha_0)$, which is given by (3.54) . So that using the conditional SER $P_s(\xi|\boldsymbol{a}_i, v_\Delta, |\alpha_0|)$ derived in (4.18), $CRB|_{\alpha_0}$, aforementioned $f_v(v_\Delta)$ and (4.1), we can derive the SER, following

almost the same set of arguments which were used in the derivation of SER in Section 4.2.3.1. The following parameter changes should be noticed carefully:

$$I_1(\mu, \lambda) = Q\left(\frac{\mu}{1 + \Lambda\lambda^2}\right) \tag{4.29}$$

and $I_2(\mu, \lambda_1, \lambda_2)$ defined in (4.10) as mentioned before is

$$I_2(\mu, \lambda_1, \lambda_2) = \frac{1}{2\pi}\int_0^{\frac{\pi}{2}-\phi_1} \exp\left(\frac{-\mu^2}{2{b_1}^2 \sin^2\phi}\right) d\phi + \frac{1}{2\pi}\int_0^{\frac{\pi}{2}-\phi_2} \exp\left(\frac{-\mu^2}{2{b_2}^2 \sin^2\phi}\right) d\phi \tag{4.30}$$

with slight parameter changes, where $b_1 = \sqrt{\lambda_{1\Lambda}^2 + 1}$, $b_2 = \sqrt{\lambda_{2\Lambda}^2 + 1}$,

$$a_1 = \frac{\lambda_{1\Lambda}^2 - \lambda_{1\Lambda}\lambda_{2\Lambda} + 1}{\sqrt{(\lambda_{1\Lambda}^2 + 1)(\lambda_{1\Lambda}^2 + \lambda_{2\Lambda}^2 + 1)}}$$

$$a_2 = \frac{\lambda_{2\Lambda}^2 - \lambda_{1\Lambda}\lambda_{2\Lambda} + 1}{\sqrt{(\lambda_{2\Lambda}^2 + 1)(\lambda_{1\Lambda}^2 + \lambda_{2\Lambda}^2 + 1)}}$$

$\phi_1 = \tan^{-1}(a_1 b_1)$ and $\phi_2 = \tan^{-1}(a_2 b_2)$, where $\lambda_{1\Lambda} = \sqrt{\Lambda}\lambda_1$ and $\lambda_{2\Lambda} = \sqrt{\Lambda}\lambda_2$. Hence the SER and the corresponding conditional SER are given by (4.16) and (4.15) respectively.

4.3 Performance Analysis with Channel-Dependent Residual CFO for 4-QAM OFDM Systems

Same as we discussed previously in (3.56) For the channel-dependent residual CFO case in 4-QAM, SER on a particular (say 0th) subcarrier of the ith OFDM symbol conditioned on the other $N-1$ sub-carrier symbols is obtained by solving

$$P_s\left(\xi|\boldsymbol{a}_i\right) = \int\int P_s\left(\xi|v_\Delta, \boldsymbol{h}, \boldsymbol{a}_i\right) f_v(v_\Delta|\boldsymbol{h}) f(\boldsymbol{h}) dv_\Delta d\boldsymbol{h}$$

4.3.1 Frequency-flat Rayleigh Fading Channel

For the channel-dependent residual CFO scenario, the symbol error probability is given by (3.56). The closed-form solution to (3.56) for the frequency-flat Rayleigh fading channel in the case of 4-QAM is presented in the following. However, solving the above problem for the frequency-selective case appears to be intractable. The variance of the conditional Gaussian random variable $v_\Delta|\alpha_o$ for the frequency-flat Rayleigh fading channel is given by (3.53) for the MLE estimator (**Morelli and Mengali**, 2000) as mentioned before. Then averaging the conditional SER $P_s\left(\xi|\boldsymbol{a}_i, v_\Delta, |\alpha_0|\right)$

using $f_v(v_\Delta|\boldsymbol{h})$ we can obtain $P_s\left(\xi|\boldsymbol{a}_i,|\alpha_0|\right)$ as

$$P_s\left(\xi|\boldsymbol{a}_i,|\alpha_0|\right)=\frac{1}{2}E\Big\{Q\left(\sqrt{2\gamma}\big[|\alpha_0|+\sqrt{\Lambda}\alpha_{Ii}X\big]\right)\Big\}+$$
$$\frac{1}{2}E\Big\{Q\left(\sqrt{2\gamma}\big[|\alpha_0|+\sqrt{\Lambda}\beta_{Ii}X\big]\right)\Big\}.....$$
$$.....-\frac{1}{4}E\Big\{Q\left(\sqrt{2\gamma}\big[|\alpha_0|+\sqrt{\Lambda}\beta_{Ii}X\big]\right)Q\left(\sqrt{2\gamma}\big[|\alpha_0|-\sqrt{\Lambda}\beta_{Qi}X\big]\right)\Big\} \quad (4.31)$$

where the statistical expectation is taken with respect to the random variable $X=\frac{v_\Delta|\alpha_0|}{\sqrt{\Lambda}}$ and $X\sim\mathcal{N}(0,1)$. It is obvious that by observing the functions $I_1(\mu,\lambda)$ and $I_2(\mu,\lambda_1,\lambda_2)$ in Section 4.2.3.2, we can write

$$P_s\left(\xi|\boldsymbol{a}_i,|\alpha_0|\right)=\frac{1}{2}I_1(\sqrt{2\gamma}|\alpha_0|,\sqrt{2\gamma}\alpha_{Ii})+....$$
$$....-\frac{1}{4}I_2(\sqrt{2\gamma}|\alpha_0|,\sqrt{2\gamma}\beta_{Ii},-\sqrt{2\gamma}\beta_{Qi}). \quad (4.32)$$

Next, after integrating $P_s\left(\xi|\boldsymbol{a}_i,|\alpha_0|\right)$ with $f_{\alpha_0}(|\alpha_0|)$ to remove the dependency of $|\alpha_0|$, we obtain the conditional SER $P_s\left(\xi|\boldsymbol{a}_i\right)$ as

$$\begin{aligned}P_s\left(\xi|\boldsymbol{a}_i\right)=&\frac{1}{2}I_1^*(\sqrt{2\gamma},\sqrt{2\gamma}\alpha_{Ii})+\frac{1}{2}I_1^*(\sqrt{2\gamma},\sqrt{2\gamma}\beta_{Ii})+\frac{1}{2}I_1^*(\sqrt{2\gamma},-\sqrt{2\gamma}\alpha_{Qi})\\&+\frac{1}{2}I_1^*(\sqrt{2\gamma},-\sqrt{2\gamma}\beta_{Qi})-\frac{1}{4}I_2^*(\sqrt{2\gamma},\sqrt{2\gamma}\alpha_{Ii},-\sqrt{2\gamma}\alpha_{Qi})\\&-\frac{1}{4}I_2^*(\sqrt{2\gamma},\sqrt{2\gamma}\alpha_{Ii},-\sqrt{2\gamma}\beta_{Qi})-\frac{1}{4}I_2^*(\sqrt{2\gamma},\sqrt{2\gamma}\beta_{Ii},-\sqrt{2\gamma}\alpha_{Qi})\\&-\frac{1}{4}I_2^*(\sqrt{2\gamma},\sqrt{2\gamma}\beta_{Ii},-\sqrt{2\gamma}\beta_{Qi}) \quad (4.33)\end{aligned}$$

where

$$I_1^*(t_0,t_1)=\int_0^\infty I_1(t_0|\alpha_0|,t_1)f_{\alpha_0}(|\alpha_0|)d|\alpha_0|$$
$$I_2^*(t_0,t_1,t_2)=\int_0^\infty I_2(t_0|\alpha_0|,t_1,t_2)f_{\alpha_0}(|\alpha_0|)d|\alpha_0|.$$

We can obtain the solutions to above integrations as follows.

$$I_1^*(t_0,t_1)=\left[\frac{1}{2}-\frac{t_0\sigma_R}{\sqrt{1+t_0^2\sigma_R^2+\Lambda t_1^2}}\right] \quad (4.34)$$

$$\begin{aligned}I_2^*(t_0,t_1,t_2)=&\frac{1}{2}-\frac{\psi_1+\psi_2}{2\pi}-\frac{\varepsilon_1}{2\pi\sqrt{1+\varepsilon_1^2}}\left(\frac{\pi}{2}-\tan^{-1}\left[\frac{t_0\sigma_R a_1}{\sqrt{1+\varepsilon_1^2}}\right]\right)\\&-\frac{\varepsilon_2}{2\pi\sqrt{1+\varepsilon_2^2}}\left(\frac{\pi}{2}-\tan^{-1}\left[\frac{t_0\sigma_R a_2}{\sqrt{1+\varepsilon_2^2}}\right]\right) \quad (4.35)\end{aligned}$$

where $\varepsilon_1=\frac{t_0\sigma_R}{b_1}$, $\varepsilon_2=\frac{t_0\sigma_R}{b_2}$, $b_1=\sqrt{t_{1\Lambda}^2+1}$, $b_2=\sqrt{t_{2\Lambda}^2+1}$,

$$a_1=\frac{t_{1\Lambda}^2-t_{1\Lambda}t_{2\Lambda}+1}{\sqrt{(t_{1\Lambda}^2+1)(t_{1\Lambda}^2+t_{2\Lambda}^2+1)}}$$

$$a_2 = \frac{t_{2\Lambda}^2 - t_{1\Lambda}t_{2\Lambda} + 1}{\sqrt{(t_{2\Lambda}^2 + 1)(t_{1\Lambda}^2 + t_{2\Lambda}^2 + 1)}}$$

$\psi_1 = \tan^{-1}(a_1 b_1)$ and $\psi_2 = \tan^{-1}(a_2 b_2)$, with $t_{1\Lambda} = \sqrt{\Lambda} t_1$ and $t_{2\Lambda} = \sqrt{\Lambda} t_2$. Substituting the conditional SER in (4.33) into (4.16) will give the corresponding SER.

4.4 Results and Discussion

4.4.1 Channel-Independent CFO or Residual CFO for 4-QAM OFDM Systems

The simulations results discussed in this section are obtained by running the same set of simulation runs as mentioned in the previous section 3.5 with the only change in the symbol constellation of the transmitted signals.

From Fig. 4.1 we can observe the simulation results when the normalized CFO is uniformly distributed over $[-b, b]$ with $b = 0.05$ and $b = 0.1$ for AWGN channel. As we can see, the analytical SER curves obtained using (4.16) closely match with the simulation results for $b = 0.05$. Similar form of discrepancies which are experienced in the BPSK case are prominent for the 4-QAM case as well when $b = 0.1$. As we mentioned earlier, the small CFO assumption in the analytical development is the main reason for this. Because, the CFO would typically be quite small at high SNR the above discrepancy is less likely to happen in practice and thus convincing the relevance of the analytical result.

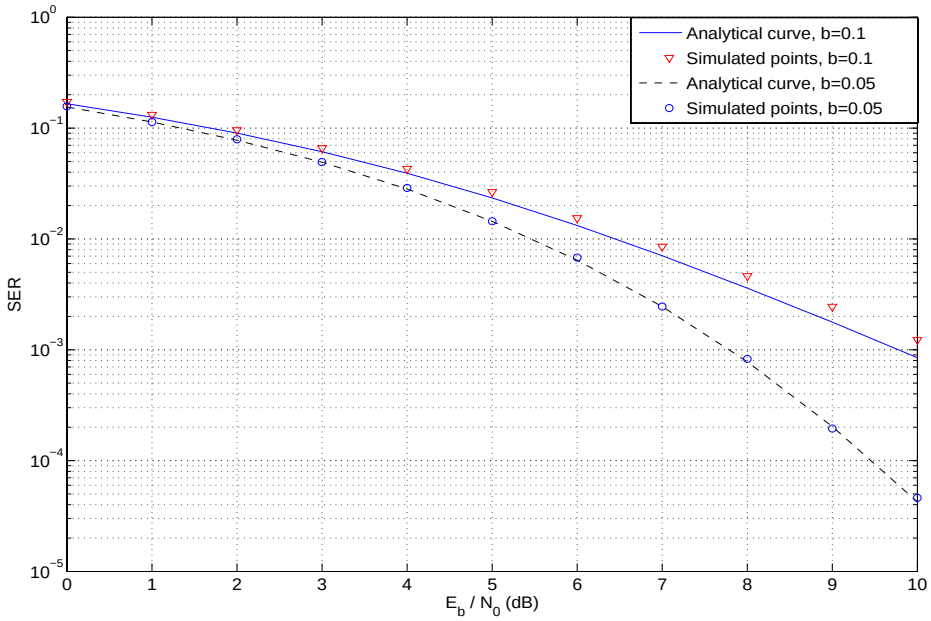

Figure 4.1: BER curves for AWGN channel with N=8 subcarriers and b=0.1, b=0.05 for 4-QAM OFDM Systems.

As far as flat-fading is concerned, the simulation results agree well with our analytical results for both $b = 0.05$ and $b = 0.1$ cases, confirming the accuracy of our analytical expressions given (4.25) and (4.16). We can observe from the Fig. 4.2 that the deviations of the simulation points when $b = 0.1$ is not significant as compared to the case of AWGN channel at high SNR. This is due to the fact that, even at low SER values the contribution from CFO has a less dominant effect on SER than the fading does and hence the small CFO assumption in the analytical development for flat fading is more realistic.

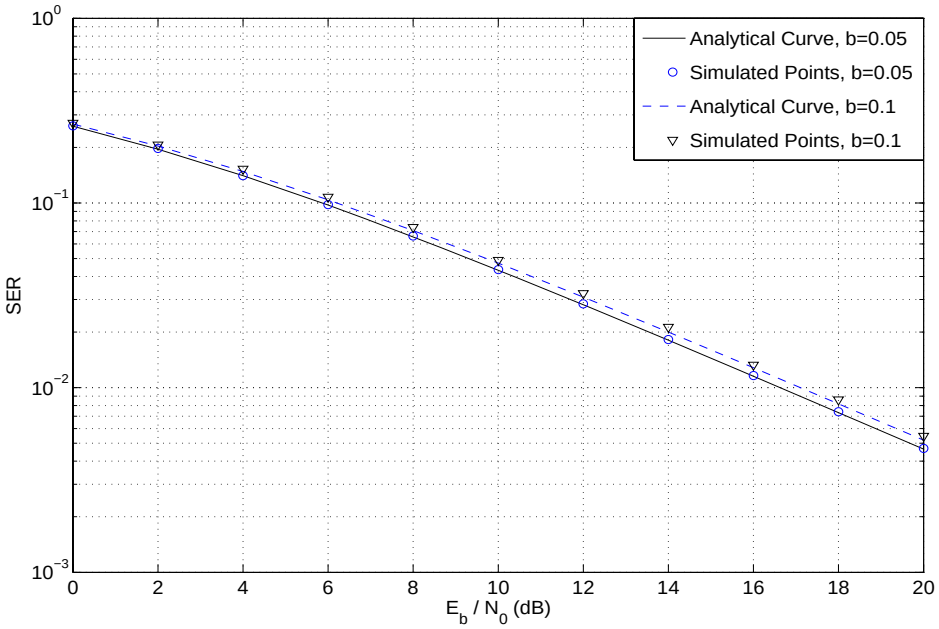

Figure 4.2: BER curves for the frequency-flat Rayleigh fading channel with N=8 subcarriers and b=0.1, b=0.05 for 4-QAM OFDM Systems.

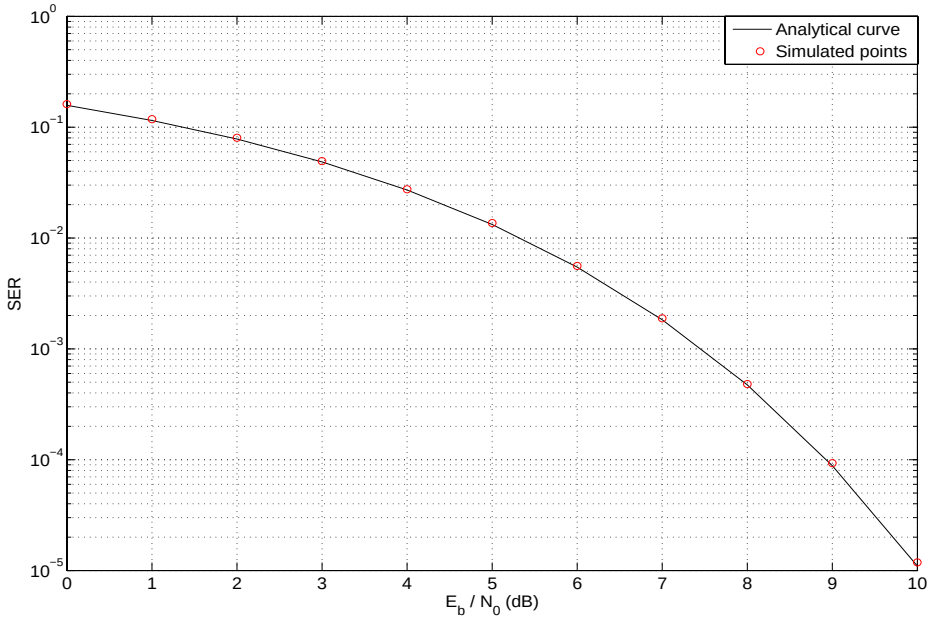

Figure 4.3: BER curves for the AWGN channel (setting I) with N=16 subcarriers for 4-QAM OFDM Systems.

As we have discussed earlier channel independence can be achieved using perfect power controlling as well. The corresponding simulation results for AWGN channel is shown in the Fig. 4.3 and Fig. 4.4 for Setting I and Setting II[1] respectively. OFDM system with $N = 16$ with one OFDM preamble/training symbol followed by only one OFDM data symbol is simulated without considering the CFO-induced, symbol-index-dependent phase shift as we discussed in the section 3.5.1. The correctness of the analytical derivations (section 4.1.3.1) is noticeable by observing the closeness of the analytical curve and the simulation points in the Fig. 4.3. Moreover the Fig. 4.4 reinforce the fact that, the applicability of our analytical results to practical systems with a CFO estimator. The simulation results under perfect power control for the

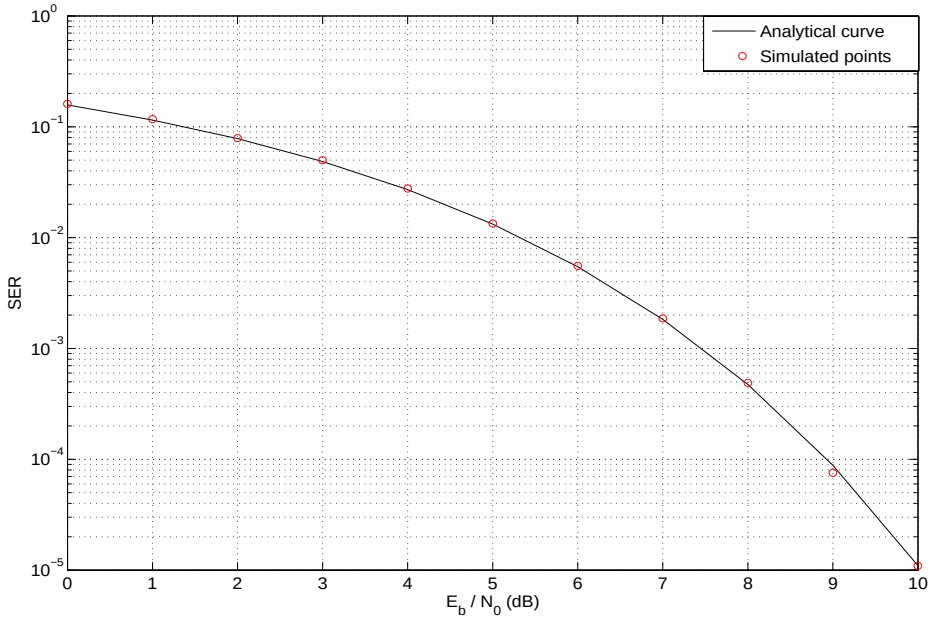

Figure 4.4: BER curves for the AWGN channel (setting II) with N=16 subcarriers for 4-QAM OFDM Systems.

frequency-flat fading channel are shown in Fig. 4.5 - Fig. 4.8. The corresponding Setting I and Setting II results are depicted in Fig. 4.5 and Fig. 4.6 with $N = 52$, which reveals the accuracy of analytical derivations given in the section 4.1.3.2 and indeed applicable to practical systems. Careful observations of Fig. 4.6, Fig. 4.7 and Fig. 4.8 (all are under Setting II) show that, the discrepancy of the simulated points and the analytical results increases as N decreases. The reason behind this phenomenon is the asymptotic behaviour of the ML estimate as shown in (3.42). That is higher the N higher the accuracy of (3.43). As far as the applications of OFDM is concerned, the number of subcarriers used (N) is typically not a small number, For example IEEE Std 802.11a and IEEE Std 802.16 have $N = 52$ and $N = 256$ respectively (**IEEE Std 802.11a-1999(R2003)**, 2003; **IEEE Std 802.16^{TM}-2004**, 2004) thus confirming the practical applicability of our derivations.

[1] see the section 3.5.1

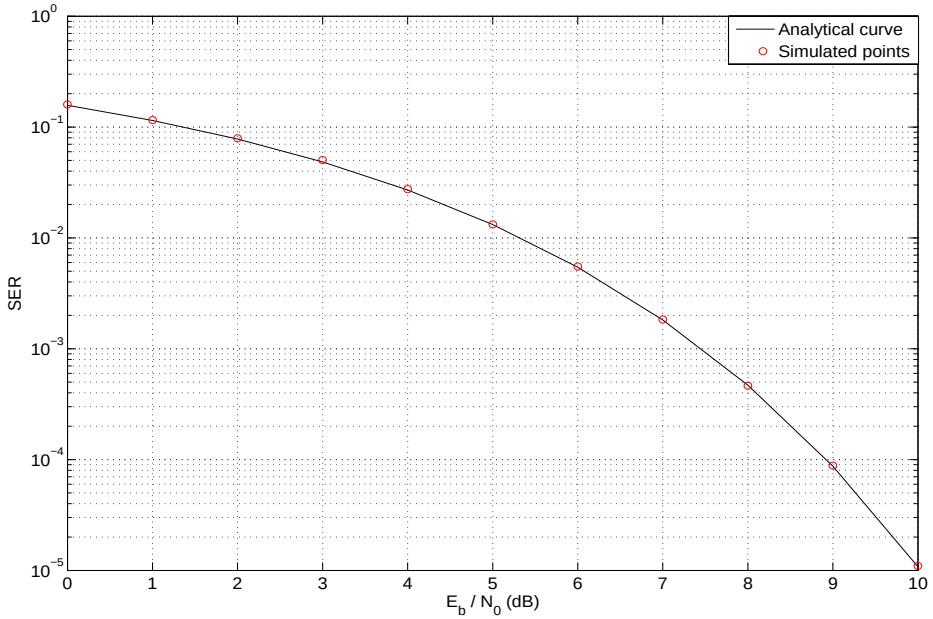

Figure 4.5: BER curves for the frequency-flat Rayleigh fading channel (setting I) with perfect power control and N=52 subcarriers for 4-QAM OFDM Systems.

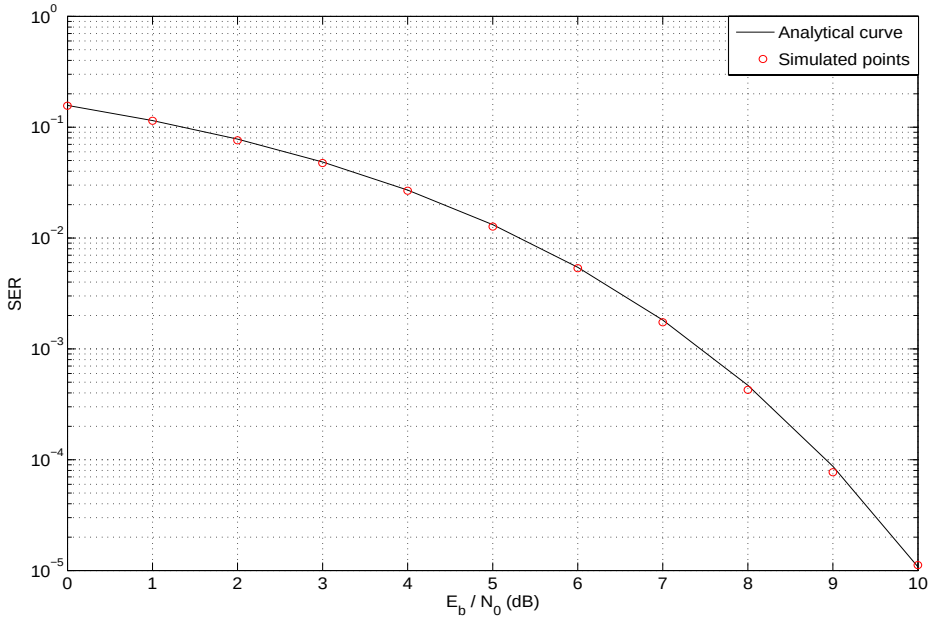

Figure 4.6: BER curves for the frequency-flat Rayleigh fading channel (setting II) with perfect power control and N=52 subcarriers for 4-QAM OFDM Systems.

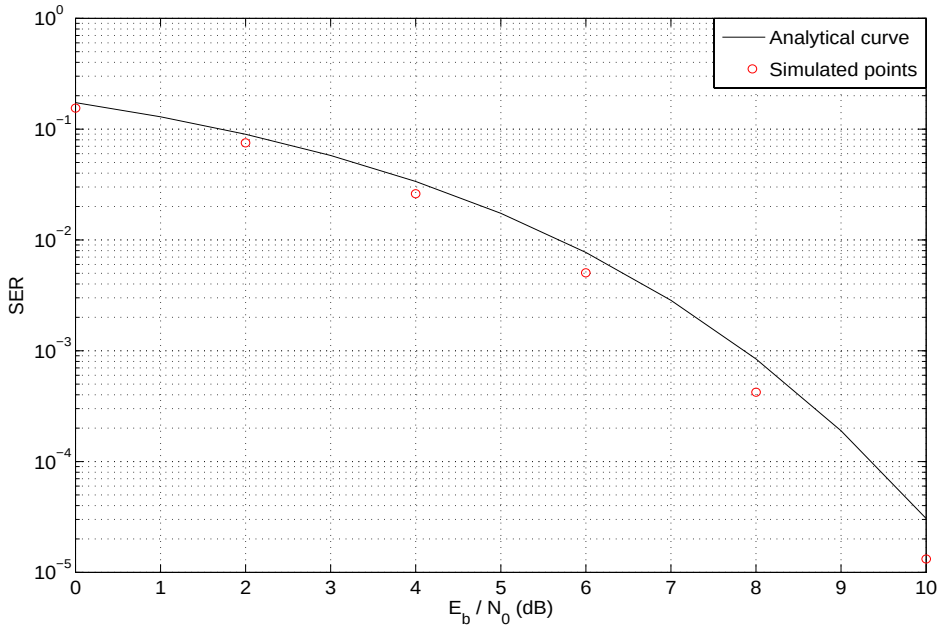

Figure 4.7: BER curves for the frequency-flat Rayleigh fading channel (setting II) with perfect power control and N=20 subcarriers for 4-QAM OFDM Systems.

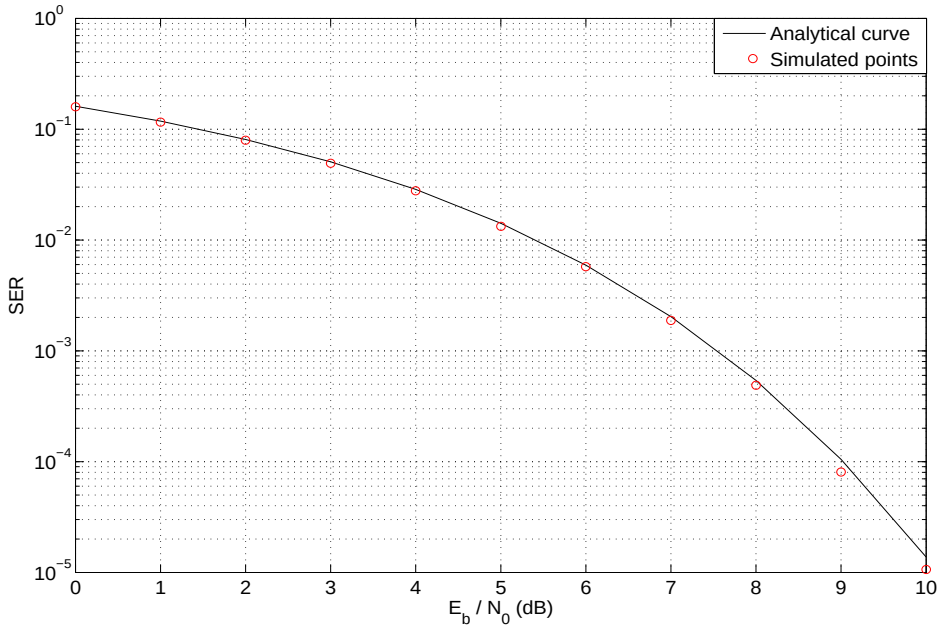

Figure 4.8: BER curves for the frequency-flat Rayleigh fading channel (setting II) with perfect power control and N=32 subcarriers for 4-QAM OFDM Systems.

4.4.2 Channel-Dependent Residual CFO for 4-QAM OFDM Systems

This section describes the simulation results associated to the analytical derivation presented in the section 4.2.1.

The simulation results in Fig. 4.9 and Fig. 4.10 show how the analytical results are matching with the simulated results for OFDM systems with $N = 32$ in the cases of Setting I and Setting II respectively. As pointed out previously, Fig. 4.10, Fig. 4.11 and Fig. 4.12 (all are under Setting II) is presented to demonstrate the behaviour of the discrepancy or the deviation of our analytical result and the simulation results. Indeed this arises due to the asymptotic nature of the ML estimate as mentioned before. Again we can conclude that, higher the N higher the accuracy of (3.43) assuring the applicability and the correctness of the analytical results as far as practical OFDM systems are concerned.

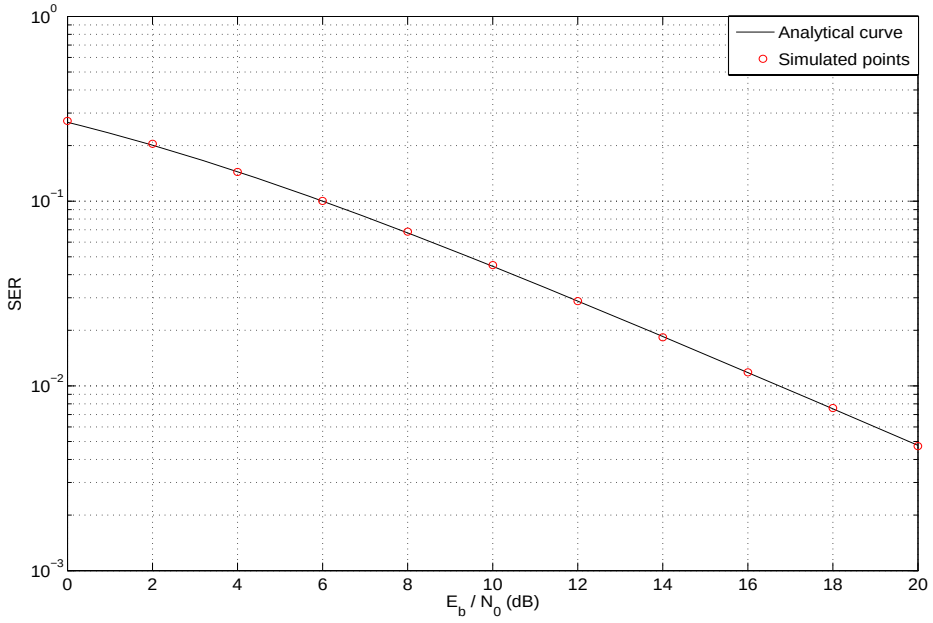

Figure 4.9: BER curves for the frequency-flat Rayleigh fading channel (setting I) with no power control and N=32 subcarriers for 4-QAM OFDM Systems.

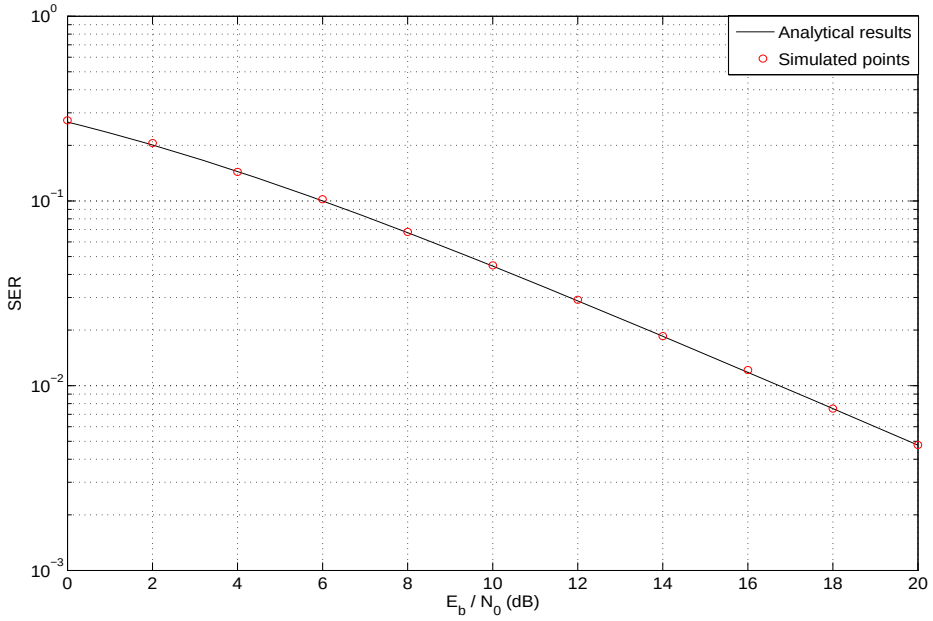

Figure 4.10: BER curves for the frequency-flat Rayleigh fading channel (setting II) with no power control and N=32 subcarriers for 4-QAM OFDM Systems.

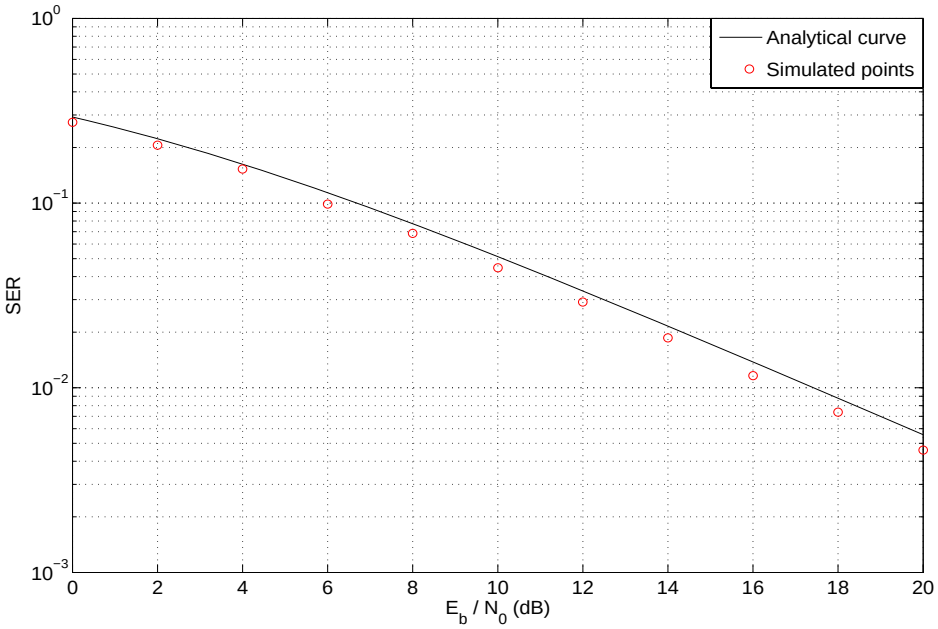

Figure 4.11: BER curves for the frequency-flat Rayleigh fading channel (setting II) with no power control and N=8 subcarriers for 4-QAM OFDM Systems.

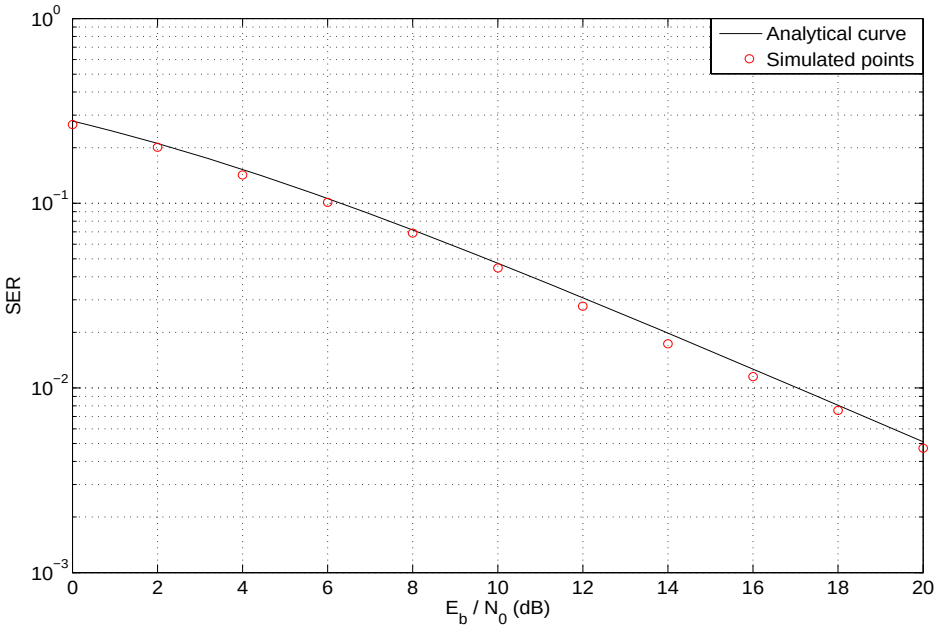

Figure 4.12: BER curves for the frequency-flat Rayleigh fading channel (setting II) with no power control and N=16 subcarriers for 4-QAM OFDM Systems.

CHAPTER 5

CONCLUSIONS AND RECOMMENDATIONS

5.1 Conclusions

The Main objective in this thesis is to carryout a comprehensive investigation on performance degradation in OFDM systems due to carrier frequency offset in the transmitter and the receiver. Eventhough in the literature this problem has been addressed in several occasions, none of them have attempted to incorporate the randomness of CFO in their derivations. The CFO is a random parameter for which the probability density function should clearly be identified.

In essence, the identification of the nature of the random variable CFO is twofold in our case where it is treated as either uniformly distributed or Gaussian distributed. Consider a situation where a CFO estimator at the receiver is not implemented. The possible scenario might be where the transceivers use highly stable crystal oscillators and skip CFO estimation to save energy. In this case we can say that the CFO is uniformly distributed showing the applicability of our derivations in the sections 3.2.1-3 and 4.1.1-3 for BPSK and 4-QAM OFDM systems respectively.

The ML estimates are Gaussian distributed and using this observation, we obtain the rest of the derivations accordingly identifying the probability distribution function of the residual CFO. Another important fact that should be mentioned in the derivations with Gaussian pdf is the distinction between perfect power control and no power control. We carry out our derivation with no channel energy fluctuations, or in other words, in situations where the statistics of the estimated residual CFO does not depend on the channel since the power control compensates the channel energy fluctuations. On the other hand, no power control will not consider stabilizing the channel energy fluctuations. These concepts are important in the training signal design aspects for OFDM systems showing the significance of our derivations in the performance analysis of such systems.

It should be emphasized that, the analytical BER expressions derived for a variety of situations here cannot be obtained with the use of existing ICI expressions (**Sathananthan and Thellambura**, 2001; **Dharmawansa et al.** [a] [b], 2006). As we consider the CFO or residual CFO to be random, it should remain in a form where we can mathematically utilize it and further apply it in the problem to obtain satisfactory solutions. Thus the derivation of the new approximated ICI expression given in (3.12) is the most useful result which enables us in getting through all the other derivations.

In summary, we derive BER/SER expressions for AWGN channel, frequency-flat and frequency-selective Rayleigh fading channels with the symbols coming from BPSK and 4-QAM constellations. The simulation results confirm the accuracy and the applicability of those in analysing the performance of practical OFDM systems.

5.2 Recommendations

In this section we suggest recommendations and potential future directives which may be investigated more thoroughly to make the results more realistic. Moreover some of these can be considered as modifications or amendments which should be investigated to explore the performance degradations or improvements in different kind of channel representations and system model representations.

1. In the section 3.3.2 we discuss the BER analysis in the case of frequency-selective Rayleigh fading channel with uniformly distributed CFO for BPSK OFDM systems. But the corresponding analysis is not performed for the 4-QAM OFDM systems, and hence can be considered.

2. In our derivations we did not consider the CFO-induced, symbol-index-dependent phase shift of $\exp(j2\pi v_{\Delta} m(N + N_g)/N)$ where m is the OFDM symbol index and N_g is the number of guard samples. We simply assume that every symbol is phase synchronized, so that the receiver is able to perfectly compensate for the aggregated phase-shift term (**Rugini and Banelli**, 2005). Incorporating this cumulative phase-shift in to the system equation deserves attention.

3. All the associated fading coefficients in our derivations are taken to be circularly symmetric complex Gaussian random variables which imitate a Rayleigh fading environment. In addition therefore the mathematical tractability of the performance analysis with different types of fading coefficients (e.g Nakagami-m, Rice, etc.) should be obtained.

4. Since we concentrate only on BPSK and 4-QAM symbol constellation schemes, the impact of using higher order symbol constellations needs to be investigated. A careful observation of equation (4.5) reveals that, M-QAM symbol constellations will have the conditional probability expressions to be lengthy thus resulting more complex SER expressions. Hence, investigation of possible complexity reduction method is of significance.

5. MIMO technology has attracted attention in wireless communications, since it offers significant increases in data throughput and link range without additional bandwidth or transmit power. The performance degradation in these systems due to the presence of ICI in MIMO OFDM systems (space-frequency coded OFDM, space-time coded OFDM) should be thoroughly investigated.

5.3 List of Publications

1. Chathuranga Weeraddana, Nandana Rajatheva, and Hlang Minn, *Probability of Error Analysis of BPSK OFDM Systems with Residual Frequency Offset*, submitted to the IEEE Transactions on Communications, accepted subject to revision.

2. Chathuranga Weeraddana and Nandana Rajatheva *Probability of Error Analysis of OFDM Systems with Residual Frequency Offset*, accepted for IEEE VTC-Spring 2007.

3. Chathuranga Weeraddana, Nandana Rajatheva, and Hlang Minn ,*Probability of Error Analysis of 4-QAM OFDM Systems with Random Residual Frequency Offset*, submitted to the IEEE GLOBECOM 2007 (under review).

REFERENCES

Armada A. G. (1998, January). Phase noise and sub-carrier spacing effects on the performance of an OFDM communication systems. *IEEE Commun. Lett.*, vol. 2 no. 1, pp. 11-13

Armstrong J., & (1999, March). Analysis of new and existing methods of reducing intercarrier interference due to carrier frequency offset in OFDM. *IEEE Trans. Communications*, vol. 47, pp. 365-369

Cai X., & Akansu A. N. (2000, July). A subspace method for blind channel identification in OFDM systems. *Prc. ICC New Orlean, LA*, pp. 929-933

Chow J. S., Tu J. C., and Cioffi J. M (1991, Aug). A Descrete Multitone Transceiver System for HDSL Applications. *IEEE J. Sel. Areas Communications*, vol. 9 no. 5, pp. 895-908

Cioffi J. M. , & A MulticarrierPrimer. *Amati Communications Corporation and Stanford Univercity*, Retrieved April 2007, from Website: http://www-isl.stanford.edu/people/cioffi/pdf/multicarrier.pdf,

Cimini L. J. (1985, July). Analysis and Simulation of a Digital Mobile Channel Using Orthogonal Frequency Division Multiplexing. *IEEE Trans. Communications*, vol. COM-33, pp. 665-675

Dharmawansa K. D. P., Rajatheva R. M. A. P. and Minn H. [a] (2006, October). An exact error probability analysis of OFDM systems with frequency offset. *IEEE MILCOM 2006*,

Dharmawansa K. D. P., Rajatheva R. M. A. P. and Minn H. [b] (2006). An exact error probability analysis of OFDM systems with frequency offset. *under minor revisions, submitted to IEEE Trans. Communications*,

Edfors O., Sandell M., van de Beek J. and Wilson S. K. (1998, July). OFDM Channel Estimation by Singular Value Decomposition. *IEEE Trans. Communications*, vol. 46, pp. 931-939

Gradshteyn I. S. and Ryzhik I. M. (1980). Table of Integrals, Series, and Products . Cambridge, U. K.: Academic Press.

Hanzo L., Muñster M. and Choi B. J, Keller T. (2003). OFDM and MC-CDMA for Broadband Multi-user Communications, WLANs and Broadcasting. IEEE press

Heath R. W., & Giannakis G. B. (1999, March). Exploiting input cyclostationarity for blind channel identification in OFDM systems. *IEEE Trans. Sig. Process.*, vol. 47, no. 3, pp. 848-856

Hlaing Minn., Yinghui Li, Naofal Al-Dharhir and Robert Calderbank. (2006, June). Pilot Designs for consistent frequency offset estimation in OFDM systems. *IEEE ICC 2006 ISTANBUL*, vol. 10, pp. 4566-4571

Hlaing Minn., Fu X and Bhargava V. K. (2006, June). Optimal periodic training signal for frequency offset estimation in frequency-selective fading channels. *IEEE Trans. Communications.*, vol. 54, pp. 1801-1096

Hlaing Minn., & Al-Dhahir N. (2006, May). Optimal training signals for MIMO OFDM channel estimation. *IEEE Trans. Wireless Commun.*, vol. 5 no. 5, pp. 1158-1168

Hlaing Minn., & Xing S. (2005, Feb). An optimal training signal stucture for frequency offset estimation. *IEEE Trans. Communications.*, vol. 53, pp. 343-355

IEEE Std 802.11a-1999(R2003), (2003, June). Part 11: Wireless LAN Medium Access

Control (MAC) and Physical Layer (PHY) specifications, High-speed Physical Layer in the 5 GHz Band. *IEEE-SA Standard Board*, Retrieved April 2007, from Website: http://standards.ieee.org/getieee802/portfolio.html

IEEE Std 802.16^{TM}-2004, (2004, October). IEEE Standards for Local and Metropolitan Area Networks, Part 16: Air Interface for Fixed Broadband Wireless Access Systems. *IEEE Computer Society and the IEEE Microwave Theory and Technique Society*, Retrieved April 2007, from Website: http://standards.ieee.org/getieee802/portfolio.html

Jing Lei., & Tung-Sang Ng. (2004, March). A consistent OFDM carrier frequency offset estimator based on distinctively spaced pilot tones. *IEEE Trans. Wireless Communications*, vol. 3 no. 2, pp. 588-599

Kay S. M. (1993). Fundamentals of Statistical Signal Processing: Estimation Theory. Englewood Cliffs NJ: Prentise-Hall.

Keller T., & Hanzo L. (2000, May). Adaptive multicarrier modulation: A convenient framework for time-frequency processing in wireless communications. *Proc. IEEE*, vol. 88, pp. 611-640

Marvin K. S, & Alouini M. S (2005). Digital Communications Over Fading Channels (2nd ed.).. John Wiley & Sons, Inc.

Miller K. S. (1969, October). Complex Gaussian processes. *SIAM REVIEW*, vol. 11, pp. 544-567,

Moose P. H. (1994, October). A Technique for orthoganalfrequency division multiplexing frquency offset correction. *IEEE Trans. Communications*, vol. 42 no.10, pp. 2908-2914

Morelli M., & Mengali U. (1999, March). An improved frequency offset estimator for OFDM applications. *IEEE Commun. Lett.*, vol. 3 no. 3, pp. 75-77

Morelli M., & Mengali U. (2000, September). Carrier-frequency estimation for transmission over selective channels. *IEEE Trans. Communications*, vol. 48, pp. 1580-1589

Muquet B., de Courville M. and Duhamel P. (2002, July). Subspace-based blind and semi-blind channel estimation for OFDM systems. *IEEE Trans. on Sig. Process.*, vol. 50, no. 7, pp. 1699-1712

Pollet T., Blade M. V. and Moeneclaey M. (1995, Feb./Mar./Apr.). BER sensitivity of OFDM systems to carrier frequency offset and Wiener phase noise. *IEEE Trans. Communications*, vol. no. 2/3/4, pp. 191-193

Proakis J. G. (1995). Digital Communications (3rd ed.).. New York: McGraw-Hill.

Rugini L., & Banelli P. (2005, September). BER of OFDM systems impaired by carrier frequency offset in multipath fading Channels. *IEEE Trans. Wireless. Communications*, vol. 4, pp. 2279-2288

Russell M., & Stüber G. L. (1995, July). Interchannel interference analysis for OFDM in a mobile environment. *IEEE Vehicular Technology Conf., Chicago*, vol. 2, pp. 820-824

Sathananthan K., & Tellambura C. (2001, November). Probability of error calculation of OFDM systems with frequency offset. *IEEE Trans. Communications*, vol. 49, pp. 1884-1888

Schmidl T. M., & Cox D. C. (1997, December). Robust frequency and timing synchronisation for OFDM. *IEEE Trans. Communications*, vol. 45 no. 12, pp. 1613-1621

Shentu J., Panta k. and Armstrong J. (2003, June). Effects of Phase Noise on Performance of OFDM Systems Using an ICI Cancellation Scheme. *IEEE Trans. Communications*, vol. 49 no. 2, pp. 221-224

Stantchev B., & Fettweis G. (1994, September). Time-variant distortions in OFDM. *IEEE Commun. Lett.*, *v*ol. 4, pp. 312-314

St*ü*ber G. L. (2001). Principles of Mobile Communication(2nd ed.).. Kluwer Academic Publishers Boston/Dordrecht/London

Tureli U., Liu H. and Zoltowski M. D. (2000, September). OFDM blind carrier offset estimation:ESPRIT. *IEEE Trans. Communications*, *v*ol. 48, pp. 1459-1461

Van de Beek J-J., Sandell M. and B*ö*rjesson P. O. (1997, July). ML estimation of time and frequency offset in OFDM systems. *IEEE Trans. Signal Proc.*, *v*ol. 45 no. 7, pp. 1800-1805

Verdu S. (1998). Multiuser Detection. Cambridge University Press.

Wang Z., & Giannakis G. B. (2000, May). Wireless multicarrier communications. *IEEE Sig. Process. Mag*, *v*ol. 17 issue. 3, pp. 29-48

Weinstein S. B., & Ebert P. M. (1971, October). Data transmission by frequency-division multiplexing using the discrete Fourier transform. *IEEE Trans. Commun. Technol.*, *v*ol. COM-19, pp. 628-634

Zhao Y., & Häggman S. G. (1996, April-May). Sensitivity to Doppler shift and carrier frequency errors in OFDM systems-the consequences and solutions. *IEEE VTC'96*, *v*ol. 3, pp. 1564-1568

APPENDIX A

SOME OF THE INTERGRATIONS RELATED WITH Q-FUNCTION

1.

$$I = \int Q(c + dx)dx \tag{A.1}$$

Q- function is defined bu

$$Q(x) = \frac{1}{\sqrt{2\pi}} \int_x^\infty \exp\left\{ - \frac{y^2}{2} \right\} dy \tag{A.2}$$

Dfferentiating (A.2) with respect to x yeilds

$$\frac{d}{dx}Q(x) = Q'(x) = -\frac{1}{\sqrt{2\pi}} \exp\left\{ - \frac{x^2}{2} \right\} \tag{A.3}$$

so that we can perform the part by integration as

$$\int Q(x)dx = \int Q(x)\frac{d}{dx}xdx = xQ(x) - \frac{1}{\sqrt{2\pi}} \exp\{-\frac{x^2}{2}\} \tag{A.4}$$

Using (A.4) we can solve the indefinite integral $\int Q(c + dx)dx$ to obtain

$$\int Q(c + dx)dx = \frac{1}{d}\left[(c + dx)Q(c + dx) - \frac{1}{\sqrt{2\pi}} \exp\left\{ - \frac{(c + dx)^2}{2} \right\}\right] \tag{A.5}$$

where c and d are arbitary constants with $d \neq 0$.

2.

$$I = \int_0^\infty Q(a_1x)Q(a_2x)\frac{x}{\sigma_R^2} \exp\left(- \frac{x^2}{2\sigma_R^2} \right) dx \tag{A.6}$$

To perform part by integration we arrange (A.6) as

$$I = \int_0^\infty Q(a_1x)Q(a_2x)\frac{d}{dx}\left(- \exp\left[- \frac{x^2}{2\sigma_R^2} \right] \right) dx \tag{A.7}$$

After having some mathematical manipulations on (A.7) we can obtain

$$I = \frac{1}{4} - \int_0^\infty \frac{a_2}{\sqrt{2\pi}} Q(a_1x) \exp\left[- \frac{x^2}{2}\left({a_2}^2 \frac{1}{\sigma_R^2} \right) \right] dx \\ - \int_0^\infty \frac{a_1}{\sqrt{2\pi}} Q(a_2x) \exp\left[- \frac{x^2}{2}\left({a_1}^2 \frac{1}{\sigma_R^2} \right) \right] dx \tag{A.8}$$

Using (**Gradshteyn and Ryzhik**, 1980 : eq 6.285) and followed by some triagonometric manipulations gives

$$I = \frac{1}{4} - \frac{a_2m_2}{4} - \frac{a_1m_1}{4} + \frac{a_2m_2}{2\pi} \cot\left(\frac{1}{a_1m_2} \right) + \frac{a_1m_1}{2\pi} \cot\left(\frac{1}{a_2m_1} \right) \tag{A.9}$$

3.

$$I(\mu) = \int_{-\infty}^{\infty} Q(\mu + \lambda_1 x) Q(\mu + \lambda_2 x) \frac{1}{\sqrt{2\pi}} \exp\left(- \frac{x^2}{2} \right) dx \tag{A.10}$$

As differential coefficients inside the integral are well defined over the range $(-\infty, \infty)$, differentiatin of $I(\mu) = I'(\mu)$ with respect to μ yields

$$I'(\mu) = I_1(\mu) + I_2(\mu) \tag{A.11}$$

where

$$I_1(\mu) = -\frac{1}{2\pi} \int_{-\infty}^{\infty} Q(\mu + \lambda_2 x) \exp\left(- \frac{x^2 + \frac{2\mu\lambda_1 x}{\lambda_1^2+1} + \frac{\mu^2}{\lambda_1^2+1}}{\frac{2}{\lambda_1^2+1}} \right) dx \tag{A.12}$$

with some rearrangements we can further reduced (A.12) as

$$I_1(\mu) = -\frac{1}{\sqrt{2(\lambda_1^2+1)}} Q\left(\frac{\mu_F}{\sqrt{\lambda_F^2+1}} \right) \exp\left(- \frac{\mu^2}{2(\lambda_1^2+1)} \right) \tag{A.13}$$

where $\mu_F = \mu\big(1 - \frac{\lambda_1\lambda_2}{\lambda_1^2+1}\big)$ and $\lambda_F = \frac{\lambda_2}{\sqrt{\lambda_1^2+1}}$. Note that $I_2(\mu)$ has the same definition as $I_1(\mu)$ with λ_1 and λ_2 interchanged. With the fact that $I(\infty) = 0$

$$\begin{aligned} - I(\mu) = \int_{\mu}^{\infty} I'(t) dt = &- \frac{1}{\sqrt{2\pi(\lambda_1^2+1)}} \int_{\mu}^{\infty} \exp\left(- \frac{t^2}{2b_1^2} \right) Q(a_1 t) dt \\ &- \frac{1}{\sqrt{2\pi(\lambda_2^2+1)}} \int_{\mu}^{\infty} \exp\left(- \frac{t^2}{2b_2^2} \right) Q(a_2 t) dt \end{aligned} \tag{A.14}$$

where $b_1^2 = \lambda_1^2 + 1$, $b_2^2 = \lambda_2^2 + 1$, $a_1 = \frac{\lambda_1^2 - \lambda_1\lambda_2 + 1}{\sqrt{(\lambda_1^2+1)(\lambda_1^2+\lambda_2^2+1)}}$ and $a_2 = \frac{\lambda_2^2 - \lambda_1\lambda_2 + 1}{\sqrt{(\lambda_2^2+1)(\lambda_1^2+\lambda_2^2+1)}}$. Considering only the first integral term in (A.14) we can deduce that

$$\begin{aligned} &- \frac{1}{\sqrt{2\pi(\lambda_1^2+1)}} \int_{\mu}^{\infty} \exp\left(- \frac{x^2}{2b_1^2} \right) Q(a_1 x) dx \\ &\qquad = - \frac{1}{\sqrt{2\pi}} \int_{\frac{\mu}{b_1}}^{\infty} \exp\left(- \frac{t^2}{2} \right) Q(a_1 b_1 t) dt \\ &\qquad = - \frac{1}{2\pi} \int_{\frac{\mu}{b_1}}^{\infty} \int_{a_1 b_1 t}^{\infty} \exp\left(- \frac{y^2}{2} \right) \exp\left(- \frac{t^2}{2} \right) dy dt \end{aligned} \tag{A.15}$$

Thus we can simply move from rectangular cordinates to polar cordinates and thus rewrite the integral

$$\begin{aligned} &- \frac{1}{2\pi} \int_{\frac{\mu}{b_1}}^{\infty} \int_{a_1 b_1 t}^{\infty} \exp\left(- \frac{y^2}{2} \right) \exp\left(- \frac{t^2}{2} \right) dy dt \\ &\qquad = - \frac{1}{2\pi} \int_{\beta_1}^{\frac{\pi}{2}} \int_{\frac{\mu \sec\theta}{b_1}}^{\infty} r \exp\left(- \frac{r^2}{2} \right) dr d\theta \end{aligned} \tag{A.16}$$

with $\beta_1 = \tan^{-1}(a_1 b_1)$. Then we can easily come up with a solution to $I(\mu)$ as

$$I(\mu) = \frac{1}{2\pi}\int_0^{\frac{\pi}{2}-\beta_1} \exp\left(\frac{-\mu^2}{2{b_1}^2\sin^2\phi}\right)d\phi + \frac{1}{2\pi}\int_0^{\frac{\pi}{2}-\beta_2} \exp\left(\frac{-\mu^2}{2{b_2}^2\sin^2\phi}\right)d\phi \quad \text{(A.17)}$$

$I(\mu)$ cannot be evaluated in closed-form and it shows similarities to the well known Craig's formula. So that $b_1 = \sqrt{\lambda_1^2 + 1}$, $b_2 = \sqrt{\lambda_2^2 + 1}$,

$$a_1 = \frac{\lambda_1^2 - \lambda_1\lambda_2 + 1}{\sqrt{(\lambda_1^2+1)(\lambda_1^2+\lambda_2^2+1)}}$$

$$a_2 = \frac{\lambda_2^2 - \lambda_1\lambda_2 + 1}{\sqrt{(\lambda_2^2+1)(\lambda_1^2+\lambda_2^2+1)}}$$

with $\beta_1 = \tan^{-1}(a_1 b_1)$ and $\beta_2 = \tan^{-1}(a_2 b_2)$.